# The quantum and the gravity: Newtonian and Cosmological applications

by

Natacha Altamirano

A thesis
presented to the University of Waterloo
in fulfillment of the
thesis requirement for the degree of
Doctor of Philosophy
in
Physics

Waterloo, Ontario, Canada, 2018

**Examining Committee Membership**

The following served on the Examining Committee for this thesis. The decision of the Examining Committee is by majority vote.

| | |
|---|---|
| External Examiner: | Miles Blencowe<br>Professor, Dartmouth College |
| Supervisor: | Robert B. Mann<br>Professor, Dept. Physics and Astronomy,<br>University of Waterloo. |
| Co-Supervisor: | Niayesh Afshordi<br>Associate Professor, Dept. Physics and Astronomy,<br>University of Waterloo.<br>Associate Professor, Perimeter Institute for Theoretical Physics. |
| Internal Member: | Avery Broderick<br>Associate Professor, Dept. Physics and Astronomy,<br>University of Waterloo.<br>Associate Professor, Perimeter Institute for Theoretical Physics. |
| Internal-External Member: | Achim Kempf<br>Professor, Dept. Applied Mathematics,<br>University of Waterloo. |
| Other Member(s): | Lucien Hardy<br>Adjunct Professor, Dept. Physics and Astronomy,<br>University of Waterloo.<br>Professor, Perimeter Institute for Theoretical Physics. |

This thesis consists of material all of which I authored or co-authored: see Statement of Contributions included in the thesis. This is a true copy of the thesis, including any required final revisions, as accepted by my examiners.

I understand that my thesis may be made electronically available to the public.

## Statement of Contribution

The chapters of this thesis contain material produced in different collaborations. Chapter II was in collaboration with Magdalena Zych, Paulina Corona-Ugalde and Robert Mann. Chapter III was in collaboration with Kiran Khosla. Chapter IV was in collaboration with Magdalena Zych, Paulina Corona-Ugalde and Robert Mann. Part III of this thesis includes material produced in collaboration with Kiran Khosla, Paulina Corona-Ugalde, Romain Pascalie, Robert Mann and Gerard Milburn.

**Abstract**

The gravitational decoherence field studies the suppression of coherence in quantum systems caused by effects rooted in the gravitational interaction. This models are not just important to yield interesting ideas about the search, in regimes others than the Planck scale, for the interplay between quantum mechanics and general relativity, but also from a theoretical point of view. The fact that the gravitational field can not be shielded opens the question of how strong will the gravitational 'environment' decohere a quantum system? and if this decoherence can somehow explain the absence of macroscopical superpositions? This thesis studies in depth the 'Classical Channel Gravity' (CCG) model, a recent proposal of gravitational decoherence that assumes that the gravitational interaction is always accompanied with an intrinsic decoherence mechanism which ensures that there is no transmission of quantum information between the parties involved. This model can be understood a series of weak continuous quantum measurements accompanied with a feedback term produced by some underlying hidden gravitational degrees of freedom. We first study all the possible emergent dynamics from collisional Markovian dynamics; these ones range from exact unitary to arbitrary fast decoherence (Zeno effect). The second part of the thesis is devoted to study the Newtonian and post Newtonian limits of the CCG model, with particular focus on the testability features of CCG. In particular, we apply this model to coupled clocks and find that the amount of decoherence predicted by CCG is the same as the decoherence that an 'environment of clocks' will imprint in a single clock in the context of unitary evolution. On the other hand, we find that this effect is far from being detectable with the current achieved time accuracy. However, CCG as a model for multi partite systems and two systems with very different masses seems to yield an amount of decoherence that is not only able to be detectable with current experiments but also seems to indicate that this model is ruled out. Nevertheless, we also mention potential caveats with our assumptions and discuss other physically motivated directions to further study this result. Finally, we also explore the extension of CCG for the cosmological scenario. In this context the scale factor is being decohered by test particles 'sitting' on spacetime. We find that this decoherence will be seen by an observer unaware of the CCG fundamental mechanism as an emergent form of dark energy filling the universe.

**Acknowledgements**

I would like to thank all the people that supported me, either directly or indirectly, along this time and that helped me professionally or personally. I would like to start with the Canadian tax payers, Ontario Government and public and private funds who support Perimeter Institute for the economic support I've received from you. Moving to Canada and affording education would have not been possible without it.

I am lucky to have had two PhD supervisors that not only supported me professionally but are also great people. I've learnt a great deal from them and this goes beyond physics. My experience with them have shaped my understanding of science and academia, they have supported me in my many struggles and I am in debt with them for always taking the time for me. Thank you Robb for your generosity, for always finding the time to have meetings and for for introducing me to amazing people from whom I've learnt a lot. Niayesh's intuition will never cease to amaze me; there is not a problem you present to him he can not understand, a code he can not fix or a factor of 2 he will miss. He has introduced me to the exciting world of cosmology and astrophysics, and taught me the importance of testable science. I can not thank you both enough for sharing your knowledge with me. I would also like to thank David Kubiznak for his guidance during my first year at PI. My special acknowledgement goes for Sergio Dain, his advice during my time in Argentina will always stay with me and if I need to pick a role model then that is certainly Sergio, gracias!

Doing my PhD involved a lot thinking, computing and writing and my most memorable memories about it always include a collaborator sharing that with me. A special thank to all of them, Chiamaka, Beth, Romain, Jamie, Matt, Paulina, Nima, Shant and Gerard. My special thanks go for Kiran, with whom I've spent endless time doing physics and thinking about it, and some of this thesis is the result of scratching our heads together. My special admiration goes for Magdalena, you are one of the greatest scientist I know! I have learnt and tried to copy your passion for physics and hard work during my PhD. I will also like to thank Alex and Fil for embarking with me in organizing the workshop 'Spacetime and Information'.

I probably spent a third of my time in Canada inside the Perimeter Institute and I have met and shared with incredible people there. Thank you Debbie for your dedication in the academic program. Thank you to the reception staff, Tom and Amy, who have received me every single morning with a smile, making the difference in my days. I would like to thank all the staff that have, in one way or another, supported me during the last year at PI to

find my next move for my professional career. My special thanks goes for the bistro staff, that have coped with my pickiness for food for 5 years. Thank you Chiamaka and Yasaman for making the office a special spot. I would like to thank the Women in Physics community at PI: meeting with all of you regularly has made me feel much more comfortable and stronger. Thank you for sharing your many experiences with me. In particular I would like to acknowledge Bianca, Maite, Bel, Lauren and Gang for sharing the the sensitive task of running the Diversity Committee at PI. These 5 years were full of challenges and one of them was to learn to play violin. Thanks to Dan for being my indirect teacher and all the members of the PI orchestra for being patient with me and push me to learn new things.

Waterloo would have really been *Winterloo* if it wasn't for the warmth of my many friends here. Finding female physicists with whom I could share my experience and relate to theirs wasn't easy but I am lucky to have found Shira and Fiona: your friendship and support made academia a little less crazy, thank you very much for listening to me and advising me! Thank you to the *Latinos*: Néstor, Andrés, Lucía, Pablo, Nayeli, Caro y Julián for the latin parties and the many *taco entraña* shared. A very special thanks to the Argentinians at PI: Damián, Bel and Juani for sharing with me and for being a very strong emotional support. You brought home a little bit closer! I would like to thank Luis Lehner for his generosity and Lucy for making Waterloo seem a little less far from Argentina in my first year here! I will like mention the support from my old friends back home, Merce, Maty, Xime, Nico, Andres, Meli, Naty, Agus, Pablo.

I strongly believe I wouldn't have reached this step in my life if it wasn't for the unconditional support of my family. This thesis is dedicated to my Mom and my Dad who have always believed in me, who taught me not to be afraid of anything. Their efforts for the wellbeing of my sister and me since we were kids is in part my motivation to achieve great things, only we know how many sacrifices they made for us to be were we are. I want to thank my sister Ani, with who I share an honest friendship the type that is unconditional and the strongest of all. Estoy convencida de que no hubiera podido alcanzar esta meta sin el apoyo incondicional de mi familia. Esta tesis está dedicada a mi Mamá y Papá quienes siempre creyeron en mi y me enseñaron a no tenerle miedo a nada. Sus esfuerzos por mi bienestar y el de mi hermana desde que eramos chicas es en parte mi motivación para alcanzar grandes metas. Solo nosotros sabemos todos los sacrificios que hicieron para que estemos donde estamos hoy. Quiero agradecerle a mi hermana, Ani con quien comparto una verdadera y honesta amistad, de esas que son incondicionales y las más fuerte de todas.

I do not have words to thank Gabriel enough who has been my strongest supporter

during all this period and the one who is behind the scenes of this thesis. Only he knows that parts of this period have been difficult for me. Many hours of work not yielding the results I expected or my struggles with academia or even my ups and downs as a person found relief arriving home and having him to share this with. Your positivity, support and encouragement have been a motor for me, THANK YOU for sharing all this with me, I love you!

*A Mamá y Papá,*
*por siempre creer en mi.*

*To mom and dad,*
*who always believed in me.*

# Table of Contents

# List of Tables

# List of Figures

# Chapter 1

# Introduction

## 1.1 Motivation

Quantum Mechanics (QM) and General Relativity (GR) are both successful theories in their own domains, being able to explain a broad range of natural phenomena and tested with high accuracy [9]. On the one hand, QM, and its relativistic extension to fields, undergirds the explanation of most of the known forces of nature and the construction for the standard model of particle physics. On the other hand, GR has passed several tests over different mass scales ranging from the everyday (in its Newtonian limit) to the entire universe, covering the recent discovery of gravitational waves for black holes and neutron star mergers [10, 11, 12] (for a full characterization of the tests of GR on all scales refer to [13]).

Despite their success, these theories present us with several open problems. Among others, on the QM side we have the measurement problem and the lack of macroscopic superposition whereas on the GR side we have the singularity problem and the dark energy and dark matter problems. However, we should also mention the most ambitious of all the open problems: to find a coherent unification between quantum physics and general relativity. This is a conundrum that has intrigued physicists and philosophers for decades and a journey from which we have learned plenty. To attack this task one has several options:

- String theory [14] and loop quantum gravity [15]. The most challenging aspect of this option is how far we are experimentally from reaching the Planck scale ($l_P = 10^{-35}$m, $t_P = 10^{-44}$s, $m_P = 10^{-8}$kg) where effects of a *quantum space-time* will be significant.

- *Gravitize* quantum mechanics [16].
- Construct a new framework with ingredients of both theories [17].

Ultimately, the contrast between the predictions of these models and experiments will shed light on the correct theory. However, waiting for experiments to reach the Planck scale is not an efficient short term idea and so far we are still left with many open questions. How does quantum matter gravitate? How is the gravitational field of a quantum superposed state? What is the correct GR approach/set of observables that should be quantized? Nevertheless, because of advancements in technology, the regime where we can test the interplay between QM and GR is becoming reachable phenomenologically. We'll discuss this in two main categories:

- quantum field theory (QFT) in curved space time and perturbative quantum gravity and
- gravitational decoherence.[1].

Perturbative quantum gravity and QFT in curved spacetime have provided a great deal of insight regarding cosmology and has predicted interesting phenomena like black hole radiation. With the discovery of the cosmic microwave (CMB) background physicists were left with the questions of why the anisotropies of the CMB were correlated on scales that were never in causal contact (the horizon problem) and why the universe seams to be spatially flat (the flatness problem). Inflation plays a major role *solving* these problems and moreover, inflation + ΛCDM (a universe with cosmological constant and cold dark matter) explains, with only six parameters, the observable universe better than any other model tested so far [18]. There is still the open problem of finding the right extension to the standard model or a modified theory of gravity to consistently include and explain the nature of dark matter and dark energy.

In addition, QFT in curved spacetime allowed the theoretical exploration of quantum effects on a fixed classical background. Unruh [19] showed that a uniformly accelerated observer in a flat background will see a thermal bath with temperature proportional to its acceleration. A related effect is what we now know as Hawking radiation [20, 21], which

[1]There are models of gravitational decoherence that use QFT in curved spacetime techniques and there are models of gravitational decoherence that can not be *testable* – or at least phenomenologically constrained, but in this category we are including all those models that study the interplay between quantum mechanics and general relativity that: 1) produce decoherence and 2) do not fit solely in the other categories.

is the prediction that a black hole will thermally radiate. When radiating, the black hole will shrink, ultimately disappearing completely. The study and understanding of this final state has led to the black hole information paradox (see [22] for a review): after complete evaporation there will be only thermal radiation, even if the system that collapsed began a pure state. This means that the system would have evolved from a pure state into a mixed state, thus conflicting with quantum mechanics since this is something that is not allowed by unitary evolution. Some of the possible resolutions of the paradox rely on abandoning the classical and semi classical description of black hole horizons for more exotic ideas like the fuzzball program [23, 24].

Until very recently these predictions did not leave the 'theoretical bubble' – at most we have their confirmation in analogue setups [25]. However, the recent discovery of gravitational waves [10, 11, 12] opened a new window into regimes to test this phenomenologically, and we can barely imagine what the improvement of sensitivity, detectors and more events will teach us about this unexplored regime. In fact Abedi and collaborators [26] have recently discovered an 'echo' signature, with $2.5\sigma$ significance, in the black hole merger data that is consistent with the predictions of the fuzzball program. In addition they have also found echo signals with $4.5\sigma$ significance for the neutron star merger data [27]. Finally, the Event Horizon Telescope initiative will observe black holes in the millimetre wavelength scale where the accretion disks of blackholes become optically thin. In these frequencies one is able resolve the shadows of the event horizon (or the photon unstable orbits)[2]. This technique will not just be able to provide new tools to understand gravity in the strong field regime, but it might also shed light about the interplay between gravitational physics and quantum mechanics near the horizon [28, 29].

Let's now switch gears to the other category to study the interplay between GR and QM. Gravitational decoherence refers to those models that predict a loss of coherence of quantum (matter or spacetime itself) fields that can be related to gravitational effects. The aim of these models is to understand the interplay between quantum mechanics and gravitational physics, which is a much less ambitious program than constructing a fundamental framework, but still interesting from the experimental point of view at low energy. Of course, the real challenge is to build an experiment with masses large enough to detect their gravitational interaction and small enough to prepare in a quantum state. This is a 20 order-of-magnitude problem: the smallest mass for which we measure gravitational interaction is of the order of $10^{-2}$ kg and it was achieved with a torsion balance experiment [30], whereas the largest mass that has been put in superposition is $10^{-22}$ kg for organic molecules [31, 32, 33]. The proposals to test these models range from optomechanical experiments [34, 35], matter wave interferometry [36, 2, 37, 38], and torsion balance ex-

[2] eventhorizontelescope.org, Odyssey education.

periments [39] (or a combination [40])– for a full description of the *state of the art* on the phenomenological and experimental side of gravitational decoherence refer to the recent review [41].

Under this broad description of gravitational decoherence many models fall in this category. The goal of this thesis is to analyze consequences, from theoretical and experimental perspectives, in both the Newtonian and cosmological regimes. Before we dive into the revision of the specific model let's briefly describe the *state of the art* in the gravitational decoherence field.

## 1.2 Gravitational decoherence

Decoherence refers to the loss of coherence of a quantum state. The most basic example is the interaction of the system with an environment; when the environmental degrees of freedom are traced out, we are left with the off-diagonal terms of the density matrix being exponentially suppressed.

Consider a system and an environment that is effectively measuring the system with the interaction Hamiltonian

$$H_{\text{int}} = \sum_n |\, n\rangle\langle n\,| \otimes \hat{A}_n\,, \tag{1.1}$$

where $|\, n\rangle$ are the states of the system that can be measured and $\hat{A}_n$ is the coupling observable from the environment with the system, that can a priori be very general but will depend on $n$. If the initial state of the system is $|\, n\rangle$ and the one for the environment is $|\, \Phi_0\rangle$, the time evolution under the interacting Hamiltonian is

$$|\, n\rangle|\, \Phi_0\rangle \xrightarrow{t} \exp(-i\, t\, H_{\text{int}})|\, n\rangle|\, \Phi_0\rangle = |\, n\rangle\exp(-i\hat{A}_n t)|\, \Phi_0\rangle := |\, n\rangle|\, \Phi_n(t)\rangle\,. \tag{1.2}$$

If we now consider that the system is in a state of superposition ($\sum_n c_n|\, n\rangle$) then the evolution is

$$\left(\sum_n c_n|\, n\rangle\right)|\, \Phi_0\rangle \xrightarrow{t} \sum_n c_n|\, n\rangle|\, \Phi_n(t)\rangle\,, \tag{1.3}$$

and upon tracing the degrees of freedom of the environment we get the reduced density

matrix of the system

$$\rho_S(0) = \sum_{n,m} c_n c_m^* |\, n\rangle\langle m\,| \xrightarrow{t} \mathrm{Tr}[\rho]_{\mathrm{E}} = \mathrm{Tr}\Big[\sum_{n,m} c_n c_m^* |\, n\rangle\langle m\,|\,\Phi_n\rangle\langle\Phi_m\,|\Big]_{\mathrm{E}}$$
$$= \sum_j \sum_{n,m} \langle\Phi_j\,|c_n c_m^*|\, n\rangle\langle m\,|\,\Phi_n\rangle\langle\Phi_m\,|\,\Phi_j\rangle$$
$$= \sum_j |c_j|^2\,|\, j\rangle\langle j\,|\,, \tag{1.4}$$

where we have used the fact that the states of the environment are orthogonal $\langle\Phi_n\,|\,\Phi_m\rangle = \delta_{nm}$[3]. This means that after interaction with the environment the off-diagonal terms of the density matrix are zero, suppressing all the coherence present in the initial state and giving a final state that is an ensemble with classical uncertainties, or, in other words, a statistical mixture.

In this context gravitational decoherence encapsulates all those models where the coherence suppression is related to a gravitational process. This field is relatively young and we still lack a unifying framework for all the proposed models. However, these models can be separated into different categories[4]:

1. Models where quantum matter is interacting with a random gravitational field where *quantum or classical fluctuations of spacetime* are the source of decoherence. In these scenarios the fluctuations take the role of the environment that gets entangled, and thus causing decoherence when these degrees of freedom are traced out. Examples of this cover the effective Schrödinger equation in a fluctuating spacetime [42, 43, 44, 45], producing a localization in energy for the matter fields, ultimately conserving the expectation value of the Hamiltonian; stochastic semiclassical gravity [46], governed by the Einstein-Langevin to produce corrections to semiclassical gravity; decoherence arising from a thermal bath of gravitons [47]; generic fluctuations for gravitational perturbations in the ADM formalism [48]; and fluctuations of the time parameter in the Schrödinger equation [49, 50].

2. *Spontaneous wave function collapse* models have at their core the measurement problem (for a review on the status of collapse models see [51]). As we discussed above,

[3] In general this inner product is not zero but it asymptotes very rapidly to zero because of the many degrees of freedom that the environment contains.

[4] Here we follow the characterization provided in [41] and we strongly encourage the reader to refer to it for an extensive comparison.

quantum mechanics has been able to pass many different kinds of experimental tests, but it has not been able to consistently explain the most obvious of all tests: why in everyday life we do not see superpositions of macroscopic systems?[5]. This is fundamentally even deeper: in quantum mechanics if you have two solutions $\psi_1$, $\psi_2$ of the Schrödinger equation then $\psi = \psi_1 + \psi_2$ is also a solution (linearity of the Schrödinger equation), whereas for classical systems two solutions cannot be added to give another solution due to the fact that the Hamilton-Jacobi equations are non-linear. The absence of macroscopic superpositions is also related to the measurement problem. Since in a measurement a quantum system gets entangled with a macroscopic measurement device, the final state for the system-measurement device is a linear superposition of states of the joint Hilbert space of the system and the measurement device. If one evolves this state under the Schrödinger equation this linear superposition is preserved. However after a measurement we see that the measurement device is in a single macroscopic state, producing the collapse of the wave function (under the measurement postulate). The determinism is broken and probabilities emerge: after the measurement the quantum system is in one or another state with certain probabilities given by the Born rule. Gravitational collapse models propose a stochastic non-linear modification of the Schrödinger equation to produce the collapse of the wave function for macroscopic enough systems due to gravitational effects. Examples of such models are the Diósi-Penrose model [52, 5, 53], which uses principles of general relativity to limit the lifetime of spatial quantum superpositions and, as a result, breaks the unitary evolution of the wavefunction. Other models include Adler's model [54], Károlyházy's model [55], and the Schrödinger-Newton equation [56, 57].

3. Finally, there are models of gravitational decoherence within a static spacetime such as the recent proposal of universal decoherence from time dilation [58] and decoherence in clocks due to the mass-energy equivalence [59]. Furthermore, there are models of *self* decoherence in fields in the context of inflation and the cosmic background [60, 61, 62, 63]. These models explore decoherence of different modes of fields with others of different wavelength.

So far we have discussed the interplay between quantum mechanics and general relativity. However the possibility that gravity remains classical at a fundamental level is considered viable or even necessary [55, 64, 65, 66, 52, 5, 67, 68, 16, 69], with a range of arguments invoked to support such a position: the absence of direct observations of

[5]Linear superposition has been seen in molecules as massive as $10^{-22}$ kg and on the other hand the absence of superposition (classical behaviour) holds for masses as low as $10^{-6}$ kg.

quantum gravitational phenomena [70], anticipated pernicious tensions between the foundational principles of quantum theory and general relativity [68, 16, 71] (see e.g. [72, 73] for different views), and lack of a complete framework for quantum gravity [74].

From an information-theoretic perspective, classicality of an interaction is defined as the inability of the resulting channel to increase entanglement. Thus, in order to verify whether gravity is a quantum or a classical entity it has been proposed to test its entangling capacity using a pair of masses in two close-by interferometers [75, 76, 77]. However, note that this is still a source of debate among the community. Anastopoulos and Hu [78] pointed out that such experiments might only be able to test the interplay between quantum mechanics and gravity and will not yield evidence of the existence (or not) of quantum gravity.

Since a unitary interaction in general does increase entanglement, an interaction with a known unitary part must be accompanied by decoherence in order for the resulting channel to be entanglement non-increasing – a model-independent result shows that this decoherence must be at least twice the interaction strength [79] (see [80, 81] for a broader context of effective dynamics in a classical stochastic environment).

The presence of the unitary Newtonian term in the Schrödinger equation is experimentally well established [82, 83, 1, 84, 85]. Therefore, for gravity to be a fundamentally classical channel the unitary Newtonian term must be accompanied by certain minimal decoherence – first shown in a series of works by Kafri, Taylor and Milburn [79, 8, 86]. The significance of this approach is that it provides a broad framework for understanding how to describe gravitational interactions in an information-theoretic manner, and their lower bound on decoherence distinguishes theories where low-energy particles can or cannot develop entanglement through the Newtonian interaction.

This model is at the core of this thesis and for this reason we provide a detail explanation of it in the next section.

## 1.3 A classical channel model for gravitational decoherence

All forces in the standard model are currently understood in terms of local quantum interactions and long range forces emerge as fluctuations of underlying gauge fields in the low energy limit, such as photons for the Coulomb force [87]. Interactions in quantum field theory are described by quantum gauge fields that act as *force carriers* and, as they admit a quantum description, they can carry quantum information. As we discussed above, gravity cannot be consistently understood in these terms as of now. Recently, a new approach [8]

suggested that gravity is fundamentally classical and therefore cannot carry quantum information [88]. This approach is motivated by the fact that gravity cannot be shielded and therefore any observer can in principle gain information about the quantum state sourcing gravity.

The process of gaining (partial) information about a quantum state is equivalent to making weak measurements [89], and is consistent with the standard approach for describing open quantum systems [90]. For example, a test particle in a quantum potential will become entangled with the source of the potential, and an observer who is not aware of the test particle (i.e. who traces over the test particle degrees of freedom) will necessarily see decoherence in the evolution of the source particle. This decoherence mechanism is present for any quantum potential (for example the Coulomb interaction), and is not limited to gravity. The distinction between the electric and gravitational potential is the ability to, in principle, shield this effect: a superconducting shell around a source charge eliminates the test-source interaction thereby shielding the decoherence; however there is no such shield for gravity. This form of decoherence, perfectly compatible with the unitary evolution of standard quantum mechanics, motivated consideration of a classical channel model for gravitational interactions proposed by Kafri, Taylor and Milburn [8].

In the CCG model, the gravitational potential is assumed to be fundamentally classical even though it can be sourced by quantum states. This quantum-classical interaction induces unavoidable decoherence on the quantum systems [91, 92]. This form of decoherence is not a consequence of tracing over an entangled state (as in the case of quantum potentials) but is rather a modification of unitary evolution as a consequence of quantum-classical interactions. The key premise of this model is that Newtonian gravity is a fundamentally classical interaction that cannot increase entanglement between any two systems. This premise is applicable to any non-relativistic system, though the original proposal considered a pair of harmonic oscillators for testing that idea.

The CCG framework is an application of pairwise continuous measurement with feedback [80, 81] to gravitational interactions. It can also be obtained from a quantum collisional model, where the systems interact with a Markovian environment[6] in a suitably chosen parameter regime as we will discuss in ch. 2.

Before we dive into the specifics of the CCG model as originally discussed by [8], let's explore how decoherence appears from unitary evolution in quantum mechanics. We will use angle brackets $\langle\cdot\rangle$ to denote the expectation value of a quantum observable, and $\mathcal{E}(\cdot)$ to denote average over the classical noise. Consider two massive particles initially separated by a mean distance $d = \langle\hat{x}_1(0) - \hat{x}_2(0)\rangle$, interacting under a Newtonian gravitational

[6]The enviroment is *memoryless*, in the sense that it gets freshly updated after *each collision*.

potential. The potential can then be linearized about the mean separation

$$-\frac{Gm_1m_2}{|\hat{x}_1-\hat{x}_2|} \approx -\frac{Gm_1m_2}{d}\left(1-\frac{\delta\hat{x}_1-\delta\hat{x}_2}{d}+\frac{(\delta\hat{x}_1-\delta\hat{x}_2)^2}{d^2}\right), \tag{1.5}$$

where $\delta\hat{x}_i$ is the fluctuation about the mean separation of the $i^{\text{th}}$ particle and has zero mean. The cross term in the second order expansion is the first non-trivial quantum interaction between the two particles. Therefore, the lowest order Newtonian interaction is $H_I = K\hat{x}_1\hat{x}_2$[7] where $K = 2Gm_1m_2/d^3$, using the notation from ref. [8]. Note that in general the interaction Hamiltonian $H_I$ may result in entanglement between the separated particles. Working in the interaction picture and beginning with a separable, pure initial state $\hat{\rho}(0) = \hat{\rho}_1 \otimes \hat{\rho}_2$, the joint system will unitarily evolve into

$$\hat{\rho}(\delta t) = e^{-iH_I\delta t/\hbar}\hat{\rho}_1 \otimes \hat{\rho}_2 e^{-iH_I\delta t/\hbar}, \tag{1.6}$$

after a time $\delta t$. The time $\delta t$ is assumed to be short enough such that the linearization of $H_I$ is valid over the full duration. This is standard unitary evolution, and the joint system remains pure, $\text{Tr}[(\hat{\rho}(\delta t))^2] = \text{Tr}[(\hat{\rho}_1 \otimes \hat{\rho}_2)^2] = 1$. However, an observer who is unaware of particle two will see decoherence in the reduced state of particle one, $\hat{\rho}_1(\delta t) = \text{Tr}_2[\hat{\rho}(\delta t)]$. In particular, note that even though the global evolution is non-dissipative, the observer sees decoherence in the description of their local quantum state. The decoherence is thus a consequence of thinking about the reduced evolution from the point of view of the observer, and therefore necessarily requires the presence of an observer to make sense[8].

In contrast, the key idea of the CCG model is to understand the interaction in terms of a local operation and classical communication (LOCC) protocol — e.g. a measurement and feedback process. Such a protocol is only able to exchange classical information, and is consistent with the notion that gravity may be mediated by a fundamentally classical force carrier. The LOCC protocol is modelled in the language of quantum measurement and control. The position of each mass is continuously measured, and the measurement result is used to apply a feedback on the other mass. For example, the first mass is weakly measured with measurement result $\bar{x}_1$, where the bar denotes a classical measurement value. This classical measurement result is then sent to the second mass and used to apply a conditional feedback unitary $U_{fb} = \exp[-idtK\bar{x}_1x_2/\hbar]$. The feedback Hamiltonian is chosen so as to generate an $x_1x_2$-like coupling term. However the presence of the classical

[7] Note that although this Hamiltonian is unbounded from below, reaching this regime will imply breaking the assumptions of small separations.

[8] We will further discuss this point in ch. 6, but for now we encourage the reader to refer to fig. 5.1 (top-left) for a cartoon explanation.

estimate $\bar{x}_1$ in $U_{fb}$ means there is no quantum coherence in the coupling. This process is then symmetrized by measuring the second mass and applying feedback to mass one. We emphasize that the non-unitary dynamics in CCG is fundamental and *independent* of the existence of any observer.

In the Newtonian CCG the interaction Hamiltonian is replaced by a feedback control Hamiltonian

$$H_I = K\hat{x}_1\hat{x}_2 \to H_{fb} = K\bar{x}_1\hat{x}_2 + K\bar{x}_2\hat{x}_1\,, \tag{1.7}$$

where $\bar{x}_i$ is the classical measurement outcome of a weak continuous measurement of $\hat{x}_i$. The measurement itself alters the unitary dynamics of the joint density matrix ($\hat{\rho}$) to the stochastic master equation,

$$\begin{aligned} d\hat{\rho}_c &= -\frac{idt}{\hbar}[H,\hat{\rho}] - \frac{\Gamma_1 dt}{2\hbar}[\hat{x}_2,[\hat{x}_1,\hat{\rho}]] - \frac{\Gamma_2 dt}{2\hbar}[\hat{x}_2,[\hat{x}_2,\hat{\rho}]] \\ &\quad + \sqrt{\frac{\Gamma_1}{\hbar}}dW_1\mathcal{H}[\hat{x}_1]\hat{\rho}_c + \sqrt{\frac{\Gamma_2}{\hbar}}dW_2\mathcal{H}[\hat{x}_2]\hat{\rho}_c\,, \end{aligned} \tag{1.8}$$

where $dW_i$ is a standard Wiener increment with $\mathcal{E}(dW_i) = 0$, $\mathcal{E}(dW_i dW_j) = dt\delta_{ij}$, and $\mathcal{H}[\hat{A}]\hat{\rho} = \hat{A}\hat{\rho} + \hat{\rho}\hat{A} - 2\langle\hat{A}\rangle$ for any operator $\hat{A}$. The joint state of the system is conditioned (subscript $c$) on the knowledge of the measurement outcome

$$\bar{x}_i = \langle\hat{x}_i\rangle_c + \sqrt{\hbar/2\Gamma_i}\,dW_i/dt\,, \tag{1.9}$$

and $\Gamma_i$ describes the strength of the measurement. While the derivative $dW/dt$ is not formally defined, it can be understood as a white noise process: $dW/dt = \xi(t)$ where $\mathcal{E}[\xi(t)\xi(t')] = \delta(t-t')$. This modification from unitary dynamics is from the postulate that gravity is mediated by a classical information channel and has nothing to do with the existence of an observer describing a reduced quantum state. After the instantaneous weak measurement is made, the joint system evolves under a unitary generated by the feedback Hamiltonian (1.7), $U_{fb} = \exp(-idtH_{fb}/\hbar)$, i.e.

$$\hat{\rho}(t+dt)_c = U_{fb}[\hat{\rho}(t) + d\hat{\rho}_c]U_{fb}^\dagger\,. \tag{1.10}$$

The unconditional master equation (average over all possible measurement outcomes – equivalent to an observer making an ensemble average of all possible measurement outcomes, or simply being unaware that the measurement happened) is given by

$$\frac{d\hat{\rho}}{dt} = -\frac{i}{\hbar}[\hat{H}_0 + \hat{H}_I,\rho] - \sum_i^2 \frac{\Gamma_i}{2\hbar}[\hat{x}_i,[\hat{x}_i,\rho]] - \frac{K^2}{8\hbar\Gamma_1}[\hat{x}_2,[\hat{x}_2,\rho]] - \frac{K^2}{8\hbar\Gamma_2}[\hat{x}_1,[\hat{x}_1,\rho]]\,. \tag{1.11}$$

In the particular case where $\Gamma_1 = \Gamma_2 = \Gamma$ we recover

$$\frac{d\hat{\rho}}{dt} = -\frac{i}{\hbar}[\hat{H}_0 + \hat{H}_I, \rho] - \left(\frac{\Gamma}{2\hbar} + \frac{K^2}{8\hbar\Gamma}\right)\sum_i^2 [\hat{x}_i, [\hat{x}_i, \rho]]\,. \tag{1.12}$$

Note that the feedback introduces an extra decoherence term but also *simulates* the gravitational interaction.

As we mentioned before, the previous result can be (most easily) obtained from a collisional model where a pair of particles interact with a set of ancillae (environment)[9]. The assumptions are: a) particles interact with the ancillae but not with each other; b) the interactions are local and any information transmitted through the ancillae is classical; c) the unitary part of the channel reduces to the standard Newtonian pair-potential at low energies. The ancillae can here be regarded as gravitational degrees of freedom and they facilitate measurement-and-feedback scenario, equivalent to averaging over definite but unknown measurement outcomes and correspondingly applied local feedback. The framework thus defines a Local Operations and Classical Communication (LOCC) channel [93] between the pair of masses.

A collisional model with a time-scale $\tau$ describes evolution of the state as $\rho_s(t+\tau) = \mathrm{Tr}_{\mathcal{A}}\{\hat{U}(\tau)(\rho_s \otimes \rho_a)\hat{U}^\dagger(\tau)\}$, where $\rho_s$ and $\rho_a$ are the density matrices of the system and the environment (ancillae), respectively, and $\hat{U}(\tau)$ describes their joint unitary evolution; the trace is over the ancillae.

The original CCG model, as defined in ref. [8], considers a quasi one-dimensional setting of two essentially point-like massive particles. At each step of the collisional dynamics the massive particles interact with ancillae $a_1, a_2$ via two interaction terms: the "measurement" interaction: $\hat{x}_1 \otimes \hat{p}_{a_1} + \hat{x}_2 \otimes \hat{p}_{a_2}$ (where ancillae obtain information about the positions of the particles) and the "feedback" interaction $K\hat{x}_1 \otimes \hat{x}_{a_2} + K\hat{x}_2 \otimes \hat{x}_{a_1}$ (where ancillae induce a force on the particles depending on the information about the position of the other mass, acquired in the "measurement" step). Here $\hat{x}_i$, $i = 1, 2$ are the position operators of the $i^{th}$ mass, and $\hat{x}_{a_j}, \hat{p}_{a_j}$, $j = 1, 2$ are position and momentum operators of the $j^{th}$ ancilla. For the state of ancillae giving rise to finite effective dynamics (e.g Gaussian states with width $\sigma$) and in the continuous-interaction limit of $\tau \to 0$ the following master equation results [94, 80, 81]:

$$\dot{\rho}_s = -\frac{i}{\hbar}[\hat{H}_0 + K\hat{x}_1\hat{x}_2, \rho_s] - \left(\frac{1}{4D} + \frac{K^2 D}{4\hbar^2}\right)\sum_{i=1,2}[\hat{x}_i, [\hat{x}_i, \rho_s]],$$

[9] Chapter 2 is all devoted to characterize interactions of this type – for a full derivation of the following result see app. A.3

where $D := \lim_{\tau\to 0,\sigma\to\infty} \tau\sigma$. This corresponds to a limit in which increasingly imprecise measurements of broad width $\sigma$ occur with increasing rapidity $\tau$ such that the product $\tau\sigma$ remains finite (as we will discuss further in ch. 2). Note that for the collisional model we have used $D$ instead of $\Gamma$; these two parameters are related by $D = \frac{\hbar}{2\Gamma}$ but they represent different physical quantities.

The effective unitary interaction $V_0 = K\hat{x}_1\hat{x}_2 +$ (local terms in $\hat{x}_1$, $\hat{x}_2$). For $K := 2\frac{Gm_1m_2}{d^3}$ this approximates the Newtonian potential between masses $m_1$, $m_2$ at a distance $d+x_1+x_2$; i.e. $V_0 \approx -G\frac{m_1m_2}{|d+x_1+x_2|}$ up to second order in $x_i$, $i = 1, 2$. It is accompanied by non-unitary terms, given by the double commutators, describing decoherence in the position basis: For each particle, the magnitude of its off-diagonal elements $x_i$, $x_i'$ decays at a rate $\Gamma_{\text{CCG}} = \left(\frac{1}{4D} + \frac{K^2D}{4\hbar^2}\right)\Delta x^2$, where $\Delta x = |x_i - x_i'|$ is the "superposition size" of the $i$-th particle. Importantly, $\Gamma_{\text{CCG}}$ has a non-vanishing lower bound $\propto \frac{K}{2\hbar}$, giving rise to the master equation

$$\dot{\rho}_s = -\frac{i}{\hbar}[\hat{H}_0 + K\hat{x}_1\hat{x}_2, \rho_s] - \frac{K}{2\hbar}\sum_{i=1,2}[\hat{x}_i, [\hat{x}_i, \rho_s]]\,. \tag{1.13}$$

The decoherence rate of each particle is thus fully characterised by the gradient of the Newtonian force between the masses, $\frac{K}{2} = \frac{Gm_1m_2}{d^3}$, and by the superposition size $\Delta x$:

$$\Gamma^{min}_{\text{CCG}} = \frac{K}{2\hbar}\Delta x^2. \tag{1.14}$$

The effective interaction is necessarily accompanied by decoherence of at least the same strength since LOCC channels are entanglement non-increasing [93] (see also ch. 2 for a discussion in this specific context). If the decoherence rate is smaller than $\Gamma^{min}_{\text{CCG}}$, the unitary term $V_0$ can increase entanglement between the particles [8] – this is independent of the specific model for the channel or the ancilla. Any dynamical theory of gravity giving rise to the same unitary term as in eq. (1.13) but with smaller decoherence can in principle generate entanglement and is therefore not fundamentally classical (not compatible with an LOCC channel).

## 1.4 Content and organization

The aim of this thesis is to explore different aspects of the Classical Channel model of gravity: its fundamental construction, comparison with experiments and experimental limitations and an extension to a cosmological setting. For this we have divided the work

in three parts. Part I (based on [95]) studies in detail the different emergent dynamics of a collisional model of repeated interactions between a system and a set of anicilae. We show that, contingent on the model parameters, the resulting dynamics ranges from exact unitarity to arbitrarily fast decoherence (quantum Zeno effect). For a series of measurements the effective dynamics includes feedback-control, which for a composite system yields effective interactions between the subsystems. We quantify the amount of decoherence accompanying such induced interactions, generalizing the lower bound of the gravitational example. However, by allowing multipartite measurements, we show that interactions can be induced with arbitrary low decoherence.

Part II explores two different set ups that can constrain or test CCG. Chapter 3 (based on [96]) studies the dynamics of clocks (modelled as two level systems) that are gravitationally coupled through the mass-energy equivalence in the CCG framework. We focus on the decoherence rates and temporal resolution of arrays of $N$ clocks showing how the minimum dephasing rate scales with $N$, and the spatial configuration. Furthermore, we consider the gravitational redshift between a clock and massive particle and show that a classical channel model of gravity predicts a finite dephasing rate from the non-local interaction. We obtain a fundamental limitation on time accuracy that is intrinsic to each clock and compare this with current experiments. On the other hand in Chapter 4 (based on [97]) we show that single-atom interference experiments achieving large spatial superpositions can rule out a specific realization of the CCG model. The experiments indicate that if gravity does reduce to the pairwise Newtonian interaction with single strength between atoms at the low energies, this interaction cannot arise from the exchange of just classical information, and in principle has the capacity to create entanglement. We clarify that, contrary to current belief, CCG differs from the model of Diosi and Penrose [52, 5, 68], which is not constrained by the same data.

Finally, in Part III we present an application of CCG for cosmology in the context of a quantized Friedman-Robertson-Walker (FRW) universe. In Chapter 6 (based on [98]) we describe the fundamental difference between our approach and other models and show that it results in decoherence in the FRW state that manifests itself as a dark energy fluid that fills the spacetime. An analysis of the resulting fluid shows that the equation of state asymptotically oscillates around the value $w = -1/3$, regardless of the spatial curvature, which provides the bound between accelerating and decelerating expanding FRW cosmologies. Motivated by quantum-classical interactions this model is yet another example of theories with violation of energy-momentum conservation whose signature could have significant consequences for the observable universe. In Chapter 7 (based on [99]) we extend our analyses to a universe with primordial matter showing that its effect is always *washed off* for late time evolution. Moreover, we discuss possible observational constraints for our

model and show that – in its current formulation – eludes any meaningful constraints for current observations.

Disclaimers:

1. We have included a discussion section in each chapter and outlook section at the end of this thesis.
2. We adopt slightly different notation in each chapter; this is on purpose to be consistent with similar results in the community. However, notation will be clear and well explained in each chapter.

# Part I

# Collisional model

# Chapter 2

# Unitarity, Feedback, Interactions – Dynamics Emergent from Repeated Measurements

## 2.1 Introduction

Modern measurement theory dispenses with the description of a measurement as a *projection* onto one of the complete set of orthogonal eigensubspaces of a Hermitian operator (an observable) with the results (the observable's eigenvalues) distributed according to a probability measure [100, 101]. Rather, the measurement is understood as an *operation*, whereby the system's final state is determined by an action of a *completely positive trace non-increasing map*, corresponding to a given result, and the outcomes are described by linear operators on the system, distributed according to a *positive-operator valued measure* (POVM) [102]. This generalized description of a measurement allows achievement of tasks that are impossible with projective measurements [93] and is in fact necessary in most practical situations, where measurements are made with inefficient detectors, additional noise, or provide limited information about the system [80, 81].

Of key importance is that the POVM approach unifies the theory of measurements with a general description of dynamics, the theory of open quantum systems [103]. It follows from Stinespring's dilation theorem [104] that any POVM operator can be constructed from a projective measurement on an enlarged Hilbert space: where the system of interest and an additional *ancilla* evolve under a joint unitary and then the ancilla is measured. In the context of measurement theory, the ancillae can be regarded as the measuring apparatus,

whereas in the theory of open systems they can model the system's environment. Engineering a particular measurement and engineering a particular dynamics for the system are thus two complementary aspects of the same conceptual framework. This correspondence is directly applied in quantum simulations [105], quantum control [80], quantum computation [106, 107] – in all scenarios where a particular Hamiltonian for the system is desired, or when an existing system-environment interaction needs to be suppressed [108].

Recently, a particular model was developed where repeated position measurements result in an effective long-range *interaction* between systems measured by common ancillae [79]. The interactions arise with dissipation of just the right magnitude to render the resulting dynamics classical – unable to increase entanglement. The picture of interactions as mediated by quantum systems, [109], is still missing for the gravitational case, despite a variety of efforts [74]. The above result is thus of high interest [8, 86, 67] for gravitational quantum physics. So far, an approximately Newtonian interaction was constructed from this model [8, 86], where decoherence does not only keep the resulting force classical, but is also claimed equivalent [67, 8, 34] to the Diosi-Penrose decoherence model [110, 52]. However, it is also well known that any local dynamics can be efficiently simulated by suitably chosen interactions with ancillae [93]. In particular, repeated interactions employed in the research described above correspond to a collisional model of an open system [111, 112, 113, 114], which can reproduce any Markovian dynamics [113, 114] (including recently revisited examples of effectively unitarity [115] as well as fully decoherent [116] evolutions). The questions thus arise: What are the assumptions necessary to obtain any particular type of dynamics from the continuous quantum measurement? Is it possible to induce the interactions but with less decoherence? Is it possible to generate an exact Newtonian, or even post-Newtonian, interaction from such a model?

Here we study what types of dynamics can in general emerge from a simple model of repeated measurement, where refs. [79, 8, 86, 67] are a particular example. We show that the interaction terms found in those studies, arise for a particular choice of the model parameters. We discuss the necessary conditions and highlight all relevant assumptions required for their emergence. Furthermore, we quantify the amount of decoherence arising with the effective interactions. We provide a very simple proof that for bipartite measurements dissipation accompanying effective interactions is indeed lower bounded, generalizing the observation made in the gravitational example. However, we also show how effective interactions can emerge with arbitrary low decoherence – if one allows for measurements realized through, admittedly less appealing, multipartite system-ancillae interactions.

While our results are motivated by position measurements in the gravitational sector, they also have applicability beyond these particular considerations. The very simple approach applied throughout this work shows which assumptions can be modified, and how,

in oder to obtain larger class of effective evolutions, for example, it provides a means to construct collisional models that would give Markovian master equations beyond the usual Born-Markov approximation and suggests how these can be used to recover exact Newtonian (or post-Newtonian) interaction terms from the repeated measurements. By deriving quantum filtering equations corresponding to all the different regimes of emergent dynamics our work can also provide new connections between the stochastic calculus and other approaches to open quantum systems. In this context we also note concurrent work [117] investigating emergent open dynamics of a quantum system undergoing rapid repeated unitary interactions with a sequence of ancillary systems. Our results, are commensurate with these, though the work of ref. [117] is concerned with understanding how thermalization, purification, and dephasing can emerge whereas our concern is with the continuum limit and the nature of the emergent interactions arising in such models.

The structure of this chapter is as follows: in Sec. 2.2 we revise a general model of a repeated interaction between a system and a set of independent ancillae. We show how – contingent on the relationship between the strength and duration of the interaction and the state of ancillae (moments of its probability distribution) – any type of system dynamics can emerge: from *exact* unitary evolution (related to "decoherence free subspaces" [118]), effectively unitary evolution under an "external potential" recently re-investigated in ref. [115] and decoherence, with the quantum Zeno effect (QZE) [119, 120, 116] in the extreme case. In Sec. 2.3 we generalise the model to a *sequence* of repeated interactions. In particular, we identify conditions under which coherent quantum feedback [121, 80, 81] arises. In Sec. 2.4 we consider *composite systems* under *sequences* of interactions. We identify conditions under which an effective interaction between two systems emerges and quantify the accompanying decoherence. For a particular choice of measurements we recover the emergence of a Newtonian gravitational interaction of ref. [8]. Finally, we discuss the applied method, results and outlook in Sec. 2.5, where we also discuss the connection to stochastic calculus.

## 2.2 Continuous Quantum Measurement

We consider a system $\mathcal{S}$ and a set of $n$ identically prepared ancillae $\mathcal{M}_r$, $r = 1, ..., n$. Initially, the system is uncorrelated with the ancillae, couples to the first one for a time $\tau$, decouples, then couples to the second one for time $\tau$, decouples, etc. This process repeats $n$ times, as illustrated in Figure 2.1. This is equivalent to a collisional model [111, 112, 113, 114] of an open system, modelling interaction with a Markovian environment which has relaxation time $\tau$. During an $r^{th}$ cycle the joint system $\mathcal{S} \otimes \mathcal{M}_r$ evolves under

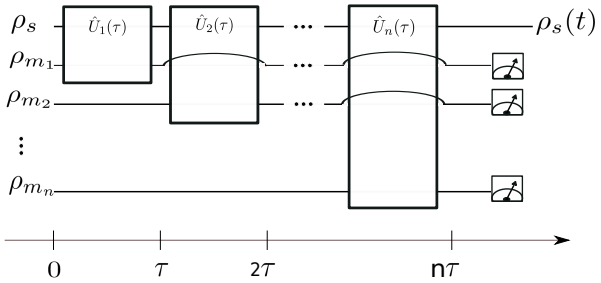


Figure 2.1: Quantum circuit illustrating time evolution of a system subject to repeated interaction with $n$ ancillae. $\rho_s$ is the initial state of the system and $\rho_{m_i}$, $i = 1, ..., n$ – of the $i^{th}$ ancillae. At each time step of duration $\tau$ the system interacts with one of the ancilla, the latter decouples and is discarded. Such a scenario is equivalent to a repeated measurement performed on the system by $n$ "meters". For identical $\rho_{m_i}$, the ancillae are also equivalent to a Markovian environment with relaxation time $\tau$. In the limit $\tau \to 0$ the scenario describes continuous quantum interaction/measurement, or a memoryless (collisional) model of the system's environment.

the Hamiltonian

$$\hat{\mathcal{H}}_{sm_r} = \hat{\mathcal{H}}_0 + g(t)\hat{\mathcal{H}}_I = \hat{S}_0 + \hat{M}_0 + g_r(t)\hat{S} \otimes \hat{M}\,, \tag{2.1}$$

where $\hat{S}_0$ acts on the system only, $\hat{M}_0$ – on the ancilla and we thus call $\hat{\mathcal{H}}_0 := \hat{S}_0 + \hat{M}_0$ the total free Hamiltonian, $\mathcal{H}_I := \hat{S} \otimes \hat{M}$ is the interaction Hamiltonian. The latter is identical at each cycle: the same operators $\hat{S}$ and $\hat{M}$ act on $\mathcal{S}$ and $\mathcal{M}_r$ for each $r$ and the interaction strength satisfies $g_r(t) = g_{r+1}(t + \tau)$, where $\mathrm{supp}(g_r) = (t_r, t_{r+1})$ and $t_{r+1} = t_r + \tau$. After the $r^{\mathrm{th}}$ interaction the joint state of the system and the respective ancilla reads

$$\rho_{sm_r}(t_{r+1}) = \hat{U}_r(\tau)\rho_{sm_r}(t_r)\hat{U}_r^\dagger(\tau)\,, \tag{2.2}$$

where

$$\hat{U}_r(\tau) = \mathcal{T}\mathrm{exp}\bigg( -\frac{i}{\hbar}\int_{t_r}^{t_r+\tau} \mathcal{H}_{sm_r}(t)dt \bigg)\,, \tag{2.3}$$

For each interaction we assume the same initial state of the ancilla and as a result the final state of the system is described by $n$ iterations of a superoperator $\mathcal{V}(\tau)[\rho_s] := \mathrm{Tr}_{\mathcal{M}}\{\hat{U}(\tau)(\hat{\rho}_s \otimes \hat{\rho}_m)\hat{U}^\dagger(\tau)\}$, where $\mathrm{Tr}_{\mathcal{M}}$ denotes the partial trace over the ancilla degrees of freedom, and $\rho_m$ is the initial state of the ancillae. We are interested in the dynamics of $\rho_s$ in the limit of a continuous interaction, given by

$$n \to \infty, \;\; \tau \to 0, \quad \text{such that} \lim_{n\to\infty,\tau\to 0} n\tau = T, \tag{2.4}$$

where $T$ is a fixed (and finite) time interval. Given the initial state of the system $\rho_s(0)$, the state at time $T$ is fully described by the map:

$$\rho_s(T) = \lim_{n\to\infty} \mathcal{V}^n\left(\frac{T}{n}\right)[\rho_s(0)]\,, \tag{2.5}$$

which is completely positive and trace preserving, but in general not unitary. The resulting dynamics in the continuous limit gives rise to a Markovian master equation, which we derive next.

If the interaction strength $g_r(t)$ is continuous and differentiable in the interval $(t_r, t_r+\tau)$, the mean value theorem allows to obtain

$$\int_{t_r}^{t_{r+1}} \hat{\mathcal{H}}_{sm}\, dt = (\hat{\mathcal{H}}_0 + \bar{g}\hat{\mathcal{H}}_I)\tau \tag{2.6}$$

where $\bar{g} = \frac{1}{\tau}\int_{t_r}^{t_r+\tau} g_r(t)\, dt$ and the Hamiltonian $\hat{\mathcal{H}} := \hat{\mathcal{H}}_0 + \bar{g}\hat{\mathcal{H}}_I$ is time independent. Under certain restrictions on the interaction strength $g_r(t)$, we can write the density matrix at a time $t_r$ as

$$\hat{\rho}_s(t_r) = \left(\hat{I} + \sum_{m=1}^{\infty} \mathcal{P}_m\right)[\hat{\rho}_s(t_{r-1})]\,, \tag{2.7}$$

where $\mathcal{P}_m$ is the super-operator consisting of $m$ commutators:

$$\mathcal{P}_m[\hat{\rho}_s(t_r)] = \frac{1}{m!}\left(-\frac{i\tau}{\hbar}\right)^m \langle[\hat{\mathcal{H}}, [\hat{\mathcal{H}}, [..., [\hat{\mathcal{H}}, \hat{\rho}_s(t_{r-1})]]]]\rangle_{\mathcal{M}_r} \tag{2.8}$$

where $\langle A\rangle_{\mathcal{M}_r}$ denotes the trace over the degrees of freedom of the r$^{\text{th}}$-ancilla. Note that eq. (2.7) holds in particular for symmetric in time switching functions, e.g. modelling constant in time interactions, and applies to typical scenarios involving photons, but also to toy models of gravitons in the recent gravitational decoherence models [8, 86, 67] – where we aim to apply results of this work. Using eq.(2.8) to expand (2.7) yields

$$\begin{aligned}
\rho_s(t_n) \;=\;& \rho_s(t_{n-1}) - \frac{i}{\hbar}\tau[\hat{S}_0 + \bar{g}\langle\hat{M}\rangle\hat{S}, \rho_s(t_{n-1})] + \frac{i\tau^2}{2\hbar^2}\bar{g}\langle i[\hat{M}, \hat{M}_0]\rangle[\hat{S}, \rho_s(t_{n-1})] + \\
-\;& \frac{\tau^2}{2\hbar^2}\Big([\hat{S}_0, [\hat{S}_0, \rho_s(t_{n-1})]] + \bar{g}\langle\hat{M}\rangle[\hat{S}, [\hat{S}_0, \rho_s(t_{n-1})]] + \bar{g}\langle\hat{M}\rangle[\hat{S}_0, [\hat{S}, \rho_s(t_{n-1})]]\Big) + \\
-\;& \frac{\tau^2}{2\hbar^2}\bar{g}^2\langle\hat{M}^2\rangle[\hat{S}, [\hat{S}, \rho_s(t_{n-1})]] + \cdots
\end{aligned} \tag{2.9}$$

where $\langle \hat{M}^k \rangle \equiv \mathrm{Tr}_{\mathcal{M}}\{\hat{M}^k \rho_m\}$ for $k \in \mathbb{N}$. Note that $i[\hat{M}, \hat{M}_0]$ is a Hermitian operator which can contribute to the effective unitary evolution of the system (see Sec. 2.2.3). The equations of motion for the system at time $T$ are finally obtained from

$$\dot{\rho}_s(T) = \lim_{\tau \to 0, n \to \infty} \frac{\rho_s(t_n) - \rho_s(t_{n-1})}{\tau}. \tag{2.10}$$

Equations (2.10) and (2.9) define a general quantum master equation that describes the effect of a repeated interactions with ancillae on the reduced state of the system. While such collisional models are well studied in the context of open quantum systems and decoherence (see e.g. refs. [113, 114]), the scope of the present work is to analyze the types of *unitary* contributions effectively arising in such models and to quantify their strength relative to the noise.

Equivalently, a repeated interaction of the form $\bar{g}\hat{S} \otimes \hat{M}$ describes a repeated measurement of the observable $\hat{S}$ on the system made by the ancillae. The ancillae play the role of "meters" (measuring apparatus) whose "pointer states" span a basis conjugate to the basis of the eigenstates of $\hat{M}$. The limit in eq. (2.4) corresponds to a continuous measurement made over time $T$. Note, that since we work with a collisional model, we shall not consider measurement channels that have no short-time expansion.

The types of dynamics arising from such a continuous measurement in general depend on the interaction strength $g(t)$, the relation between the free and the interaction terms in the total Hamiltonian eq. (2.1) and on the state of the ancillae. We shall discuss the different possibilities in the following section.

### 2.2.1 Exact unitary evolution

For an arbitrary initial state of the system the evolution under the Hamiltonian (2.1) is *exactly* unitary if and only if: $(i)$ the initial state of the ancilla is supported on a linear subspace $\mathcal{H}_M$ of eigenstates of $\hat{M}$ with a common eigenvalue and $(ii)$ the subspace $\mathcal{H}_M$ is invariant under $\hat{M}_0$. This is an analogous condition to the one derived in the context of decoherence free subspaces [118] or error correction [122], with the crucial difference that here we present conditions on the state of the ancillae, rather then the system. The proof is sketched in Appendix A.1.

The conditions above, and the proof, naturally extend to the most general case of a bipartite interaction $\sum_{i=1}^{L} g_i \hat{S}_i \otimes \hat{M}_i$. The evolution of the system is exactly unitary if the joint state of the system and ancilla is supported on a subspace where the total Hamiltonian can be written in block-diagonal form, where the system is in a joint eigenstate

of a subset of operators $\hat{S}_j$, with the corresponding eigenvalues $s_j$, and the ancilla is in an eigenstate of the operators $\hat{M}_k$ in the remaining interaction terms, with eigenvalues $m_k$. The interaction then effectively reads $\sum_j g_j s_j \hat{M}_j + \sum_k g_k m_k \hat{S}_k$. One also further requires that the free dynamics of the system and the ancilla preserve the above eigensubspaces. This generalizes the results discussed in [118] to an arbitrary interaction. The case of a general interaction, for a non-factorizable initial state, has also been studied in [123].

From the viewpoint of the measurement interpretation of interactions such a scenario is somewhat unusual, since the allowed states of the system are constrained to a specific subspace (with the exception of a single interaction term, when only the state of the ancilla is constrained). The measurement interpretation can still be applied in the sense that time evolution of the measurement apparatus (ancillae) depends on the state of the system – it is given by a Hamiltonian $\hat{h}_m \hat{M}_0 + \sum_j g_j s_j \hat{M}_j$. Analogously, the system evolves under the Hamiltonian $\hat{h}_s = \hat{S}_0 + \sum_k g_k m_k \hat{S}_k$. The system's evolution is therefore on the one hand "interaction-free" – exactly unitary – and on the other, it still depends on the state of another system, through the eigenvalues $m_k$.

### 2.2.2 Effective unitarity

Unitary evolution of a system interacting with some environment typically emerges only as an approximate description – when one assumes finite precision of any measurements made on the system to probe its dynamics. The quantitative condition for such an effective unitarity is that the terms $\propto \tau^k$ for $k \geq 2$ remain small compared to the first order ones, which is the case if

$$\lim_{\tau \to 0} \frac{\tau^k \bar{g}^k \langle \hat{M}^k \rangle}{\tau \bar{g} \langle \hat{M} \rangle} = 0 \,, \quad k = 2, 3, \cdots \tag{2.11}$$

These conditions are not automatically satisfied because the quantities $\langle \hat{M}^k \rangle$ are moments of an in principle arbitrary probability distribution over the eigenstates of $\hat{M}$ defined by the state of the ancilla[1]. If these conditions are met, from Eqs. (2.9), (2.10) the following master equation is obtained[2]

$$\dot{\rho}_s = -\frac{i}{\hbar}[\hat{S}_0 + \Xi \hat{S}, \rho_s], \tag{2.12}$$

[1]For finite-dimensional systems the number of independent moments is of course finite, as well as for continuous variable systems in e.g. a Gaussian state, which yields distribution with only two independent moments.

[2]Terms containing at least one $\hat{M}_0$ or $\hat{S}_0$ in eq. (2.9) automatically have the required limiting behaviour: the expressions $\propto \tau^k$ with $\bar{g}^{k'}$ for $k' < k$ are small compared to lower order ones, $\propto \tau^{k'} \bar{g}^{k'}$, in the limit $\tau \to 0$.

where we defined

$$\Xi := \lim_{\tau\to 0} \bar{g}\langle \hat{M}\rangle. \tag{2.13}$$

The system is effectively subject to an external potential $\Xi\hat{S}$ induced by the interactions and evolves approximately unitarily under an effective Hamiltonain $\hat{\mathcal{H}}_{eff} = \hat{S}_0 + \Xi\hat{S}$. The latter entails that in this regime the system-ancilla interaction is non-entangling.Similar results have been found in the context of classical control theory of quantum systems [124], where the system interacts with ancillae that are themselves an open quantum system. The effective Hamiltonian $\hat{\mathcal{H}}_{eff}$ and the Hamiltonian in the case of the exact unitary dynamics $\hat{h}_s$, Sec. 2.2.1, have the same general structure but the key difference is that $\hat{\mathcal{H}}_{eff}$ is valid only approximately, while $\hat{h}$ holds exactly but only for a particular state of ancillae.

From the viewpoint of the measurement interpretation, the regime of effective unitarity is tantamount to a limiting case of a weak measurement (or unsharp measurement [80]) – where the interaction between the system and the measuring apparatus is non-negligible only to lowest order. Decoherence induced by such a measurement is vanishingly small, but so is the information about the system that could be gained from the apparatus, since each of the ancillae only evolves by a global phase – as expected from general complementarity relations between information gain and state disturbance [125].

An effective unitary evolution is a generic feature of a weak interaction regime: for $\lim_{\tau\to 0} \tau\bar{g} = 0$ and a generic state of the ancilla – with fixed but arbitrary moments $\langle \hat{M}^k\rangle$ – the reduced state of the system evolves according to eq. (2.12). In this regime higher order corrections in $\tau\bar{g}$ can be made arbitrarily small by taking a suitably short time step $\tau$ (and therefore can be neglected provided that all subsequent measurements have finite resolution).

Importantly, effective unitarity can also emerge in the strong interaction regime – which we model by taking $\lim_{\tau\to 0} \tau\bar{g} = C$ with $C = 1$ for simplicity[3] – for specific states of the ancillae. The conditions in eq. (2.11) now reduce to $\lim_{\tau\to 0}\langle \hat{M}^k\rangle/\langle \hat{M}\rangle \to 0$, and we also need to ensure that $\Xi$ stays finite. An example of a suitable ancillae state is a Gaussian distribution over the eigenvalues of $\hat{M}$ with mean $\alpha\tau$ and variance $\beta\tau$, where $\alpha, \beta$ are fixed parameters. The effective potential arising from this example is $\alpha\hat{S}$.

### 2.2.3 Quantum Zeno effect

When at least one of the conditions in eq. (2.11) is not satisfied, the reduced dynamics of the system is not unitary. This can arise both in weak or strong interaction regimes,

[3]For any value of $\tau$ a function $g_r$ satisfying $\lim_{\tau\to 0} \tau\bar{g} = 1$ can be obtained from any suitably normalised family of functions that converge to a Dirac delta distribution.

depending on the state of the ancillae. We first focus on the regime of strong interactions, where non-unitarity will be shown to be a generic feature.

As in the section above, strong interaction regime is understood as $\lim_{\tau\to 0}\tau\bar{g}=1$. We consider a generic state of the ancillae, where the moments $\langle\hat{M}^k\rangle$ are in principle arbitrary but fixed, independent of $\tau$. The terms $\propto\tau^k\bar{g}^k$ in eq. (2.9) will then dominate over all others, and remain non-negligible in eq. (2.9) for arbitrary high $k$. Summing them all and denoting the magnitude of an arbitrary matrix element of the system (in the basis of $\hat{S}$) by $\rho_{ij}:=|\langle s_i|\rho|s_j\rangle|$, where $\hat{S}|s_i\rangle=s_i|s_i\rangle$, yields

$$\dot{\rho}_{ij}=\rho_{ij}\lim_{\tau\to 0}\frac{1}{\tau}\left(|\langle e^{-i\frac{\Delta s_{ij}\hat{M}}{\hbar}}\rangle|-1\right), \tag{2.14}$$

with $\Delta s_{ij}:=s_i-s_j$. The right hand side remains finite only in two cases: for diagonal elements of the system, $\rho_{ii}$, or for the ancilla in an exact eigenstate of $\hat{M}$. For a generic state of the ancilla the suppression of the off-diagonal elements of the system becomes "infinitely" fast. More precisely, $\langle e^{-i\frac{\Delta s_{ij}\hat{M}}{\hbar}}\rangle$ is a characteristic function of the probability distribution over the eigenvalues of $\hat{M}$ defined by the state of ancilla and moments of this distribution characterize the rate of decoherence. For a particular example of a Gaussian distribution $\langle e^{-i\frac{\Delta s\hat{M}}{\hbar}}\rangle=e^{-i\frac{\Delta s\langle\hat{M}\rangle}{\hbar}}e^{-\frac{\Delta s^2\sigma^2}{2\hbar^2}}$ where we set $\Delta s\equiv\Delta s_{ij}$ for simplicity, and where $\sigma=\sqrt{\langle\hat{M}^2\rangle-\langle\hat{M}\rangle^2}$ is the variance of $\hat{M}$, an exact solution to eq. (2.14) reads

$$\rho_{ij}(t)=\rho_{ij}(0)\lim_{\tau\to 0}e^{-\frac{t}{\tau}(1-e^{-\sigma^2\Delta s^2/2\hbar^2})} \tag{2.15}$$

for $i\neq j$. Approximating (2.15) yields

$$\rho_{ij}(t)\approx\rho_{ij}(0)\lim_{\tau\to 0}(1-\frac{\sigma^2\Delta s^2}{2\hbar^2}\frac{t}{\tau}) \tag{2.16}$$

to first non-vanishing order in $\sigma$. eq. (2.16) is a generic result at this order – valid for any state of ancilla when keeping up to second moments of its distribution.

In this regime, the interaction $\bar{g}\hat{S}\otimes\hat{M}$ is diagonalizing the system in the eigenbasis of $\hat{S}$ at an arbitrarily fast rate $\omega_D\approx\lim_{\tau\to 0}\frac{\sigma^2\Delta s^2}{2\hbar^2\tau}$. Unitary evolution, stemming from typically leading order term $\propto\langle\hat{M}\rangle[\hat{S},\rho]$, becomes irrelevant – it only acts non-trivially on the off-diagonal elements, but these are "instantaneously" suppressed. From the viewpoint of the measurement-interpretation, this "infinite" decoherence is simply the QZE effect: the measurements become repeated infinitely often ($\tau\to 0$) and projective (interaction strength diverges, $\bar{g}\propto 1/\tau$) and the system "freezes" in the measurement basis.

Finally, note the reduced dynamics of the system is non-unitary – is discontinuous – even for ancillae in an eigenstate of $\hat{M}$ (with a non-zero eigenvalue), since $\dot{\rho}$ is then divergent. If only finite-precision measurements can be made on the system, decoherence and the QZE will arise also in that a case. Superposition states of the system will accumulate a relative phase at a divergent rate $\propto \lim_{\tau\to 0}\langle M\rangle\Delta s/\tau$ and thus any coarse-graining will entirely suppress their coherence. Furthermore, assuming finite precision in the preparation of the ancilla (any non-vanishing variance) decoherence will always be non-negligible in the strong interaction case – and in this sense is a generic feature of the strong interaction regime.

QZE has been realized with continuous (as well as pulsed) measurements e.g. with Bose-Einstein condensates [126] and has been theoretically studied in a number of contexts, including freezing the evolution of a two-level Jaynes-Cummings atom interacting with a resonant cavity mode [127], controlling decoherence [128] producing effective hard-core repulsions in cold atomic gases [129, 130], preparing and stabilizing the Pfaffian state in rotating harmonic traps loaded with cold bosonic atoms [131], and inducing topological states of fermionic matter via suitably engineered dissipative dynamics [132].

### 2.2.4 Finite decoherence

We now consider conditions under which only terms up to second order remain relevant. The model of repeated measurements reduces then to the usual Born-Markov master equation [103]. In analogy to $\Xi$ defined in eq. (2.2.2) we introduce

$$\Gamma := \lim_{\tau\to 0}\tau\bar{g}^2\langle\hat{M}^2\rangle\,, \qquad \tilde{M} := \lim_{\tau\to 0}\frac{\bar{g}\langle i[\hat{M},\hat{M}_0]\rangle}{2\hbar}\,, \tag{2.17}$$

and assume that all higher order terms vanish in the considered limit. This is indeed the case e.g. (a) in a strong interaction regime ($\lim_{\tau\to 0}\tau\bar{g}=1$) for ancillae in a Gaussian state with mean $\Xi\tau$ and variance $\sigma=\sqrt{\Gamma\tau-(\Xi\tau)^2}$; (b) in a *weak* interaction regime (fixed $\bar{g}$) and ancillae in a Gaussian state with fixed $\langle\hat{M}\rangle$ and $\langle\hat{M}^2\rangle=\Gamma/\tau$. Importantly, both in (a) and (b) the quantities $\Xi$, $\Gamma$ remain finite in the limit $\tau\to 0$.

Eqs. (2.9), (2.10), (2.17) yield the following master equation

$$\dot{\rho}(t) = -\frac{i}{\hbar}[\hat{S}_0+(\Xi-\tilde{M})\hat{S},\rho]-\frac{\Gamma}{2\hbar^2}[\hat{S},[\hat{S},\rho]], \tag{2.18}$$

which features two different second order contributions: The term $\tilde{M}$ contributes to the unitary system dynamics, and simply adds to the effective potential already present in eq. (2.12), and a non-unitary term $-\frac{\Gamma}{2\hbar^2}[\hat{S},[\hat{S},\rho]]$, which results in decoherence at a finite

rate. For the example (a) above the off-diagonal elements of the system are suppressed according to

$$\rho_{ij}(t) \approx \rho_{ij}(0)(1 - \frac{\Gamma \Delta s^2}{2\hbar^2} \frac{t}{\tau}), \tag{2.19}$$

(neglecting $\hat{S}_0$ for simplicity) in agreement with eq. (2.16). Decoherence vanishes provided that $\Gamma = 0$ (implying $\Xi = 0$) i.e. for an exact eigenstate of $\hat{M}$ with the eigenvalue 0, in agreement with the condition found in the QZE case (since the mean in the present example vanishes faster than the variance, unless $\langle \hat{M}^2 \rangle \equiv 0$).

The regime where eq. (2.18) applies and finite decoherence is observed corresponds to the typical case of continous weak measurements: the interactions between the system and the measuring apparatus are finite but the contributions stemming from $\Gamma$ are considered non-negligible. In that context one often considers ancillae with trivial free evolution, $\tilde{M} = 0$. The ensuing system dynamics features finite decoherence, due to noise introduced by the measurements, but with no modifications to the unitary part.

As an exemplary application of the above, for a strong interaction and a particular choice of operators: $\hat{M}_0 = 0$, $\hat{M} = \hat{p}$ (momentum operator of the ancillae), $\hat{S} = \hat{x}$ (position operator of the system), and for a Gaussian state of the ancilla with $\langle \hat{M} \rangle = 0$ and $\langle \hat{M}^2 \rangle = \tau / D$, where $D$ is a fixed parameter, our eq. (2.18) reduces to a continuous position measurement derived in ref. [94].

## 2.3 Continuous measurement of multiple observables

Here we generalize our discussion to the case when several observables are repeatedly measured on the system. This situation can be accommodated by considering that each interaction in Sec. 2.2 is composed of $p$ sub-interactions, each of duration $\tau' = \tau / p$, as shown in Figure 2.2. The total Hamiltonian in the $r^{th}$ cycle, eq. (2.1), now generalizes to

$$\hat{\mathcal{H}}^{(p)}_{sm_r} = \hat{\mathcal{H}}_0 + \sum_{i=1}^{p} g_i(t) \hat{\mathcal{H}}^I_i = \hat{S}_0 + \hat{M}_0 + \sum_{i=1}^{p} g_i(t) \hat{S}_i \otimes \hat{M}_i. \tag{2.20}$$

The operators $\hat{S}_0, \hat{S}_i$, $i = 1, ..., p$ act only on $\mathcal{S}$, and $\hat{M}_0, \hat{M}_i$ act on the $r^{th}$ ancillae, $g_i(t)$ is the switching function, now supported in the $i^{th}$ sub-step (of length $\tau'$), continuous in the interval where applied. The density matrix of the joint system at time $t_{r+1}$ is given by

$$\rho_{sm}(t_{r+1}) = \prod_{i=p}^{1} \hat{U}_i(\tau') \rho_{sm}(t_r) \prod_{i=1}^{p} \hat{U}_i(\tau')^\dagger \,, \tag{2.21}$$

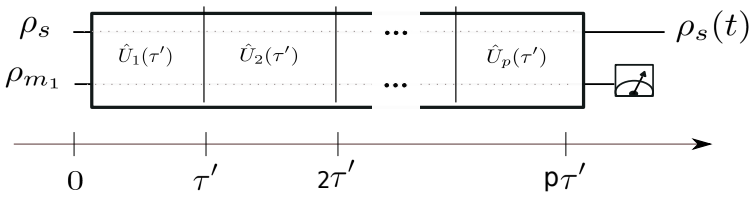


Figure 2.2: Quantum circuit illustrating time evolution of a system $\mathcal{S}$ during the first cycle of a repeated interaction with the ancillae. During each cycle, the system is subject to a sequence of $p$ different interactions with the same meter. All the subsequent cycles have the same structure.

where $U_i(\tau') = e^{-\frac{i}{\hbar}\int_{t_r}^{t_r+\tau'}(\hat{\mathcal{H}}_0+g_i(t)\hat{\mathcal{H}}_i^I)dt}$. We apply the mean value theorem, as in eq. (2.6), and define $\bar{g}_i = \frac{1}{\tau'}\int_0^{\tau'} g_i(t)dt$. Expanding eq. (2.21) in powers of $\tau$ at time $t_n$ and tracing over the ancillae degrees of freedom gives

$$\begin{aligned}\rho(t_n) &= \rho - \sum_{i=1}^{p}\Bigg\{\frac{i}{\hbar}\tau'[\hat{S}_0 + \bar{g}_i\langle\hat{M}_i\rangle\hat{S}_i,\rho] + \\ &- \frac{\tau'^2}{2\hbar^2}\sum_{j=1}^{i}(2-\delta_{ij})\Big[[\hat{S}_0,[\hat{S}_0,\rho]] + \bar{g}_j\langle\hat{M}_j\rangle[\hat{S}_0,[\hat{S}_j,\rho]] + \bar{g}_i\langle\hat{M}_i\rangle[\hat{S}_i,[\hat{S}_0,\rho]] + \bar{g}_i\langle[\hat{M}_i,\hat{M}_0]\rangle[\hat{S}_i,\rho] \\ &+ \frac{\bar{g}_i\bar{g}_j}{2}\Big(\langle[\hat{M}_i,\hat{M}_j]\rangle[\hat{S}_i,\hat{S}_j\rho+\rho\hat{S}_j] + \langle\{\hat{M}_i,\hat{M}_j\}\rangle[\hat{S}_i,[\hat{S}_j,\rho]]\Big)\Big]\Bigg\}\cdots,\end{aligned} \tag{2.22}$$

where $\{\hat{A},\hat{B}\} := \hat{A}\hat{B}+\hat{B}\hat{A}$ and $\rho \equiv \rho(t_{n-1})$. Equation (2.22) generalises eq. (2.9) to the series of $p$ repeated measurements. It introduces a new type of term

$$\langle[\hat{M}_i,\hat{M}_j]\rangle[\hat{S}_i,\hat{S}_j\rho+\rho\hat{S}_j], \tag{2.23}$$

which can contribute to the unitary part of the system dynamics. In particular, it can allow for feedback control of the system, discussed in Sec. 2.3.3.

### 2.3.1 Exact and effective unitarity

The conditions for exact unitary evolution of the system under arbitrary bipartite interaction with an ancilla were discussed in Sec. 2.2.1 and they thus apply also to the present case, where the different interactions are applied sequentially.

The conditions for effective unitarity eq. (2.11) directly generalize to the series of interactions. The resulting effective dynamics reads

$$\dot{\rho}(t) = -\frac{i}{\hbar}[\hat{S}_0 + \frac{1}{p}\sum_{i=1}^{p} \Xi_i \hat{S}_i, \rho(t)], \tag{2.24}$$

where

$$\Xi_i := \lim_{\tau' \to 0} \bar{g}_i \langle \hat{M}_i \rangle. \tag{2.25}$$

This is a straightforward generalization of eq. (2.12). The examples of interaction strengths and ancilla states discussed in Sec. 2.2.2 apply to the present case as well. Thus, for multiple measurement/interactions effective unitary dynamics are also a generic feature of a weak interaction regime, $\tau \bar{g}_i \to 0$ for $i = 1, ..., p$, but can also arise in the strong interaction regime for $\tau$-dependent preparation of the ancillae.

### 2.3.2 Generalized QZE

Here we consider the case when arbitrary high order terms contribute to the reduced dynamics of the system. Such situation arises in the regime of strong interactions, $\lim_{\tau \to 0} \tau' \bar{g}_i = 1$, $i = 1, 2$, for a generic state of the ancilla. For clarity, below we restrict to $p = 2$ repeated measurements.

In a full analogy to QZE disucssed in Sec. (2.2.3), the free evolution can be neglected compared to the interaction terms. Thus, time evolution of the matrix elements of the system reads

$$\dot{\rho}_{ij} = \lim_{\tau \to 0} \frac{1}{\tau} \left( |\mathrm{Tr}_m \{ \langle s_i | e^{-i\frac{\tau'}{\hbar}\bar{g}_2 \hat{\mathcal{H}}_2^I} e^{-i\frac{\tau'}{\hbar}\bar{g}_1 \hat{\mathcal{H}}_1^I} \rho_m \otimes \rho e^{i\frac{\tau'}{\hbar}\bar{g}_1 \hat{\mathcal{H}}_1^I} e^{i\frac{\tau'}{\hbar}\bar{g}_2 \hat{\mathcal{H}}_2^I} | s_j \rangle \}| - \rho_{ij} \right). \tag{2.26}$$

As an illustrative example one can consider a repeated measurement of the same operator on the system $\hat{S}_2 = \hat{S}_1 \equiv \hat{S}$ via two conjugate operators for the ancilla $[\hat{M}_2, \hat{M}_1] = i\hbar$. eq. (2.26) then reduces to

$$\dot{\rho}_{ij} = \rho_{ij} \lim_{\tau \to 0} \frac{1}{\tau} \left( |\langle e^{-i\frac{\Delta s_{ij} \hat{M}'}{\hbar}} \rangle| - 1 \right) \tag{2.27}$$

which is just (2.14) for $\hat{M}' := \tau' \bar{g}_1 \hat{M}_1 + \tau' \bar{g}_2 \hat{M}_2$. Another simple example is when conjugate observables are measured on the system (i.e. $[\hat{S}_2, \hat{S}_1] = i\hbar$) via the same ancilla operator $\hat{M}_1 = \hat{M}_2 \equiv \hat{M}$. eq. (2.26) then reads

$$\dot{\rho}_{i'j'} = \rho_{i'j'} \lim_{\tau \to 0} \frac{1}{\tau} \left( |\langle e^{-i\frac{\Delta s'_{ij} \hat{M}}{\hbar}} \rangle| - 1 \right), \tag{2.28}$$

where the off-diagonal elements are taken in the eigenbasis of $\hat{S}' := \tau'\bar{g}_1\hat{S}_1 + \tau'\bar{g}_2\hat{S}_2$, defining $\rho_{i'j'} := \langle s'_i | \rho | s'_j \rangle$ where $\hat{S}' | s'_i \rangle = s'_i | s'_i \rangle$ and $\Delta s'_{ij} = s'_i - s'_j$. In the most general case the decoherence basis is established from the full expression

$$e^{-i\frac{\tau'}{\hbar}\bar{g}_2\hat{\mathcal{H}}_2^I} e^{-i\frac{\tau'}{\hbar}\bar{g}_1\hat{\mathcal{H}}_1^I} = e^{-i\frac{\tau'}{\hbar}(\bar{g}_1\hat{\mathcal{H}}_1^I + \bar{g}_2\hat{\mathcal{H}}_2^I) - \frac{1}{2}\frac{\tau'^2}{\hbar^2}\bar{g}_1\bar{g}_2[\hat{\mathcal{H}}_2^I, \hat{\mathcal{H}}_1^I] + \cdots}.$$

Decoherence rates in this regime are again (cf. Sec. 2.2.3) formally divergent.

### 2.3.3 Feedback

Next we analyze conditions under which only up to second order terms contribute to the system dynamics. At the end of this section we discuss sufficient conditions for the emergence of feedback-control from the repeated measurement model.

To simplify the notation along with $\Xi_i$, eq. (2.25), we define

$$\Gamma_{ij} := \lim_{\tau' \to 0} \frac{1}{4}\tau'\bar{g}_i\bar{g}_j \langle \{\hat{M}_i, \hat{M}_j\} \rangle \qquad \tilde{M}_{ij} := \lim_{\tau' \to 0} \frac{1}{4\hbar}\tau'\bar{g}_i\bar{g}_j \langle i[\hat{M}_i, \hat{M}_j] \rangle \,. \tag{2.29}$$

From the Eqs. (2.10) and (2.22) (with $\tau = 2\tau'$) we obtain a general master equation for a system subject to two sequential measurements:

$$\begin{aligned} \dot{\rho}(t) &= -\frac{i}{\hbar}[\hat{S}_0 + (\frac{1}{2}\Xi_1 - \tilde{M}_{10})\hat{S}_1 + (\frac{1}{2}\Xi_2 - 3\tilde{M}_{20})\hat{S}_2, \rho] + \frac{i}{\hbar}\tilde{M}_{12}[\hat{S}_2, \hat{S}_1\rho + \rho\hat{S}_1] + \\ &- \frac{1}{2\hbar^2}\sum_{i=1,2}\Gamma_{ii}[\hat{S}_i, [\hat{S}_i\rho]] - \frac{1}{\hbar^2}\Gamma_{12}[\hat{S}_2, [\hat{S}_1, \rho]]), \end{aligned} \tag{2.30}$$

where in defining $\tilde{M}_{10}, \tilde{M}_{20}$ we introduced the convention $\bar{g}_0 \equiv 1$.

We now discuss how coherent feedback can result from the terms $\propto \tilde{M}_{12}$. Note that the first measurement $\hat{S}_i \otimes \hat{M}_i$ induces a translation of the state of the ancillae in the basis complementary to the eigenbasis of $\hat{M}_i$. The magnitude of this translation depends on the state of the system (on its $\hat{S}_i$-eigenvalue). The resulting state of the ancillae then determines the effective potential which arises for the system from the next interaction $\hat{S}_j \otimes \hat{M}_j$. Thus, for a suitable choice of the interactions and the state of the ancillae, an operation on the system is effectively performed that depends on its quantum state – that is coherent feedback [121, 80, 133, 81]. This makes clear why a necessary condition for feedback is $[\hat{M}_i, \hat{M}_j] \neq 0$. A sufficient condition is related with the question whether feedback is possible without introducing some decoherence. The answer is negative in the present model of ancillae. The reason is that the feedback term $\frac{i}{\hbar}\tilde{M}_{12}[\hat{S}_2, \hat{S}_1\rho + \rho\hat{S}_1]$ is

at *at most* of the same order as the decoherence terms $-\frac{1}{2\hbar^2}\sum_{i=1,2}\Gamma_{ii}[\hat{S}_i,[\hat{S}_i\rho]]$ – a direct consequence of the inequality

$$\langle(\bar{g}_1\hat{M}_1 - i\bar{g}_2\hat{M}_2)(\bar{g}_1\hat{M}_1 + i\bar{g}_2\hat{M}_2)\rangle \geq 0. \tag{2.31}$$

Therefore, independently of the weak or strong interaction regime, the state of ancillae or the repetition rate of the measurements, with the present model of ancillae-system interactions, feedback-control of the system cannot be realized without introducing dissipation lower bounded according to eq. (2.31). See also refs. [134, 135] for a comparison between coherent quantum feedback and the measurement-based feedback.

An example of a feedback-enabled control of a quantum system is a restoring force resulting from a quadratic potential $\propto \hat{S}_1^2$. It can be achieved by taking $\hat{S}_2 \propto \hat{S}_1$ in the model (2.30). More generally, feedback can take the form of a dissipative force, for $\hat{S}_2 \propto \hat{S}_1 + \beta\hat{O}$ for $[\hat{O},\hat{S}_1] \neq 0$. Taking canonically conjugate pair of ancillae operators $[\hat{M}_i,\hat{M}_j] \propto i\mathbb{I}$, results in feedback-control that is independent of the state of the ancillae.

Eq. (2.30) is valid when the quantities $\Xi_i$, $\Gamma_{ij}$, $\tilde{M}_{ij}$ remain finite in the limit $\tau' \to 0$, while contributions from higher moments vanish. A particular example of the ancillae state and operators that satisfy these conditions is a series of weak continuous position measurements first given in ref. [94], see also Appendix A.2. In this case, a harmonic potential arises as feedback and the accompanying decoherence keeps the momentum of the system finite. Experimental realization of feedback-control has been achieved with various systems, e.g. in cooling of optomechanical devices [136], trapped ions [137] or single atoms [138].

Finally, a tacit assumption was made in the above: that only measurements that are linear in the system operators can be realized by the ancillae. Relaxing this assumption would allow for noise-free feedback in the following sense: If an arbitrary measurement/interaction was allowed – of the form $\hat{V}\otimes\hat{M}$, for arbitrary $\hat{V}$ – one could induce an arbitrary potential term $\propto\langle\hat{M}\rangle\hat{V}$ already in the regime of *effective unitarity*, Sec. 2.3.1. For example, a quadratic potential arising due to weak measurement of the system position $\hat{x}$ in ref. [94] could be implemented unitarily if the ancillae would measure directly $\hat{x}^2$. We note, however, that many experimental schemes (including optical devices [139], mechanical oscillators [140], atomic ensembles [141]) indeed allow only for such linear measurements/interactions.

## 2.4 Measurement-induced dynamics for composite systems

Here consider the scenario from a previous section, but for a composite system. We allow that the different subsystems can have different interactions with the ancillae. In particular, we restrict our attention to a bipartite system subject to two continuously repeated interactions/measurements.

For a system comprising subsystems $s_1, s_2$ the operator describing the system operator describing $i^{th}$ interaction in eq. (2.20) most generally can be written as

$$\hat{S}_i = \sum_j c_j \hat{S}_{i,j}^{s_1} \otimes \hat{S}_{i,j}^{s_2} \,, \tag{2.32}$$

with real coefficients $c_j$, and where $\hat{S}_{i,j}^{s_{1(2)}}$ is an operator acting on subsystem $s_{1(2)}$. As in the previous section, we are looking for a continuous limit of a protocol whose one step of duration $\tau$ is composed of two sub-steps, each of length $\tau' = \tau/2$. Thus, the master equation for such a case can directly be obtained from eq. (2.22) for system operators given in eq. (2.32), and where the density matrix describes the state of both subsystems.

The discussions in Sec. 2.3 of the various regimes: unitarity (exact and approximate), QZE effect, finite decoherence, directly applies here. However, the physical meaning of terms describing the induced potential, feedback, and decoherence is different: Since the operators $\hat{S}_i$ connect different subsystems, in general they entail emergence of interactions between them. Moreover, decoherence basis will in general not be a product of the bases of the subsystems – they can decohere into correlated states. This follows from the discussion of decoherence basis in the QZE case of eq. (2.28) for system operators given by eq. (2.32).

Below we focus on a particular case when only bipartite interactions involving the ancillae are allowed – i.e. the ancillae only interact with one subsystem at a time. This assumption has been made in the gravitational case studied in refs. [8, 86, 67] – and is in fact crucial for the main results reported therein, as we will show at the end of this section. Under the above assumption the system operators describing the interactions take the form:

$$\hat{S}_1 = \hat{S}_1^{s_1} \otimes \hat{\mathcal{I}}^{s_2} \,, \quad \hat{S}_2 = \hat{\mathcal{I}}^{s_1} \otimes \hat{S}_2^{s_2} \,, \tag{2.33}$$

where $\hat{\mathcal{I}}^{s_i}$ is the identity operator on the Hilbert space of subsystem $s_i$. Recall that $\hat{S}_1$ acts in the first sub-step and $S_2$ in the second. For simplicity, below we take $\hat{M}_0 = 0$ (since $\hat{M}_0 \neq 0$ would give terms analogous to those discussed in Sec. 2.3.2). The total Hamiltonian acting during the entire $r^{th}$ interaction now reads

$$\hat{\mathcal{H}}^{(p)}_{s_1 s_2 m_r} = \hat{S}_0 + g_1(t) \hat{S}_1{}^{s_1} \otimes \hat{\mathcal{I}}^{s_2} \otimes \hat{M}_1 + g_2(t) \hat{\mathcal{I}}^{s_1} \otimes \hat{S}_2{}^{s_2} \otimes \hat{M}_2, \tag{2.34}$$

analogously to the case of a single system in eq. (2.20). Operators $\hat{M}_i$ act on the ancillae in the $i^{th}$ sub-step.

For the gravitational case it is natural to consider a symmetrized version of the above scenario: a second ancillae is added, which interacts with $s_2$ in the first sub-step and with $s_1$ in the second sub-step. However, since this only doubles the terms already resulting from eq. (2.34) we defer the presentation of the symmetric case to the appendix A.3. In general, we can visualize the resulting process through the circuit in Figure 2.3.

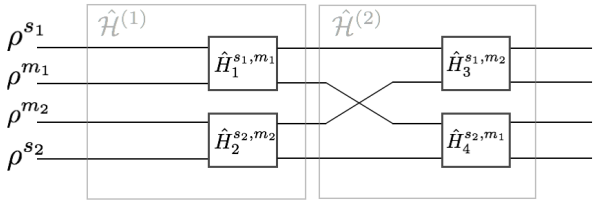


Figure 2.3: Composite system comprising subsystems $s_1, s_2$ prepared in the states $\rho^{s_1}, \rho^{s_2}$ interacting with ancillae $m_1, m_2$, initially in the states $\rho^{m_1}, \rho^{m_2}$. If each ancillae interacts with only one subsystem at a time, the resulting effective interaction between the subsystems is always accompanied by decoherence.

From the Hamiltonian in eq. (2.34), and with $\Xi_i, \Gamma_{ij}, \tilde{M}_{ij}$ defined in Eqs. (2.25),(2.29) we obtain the master equation for a composite system under two consecutive continuous measurements:

$$\begin{aligned}\dot{\rho}^{s_1,s_2}(T) &= -\frac{i}{\hbar}[\hat{S}_0 + \sum_{i=1,2}\frac{1}{2}\Xi_i\hat{S}_i^{s_i}, \rho^{s_1,s_2}] + \frac{i}{\hbar}\tilde{M}_{12}[\hat{S}_2^{s_2}, \hat{S}_1^{s_1}\rho^{s_1,s_2} + \rho^{s_1,s_2}\hat{S}_1^{s_1}] + \\ &- \frac{1}{2\hbar^2}\sum_{i=1,2}\Gamma_{ii}[\hat{S}_i^{s_1}, [\hat{S}_i^{s_i}\rho^{s_1,s_2}]] - \frac{1}{\hbar^2}\Gamma_{12}[\hat{S}_2^{s_2}, [\hat{S}_1^{s_1}, \rho^{s_1,s_2}]]),\end{aligned} \tag{2.35}$$

where $\rho^{s_1,s_2}$ is the joint state of $s_1, s_2$. Note, that this is a particular case of eq. (2.30) for the system operators defined in eq. (2.33).

We find in eq. (A.10) terms that are similar to those in eq. (2.30) for the single-system case. The terms $\propto \Xi_i$ describe effective potentials contributing to the unitary development which can arise with negligible decoherence, see Sec.2.3.1. The terms $\propto \Gamma_{ii}$ are decoherence terms for each subsystem. The term $\propto \Gamma_{12}$ in eq. (A.10), analogous to the corresponding term in eq. (2.30), expresses the fact that the decoherence basis in general is given by some combination of the operators acting on the system in the different sub-steps. Note,

however, that for to the operators in eq. (2.33), the resulting decoherence basis is still of a product form. The term $\propto \tilde{M}_{12}$, which more explicitly reads

$$\propto \bar{g}_1\bar{g}_2\langle[\hat{M}_2,\hat{M}_1]\rangle[\hat{S}_2^{s_2},\hat{S}_1^{s_1}\rho^{s_1,s_2}+\rho^{s_1,s_2}\hat{S}_1^{s_1}] \tag{2.36}$$

is analogous to the feedback term in eq. (2.23). However, the terms in eq. (2.36) connect two subsystems and they thus introduce effective *interactions* that can generate forces between them. The example of an approximately Newtonian interaction first derived in ref. [8] is presented in the Appendix A.3.

For the bipartite system-ancillae measurements, eq. (2.33), the effective interactions can only arise at the second (or higher) order. As a result, the interactions terms are not larger then the decoherence terms arising from the double commutators, in a full analogy to the case of feedback. The interactions are also lower-bounded by decoherence in the same way as feedback, as a consequence of the same inequality (2.31). In fact, these effective interactions can also be interpreted as feedback: the result of a measurement made by an ancillae on one system determines the strength of the effective potential acting on another system, which interacts with the same ancillae.

However, the conclusion about the necessary noise does not arise if one allows more general measurements. A particular example is that of measurements realized simultaneously on both subsystems, described by system operators in eq. (2.32). In such a case the potential terms in eq. (A.10) would read $\sim \Xi_i \sum_j c_j \hat{S}_{i,j}^{s_1}\otimes\hat{S}_{i,j}^{s_2}$ and could induce interactions even entangling the two systems. With such measurements the interaction terms could arise in the regime of *effective unitarity*, Sec. 2.3.1, and would thus differ from the feedback schemes where the conditional state exhibits entanglement or where non-unitary terms are present [80, 133, 142, 81, 143]. The above assumption regarding interactions, and its role, is fully analogous to the linearity assumption in the case of feedback discussed at the end of Sec. 2.3.3. Finally, we note that the above scheme differs from measurement-induced entanglement generation, where quantum correlations are created between systems interacting with a common environment by post-selecting on a particular state of the environment [144, 145, 146, 147]. (Here, the environment is assumed to be inaccessible and is always averaged over.)

## 2.5 Discussion

The very simple approach we have applied highlights several key aspects of the formalism. First, it stresses that a system subject to a repeated measurement/interaction with an ancilla can still evolve unitarily or be subject to decoherence depending on the state

of the ancilla, interaction strength and repetition rate (relaxation time of the environment). Second, in linear systems and under only bipartite system-ancillae interactions the emergence of feedback-control and of induced interactions, respectively, is accompanied by finite amount of decoherence, lower bounded by the magnitude of the induced unitary terms. However, decoherence can be made arbitrary low if more general interactions with the ancillae are permitted. For inducing interactions between different systems this would, however, require non-local (multipartite) interactions.

Our approach has implications for generating gravitational interactions and gravitational decoherence. It has recently been shown that decoherence terms first introduced ad-hoc in gravity-inspired models such as [110] could be derived from repeated interactions with the ancillae *together* with an approximately Newtonian interaction [8, 67]. The intriguing aspect of this relation is that those two approaches are aimed at enforcing distinct notions of classicality. In decoherence models the desired classical regime is that where large spatial superpositions of massive systems are suppressed. Whereas in recent works, the notion of classicality is applied to interactions [79], the classical regime being understood as eliminating the ability of interactions to generate entanglement. The approach of the present work can help clarifying to which extent these two notions of classicality have common consequences.

It would be quite remarkable if the *exact* Newtonian or post-Newtonian interaction could be reproduced from the repeated-measurements model. The resulting theory could be seen as a toy-model for quantum gravitational degrees of freedom – constructed not by quantizing their classical dynamics but by reconstructing the effective forces they generate. To this end, one would need to retain higher order terms than just first and second moments of the ancillae distribution (see appendix A.2). Our approach suggests a viable route in this direction: one can ask whether a physical state of the ancillae exists that will have higher order non-vanishing moments such that the resulting unitary corrections to the system dynamics would sum to the Newtonian potential[4]. As a further step one could extend the present approach beyond Markovian processes [148, 149] by incorporating, for example, initially correlated ancillae [150], interactions between the ancillae [151] or initially correlated system-ancillae states [152] – particularly desirable for modelling gravitational degrees of freedom. Finally, instead of constructing a classical channel from quantum degrees of freedom, one could ask if an entangling channel can arise from interactions with the ancillae in a scenario where the reduced state of the ancillae can nevertheless be described classically. The motivation here is that while the description of quantum states of matter

[4]For example, a skew Gaussian distributions have three independent moments. One can begin by asking what dynamics emerges if ancillae are prepared in such a skew-Gaussian state? Can one reconstruct a third-order approximation to the Newtonian potential within the measurement-based approach?

in a general, even curved, space-time is well understood [153], the problem lies in giving a consistent quantization of the latter.

If it is indeed possible to generate general-relativistic gravity as an effective interaction with ancillae, the resulting toy-model of quantum-gravitational degrees of freedom could shed new light on the pernicious problems associated with quantum gravity. The above questions and in particular the practical question of detection of the interaction-induced decoherence and its implications for precision tests of gravity remain interesting subjects for further study and we will discuss dome of this aspects in the following chapters.

## 2.6 Conclusion

Repeated interactions in the continuum limit are equivalent to the formalism of continuous weak measurements or collisional model of open systems. This property can be exploited to describe a broad range of phenomena, including QZE, feedback control of a system, emergence of effective potentials or of an effective interaction between two systems subject to a measurement by the same apparatus/interacting with the same environment. Also "interaction-free interactions" can emerge from such model – where evolution of a system is exactly unitary but where parameters of its Hamiltonian still depend on the quantum state of the ancillae with which it interacts.

The present approach provides a simple method for constructing collisional models of open systems beyond the Born-Markov approximation – by considering ancillae states with higher order contributing moments (as suggested above for recovery of the exact Newtonian interaction). To this end, the model considered here requires taking a probability distribution with the desired number of independent moments. The resulting more general effective interactions can be beneficial in devising novel protocols for quantum control or error-correction and in new toy-models of gravitational degrees of freedom.

# Part II

# Tests of CCG

In this part of the thesis we present two different studies related to the limits and testability of the CCG model. For this we consider the multiparticle extension of the original formulation of CCG [8]. We do this with two different set-ups: The first one (ch. 3) consider arrays of clocks interacting via the mass-energy equivalence and modelled this interaction in the CCG framework. We compare our dephasing rates with ones produce with other models and discuss the possible testability of this effect. The second one (ch. 4), posits that CCG fundamental mechanisms are applied to the 'fundamental' components of each particle interacting gravitationally. We compare our results with current experiments.

# Chapter 3

# Detecting gravitational decoherence with clocks: Limits on temporal resolution from a classical channel model of gravity

## 3.1 Introduction

The interplay between quantum mechanics and general relativity becomes fundamental when treating the nature of time operationally, specifically when considering how an observer measures time in GR and QM. Operationally, a clock is a reference and the notion of time emerges as a correlation between the clock and a system [154, 155]. Even with a fundamental flow of time, any observer limited to only measurements of quantum systems will not be able to access this fundamental flow [156] with zero uncertainty.

Recently, Castro *et.al.* [59] proposed a physically motivated quantum mechanism that produces fundamental uncertainty in measurements of coupled two level systems (clocks). The key idea in their model is that the mass-energy equivalence in quantum clocks leads to a Newtonian coupling between them. This interaction entangles the clock states, and therefore a measurement of any single clock necessarily decoheres distant clocks, limiting the temporal resolution of distant observers. In this case the decoherence is entirely a consequence of mass-energy equivalence with unitary quantum mechanics, similar to ref. [58]. In this chapter we take a different approach by treating the gravitational interaction between clocks in the context of CCG. In this context the unitary quantum interaction considered

in ref. [59] is replaced by the master equation derived in ref. [8], resulting in non-unitary dynamics for all particles that interact gravitationally. We will show that the key difference between the two proposals resides in the ability of the gravitational interaction to entangle the clocks: in ref. [59] the decoherence is a result of tracing out parts of an entangled state generated by standard unitary quantum mechanics, whereas in our model the decoherence is a consequence of the postulated quantum-classical interaction. Consequently, the limited temporal resolution is fundamental to each clock and we will discuss this in the context of operational time. There are several proposals to probe relativistic behaviour of quantum mechanics in the lab [58, 157, 158, 159], which focus on including standard principles of relativity within the framework of quantum mechanics. However, since CCG is fundamentally a modification of the equations of motion for quantum systems interacting gravitationally, we focus on potentially detectable deviations from standard quantum mechanics [160, 161] in a post-Newtonian regime – by allowing energy-mass equivalence.

This chapter is organized as follows. Firstly we show that the master equation derived in CCG results in a fundamental phase diffusion for spin $\frac{1}{2}$ systems, and the coherence time — inverse dephasing rate — is given by the gravitational interaction rate. We then extend the model to consider multiple spin $\frac{1}{2}$ systems, and characterize how the dephasing rate depends on the number of clocks, as well as their geometric arrangement comparing our results with current experiments. Finally we show that CCG implies a non-zero dephasing in spin $\frac{1}{2}$ clocks from earth's gravitational field. We conclude with a discussion of the implications of our model and its testability.

## 3.2 Coupled clocks

In the following we consider a clock with its spin processing around the z-axes of the Bloch sphere [162]. The free clock Hamiltonian is $H = \hbar\omega\sigma_z$ where $\omega$ is the clock frequency and $\sigma_z$ is the Pauli-$z$ matrix. From Einstein's mass-energy equivalence the clock has an effective mass $m = m_0 + H/c^2$ where $m_0$ is the rest mass of the clock and $c$ the speed of light. Note that this mass operator does not violate Bargmann's super selection rules [163, 164], and is in a similar spirit to Refs. [165, 166]. From the quantum correction to the mass, two clocks with rest masses $m_1$ and $m_2$, separated by a distance $d_{12}$ experience a Newtonian interaction

$$\begin{aligned} H_I &= -\frac{Gm_1m_2}{d_{12}} - \frac{G\hbar}{d_{12}c^2}\left(m_2\omega_1\sigma_z^{(1)} + m_1\omega_2\sigma_z^{(2)}\right) \\ &\quad -\frac{G\hbar^2\omega_1\omega_2}{d_{12}c^4}\sigma_z^{(1)}\sigma_z^{(2)}\,, \end{aligned} \tag{3.1}$$

that couples their internal energy states. The first term in eq. (3.1) is a constant potential, and the second term is the gravitational redshift on clock 1 (clock 2) from the rest mass of clock 2 (clock 1) which can be absorbed into the frequencies $\omega_{1,(2)}$ and therefore both terms are neglected. The last term is a coherent quantum interaction between the clocks that arises from the mass-energy equivalence. We now examine this non-local gravitational interaction as if it were mediated by a classical information channel. The natural measurement basis for the coupled clock system in CCG is the $\sigma_z$ basis and following the derivation in [8], we find the master equation that describes the interaction in eq. (3.1) in CCG is

$$\begin{aligned}\dot{\rho} &= -\frac{i}{\hbar}[H_0 + \hbar g_{12}\sigma_z^{(1)}\sigma_z^{(2)}, \rho] - \left(\frac{\Gamma_1}{2} + \frac{g_{12}^2}{8\Gamma_2}\right)[\sigma_z^{(1)}, [\sigma_z^{(1)}, \rho]] \\ &\quad - \left(\frac{\Gamma_2}{2} + \frac{g_{12}^2}{8\Gamma_1}\right)[\sigma_z^{(2)}, [\sigma_z^{(2)}, \rho]]\,, \end{aligned} \tag{3.2}$$

where $g_{12} = \frac{G\hbar\omega_1\omega_2}{d_{12}c^4}$ is the Newtonian interaction rate, $\Gamma_i$ is the measurement rate of the $i^{\text{th}}$ clock, and $\rho$ is the density matrix. The factor $g_{12}^2$ in the decoherence rate is due to the feedback from clock 1 onto clock 2 (and visa versa), and is required to get the correct magnitude of the $\sigma_z^{(1)}\sigma_z^{(2)}$ interaction. The double commutator term in eq. (3.2) prevents entanglement of the clocks thought the $\sigma_z - \sigma_z$ interaction and leads to phase diffusion in the $\sigma_z$ basis at a rate $2g_{12}$ [80]. This phase diffusion induces a fundamental limit on the time resolution of each clock that can not be avoided. Note that pure unitary evolution under the Hamiltonian in eq. (3.1) will also result in apparent dephasing if only a single clock is measured. Indeed this is exactly the type of decoherence considered in ref. [59].

For two clocks of equal frequency, where one would expect the measurement rates to be equal by symmetry, the dephasing rate is minimized when $\Gamma_1 = \Gamma_2 = g_{12}/2$; for petahertz clocks ($\omega_1 = \omega_2 = 2\pi \times 10^{15}$ Hz) as used in [167, 168] separated by 300 nm, the dephasing rate is $g_{12}/2 \approx 10^{-42}$ Hz. Such a small rate would require a clock with fractional uncertainty below $10^{-57}$ to observe, and therefore cannot be ruled out by current state of the art atomic and ion clocks which have achieved a fractional uncertainty of $10^{-18}$ [167, 169, 170].

## 3.3 Multiparticle interaction

We now extend the analysis to $N$ interacting clocks, and we investigate the enhancement of the dephasing rate due to the multiple (order $N^2 - N$) interactions. Before preceding we have to consider how information propagates in the classical channel model. There are two

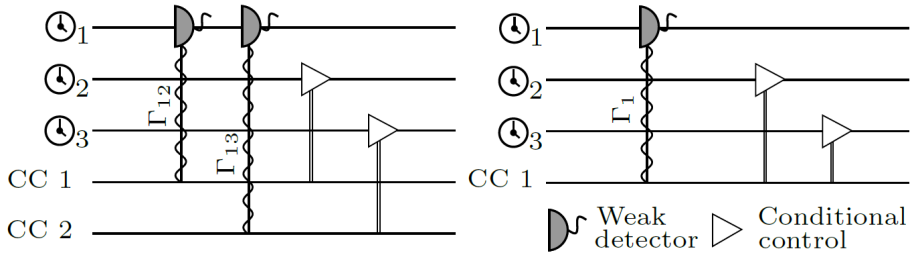


Figure 3.1: Different interpretations of the classical channel structure in CCG. We have shown only the measurements of a single clock for simplicity, but it is understood that each clock is treated equally. (left) A unique channel between each of the pairwise coupled quantum degrees of freedo. (right) A single channel used for each particle used for global feedback on all other particles.

possibilities of information propagation; pairwise measurement and feedback, fig.3.1(left), or single measurement with global feedback, fig.3.1(right). Note that both of these models are equivalent for $N = 2$ clocks and hence were not discussed in ref. [8]. The dissipative evolution of the master equation for the pairwise measurement and feedback is

$$\dot{\rho} \;=\; -\sum_i \sum_{j\neq i} \left( \frac{\Gamma_{ij}}{2} + \frac{g_{ij}^2}{8\Gamma_{ji}} \right) [\sigma_z^{(i)}, [\sigma_z^{(i)}, \rho]] \tag{3.3}$$

where $g_{ij} = g_{ji} = \frac{G\hbar\omega_i\omega_j}{d_{ij}c^4}$ is the interaction rate between clocks $i$ and $j$ and $\Gamma_{ij} > 0$ is the decoherence (dephasing) rate from the measurement of clock $i$ to generate the interaction between clocks $i$ and $j$. Note that $\Gamma_{ij}$ is related to the measurement strength, with $\Gamma_{ij} = 0$ corresponding to no measurement and $\Gamma_{ij} \to \infty$ corresponding to projective measurement of $\sigma_z$. For the moment each of the $\Gamma_{ij}$'s are still free parameters; later we show that there is a non-zero set of $\Gamma_{ij}$'s that minimize the decoherence, and thus the minimum decoherence rate has no free parameters. The decoherence terms in eq. (3.3) can be intuitively understood. Each clock is measured $N-1$ times, and each of these measurements are used to apply a independent feedback on the other $N-1$ clocks in the system. The measurements therefore contribute to a total dephasing rate of $\sum_{j\neq i} \Gamma_{ij}/2$ on the $i^{\text{th}}$ clock. The $\sum_{j\neq i} g_{ij}^2/8\Gamma_{ji}$ term for the $i^{\text{th}}$ clock is from the feedback of the $N-1$ noisy measurements form each of the other clocks in the system. Note that similar to the two clocks case, the presence of $g_{ij}^2$ in the feedback term is necessary in order to recover the correct magnitude of the systematic gravitational interaction.

In contrast to the pairwise measurement and feedback, the global feedback only requires a single measurement of the $i^{\text{th}}$ clock (single dephasing rate $\Gamma_i$), and the single measurement

| | SCENARIO | | SCALING |
|---|---|---|---|
| *A.i* | **Pairwise** | (1D) | $\log(N)$ |
| | $\mathcal{D}^{(i)}_{\rm pw} = \frac{G\hbar\omega^2}{2c^4}\sum_{j\neq i} d_{ij}^{-1}$ | (2D) | $\sqrt{N}$ |
| | | (3D) | $N^{2/3}$ |
| *A.ii* | **Global** | (1D) | $\sqrt{1-2/N}$ |
| | $\mathcal{D}^{(i)}_{\rm gl} = \frac{G\hbar\omega^2}{2c^4}\sqrt{\sum_{j\neq i} d_{ij}^{-2}}$ | (2D) | $\sqrt{\log(N)}$ |
| | | (3D) | $N^{1/6}$ |
| *B.i* | **Pairwise** | (1D) | $\sqrt{N}$ |
| | $\mathcal{G}^{(i)}_{\rm pw} = \frac{G\hbar\omega^2\sqrt{N-1}}{2c^4}\sqrt{\sum_{j\neq i} d_{ij}^{-2}}$ | (2D) | $\sqrt{N\log(N)}$ |
| | | (3D) | $N^{2/3}$ |

Table 3.1: MINIMUM DEPHASING RATES. The first column presents our results on minimization for the cases where $\Gamma_{ij}$ is pairwise defined (case $A$) and it is a fundamental constant (case $B$) as outlined in the Appendix. The second column shows the scaling with the number of clocks in the array for different dimensions, assuming $N \gg 1$ by using eq. (B.7). The coefficient of the scaling is $G\hbar\omega^2/(2L_c c^4)$, where $L_c$ is the characteristic separation between adjacent clocks in the lattice.

result is used to apply feedback on each of the other $N-1$ clocks. For global feedback, the dissipative evolution is given by

$$\dot{\rho} \;=\; -\sum_i \left(\frac{\Gamma_i}{2} + \sum_{j\neq i}\frac{g_{ij}^2}{8\Gamma_j}\right)[\sigma_z^{(i)},[\sigma_z^{(i)},\rho]]. \tag{3.4}$$

The dependence of $g_{ij}$ (which in turn depends on $d_{ij}$) in the dephasing rate of eq. (3.3) and eq. (3.4) means that the dephasing rate of the $i^{\rm th}$ clock depends on the spatial arrangement of the other $N-1$ clocks.

We consider $N \gg 1$ clocks in 1, 2 and 3D lattice configurations with a lattice constant $L_c$. In this case we can find the minimum dephasing rate on a single clock (see Appendix). Our results are presented in the second column of Table 3.1. Note that there are two

different scenarios we can consider for minimization. The first one (case $A$) is a pairwise minimization: the rate $\Gamma_{ij}$ depends only on the separation between the clocks $i$ and $j$, and the minimization is taken before including it in the general master equation. The second scenario (case $B$) minimizes the total noise in the master equation. One can estimate the scaling of these rates by assuming that $L_c$ is small compared to the macroscopic length scale, $R$, of the lattice, $L_c \ll R$. In this case, the summations in Table 3.1 are well approximated by an integral expression, eq. (B.7), for $N \gg 1$. Note that the integral approach only differs from the analytical sum by a factor of order one. We show how the dephasing rate depends on $N$ in the last column of Table 3.1. With the current experiments ($N = 10^6$, $L_c \approx 800$ nm [171]) we compute a dephasing rate of order $10^{-40}$Hz (similar for all arrangements). Note that in order to have a dephasing of the order of mHz, which can be detected in the lab, we need to have either a large number of clocks or small separation between them. For example, as considered in [59] taking $N = 10^{23}$, $L_c = 1$ fm, and a 10 GeV clock transition ($10^{26}$ Hz), results in a dephasing rate of order 1 Hz. Note however, the $\sim 1$ Hz dephasing rate here includes the spatial distribution of the clocks, whereas the the dephasing rate quoted in [59] assumed a 1 fm distance between each of the $10^{23}$ clocks. More realistically, we consider the Mössbauer effect in $^{109}$Ag [172] which has a transition frequency of $8 \times 10^5$ THz and a linewidth of 10 mHz, with adjacent atoms separated by $\approx 1$ Å. Using these parameters, CCG would predict a minimum $\gamma$-ray line width of 0.01 nHz per 100 g (1 mole) of $^{109m}$Ag, far below current experimental precision. To observe the linewidth at the order of mHz, would require $N \approx 10^{36}$ atoms, or $10^{12}$ kg of metallic silver.

## 3.4 Clocks in Earth's gravitational field

In the previous sections we were only concerned with energy-energy coupling between spatially separated clocks. However, the gravitational redshift is a relativistic effect that has been detected in quantum systems [169, 173], and therefore is a promising candidate to study the decoherence effects predicted by CCG. Again from the mass-energy equivalence, a trapped two level system with position operator $x$ will interact with any nearby object of mass $m$, and position operator $X$ via the Newtonian interaction

$$\begin{aligned} H_I &= -\hbar \frac{Gm\omega\sigma_z}{c^2|X-x|} \\ &\approx -\hbar \frac{Gm\omega}{c^2|d|}\sigma_z + \hbar \frac{Gm\omega}{c^2 d^2}\sigma_z(\delta X - \delta x) \end{aligned} \tag{3.5}$$

where $\delta x$ and $\delta X$ are deviations about the mean separation $d$ between the clock and the mass[1]. The first term is the mean redshift on the clock from the presence of the rest mass, and the second term is the lowest order Newtonian interaction between the quantum degrees of freedom. The $\sigma_z \delta x$ is a *local* interaction between the external and internal degrees of freedom of a single particle and therefore does not need to be mediated by a classical information channel. The $\sigma_z \delta X$ term however, is a non-local interaction and is replaced by an effective measurement and feedback process in CCG. In the following we consider the dephasing of a single clock from treating the nearby mass as both a composite and simple particle, where the simple particle case is just the $N = 1$ limit of the composite particle description. For the composite particle description, we treat each constituent atom as individual point particle contributing to the redshift. The dissipative part of the CCG evolution is

$$\begin{aligned} \dot{\rho}_{\text{diss}} &= -\sum_i \left( \frac{\Gamma_i}{2} + \frac{g_i^2}{8\Gamma_z} \right) [\delta X_i, [\delta X_i, \rho]] \\ &\quad - \left( \frac{\Gamma_z}{2} + \sum_i \frac{g_i^2}{8\Gamma_i} \right) [\sigma_z, [\sigma_z, \rho]] \end{aligned} \tag{3.6}$$

where $\Gamma_i$ is now the decoherence from the measurement of the position of the $i^{\text{th}}$ atom, $\Gamma_z$ is the decoherence due to measurement of the clock, and $g_i = \frac{G m_i \omega}{c^2 d_i^2}$ is the energy-position interaction between the clock and the $i^{\text{th}}$ atom of mass $m_i$ and has units of in Hz m$^{-1}$. Here we have assumed the single measurement-global feedback interpretation of the model - figure 3.1 (right) - which was shown previously to result in a lower bound for the minimum decoherence rate. The double commutator in position leads to momentum diffusion (heating) of each atom. This heating is not unique to CCG, and has been predicted in continuous spontaneous localization models [174, 175, 161] and stochastic extensions to the Schrodinger-Newton equation [176]. eq. (3.6) shows that CCG predicts a non-zero dephasing rate that accompanies the redshift, and a finite heating rate to nearby massive particles.

As $g_i$ scales as $1/d^2$, the dephasing due to the $g_i^2$ term in eq. (3.6) scales as $1/d^4$, meaning that only the closest particles to the clock significantly contribute to the dephasing rate. This is easily seen by considering a macroscopic homogenous body of $N$ atoms of equal mass $m_i = m$ (for example a single species atomic crystal) close to the clock. For such a macroscopic object, one would expect by symmetry the measurement rate of each atom to be identical, $\Gamma_i = \Gamma$. By considering gravitational interactions between neighboring atoms we use the result of ref. [8] and find $\Gamma = Gm^2/\hbar L_c^3$ where $L_c$ is now the characteristic

[1]Note that we have not included the $\delta X \delta x$ term considered by ref. [8]. This term is present but appears at sub-leading orders in this description.

separation between adjacent atoms (e.g. lattice constant for a crystal). In this case we can use eq. (B.7) to express the dephasing rate as an integral over the volume $V$ of the macroscopic object,

$$\frac{G\hbar L_c^3\omega^2}{8c^4}\sum_i \frac{1}{d_i^4} \approx \frac{G\hbar L_c^3\omega^2}{8c^4}\int_V \frac{dV}{L_c^3|r-r_0|^4} \tag{3.7}$$

where $r_0$ is the mean location of the clock, and we have used $\Gamma = Gm^2/\hbar L_c^3$. Note that the integral must converge as the point $r = r_0$ cannot be in $V$. This integral is non-trivial for a spherical body, nevertheless there is some intuition to be gained by considering a shell of mass centered around the clock even though there is no net redshift at the center of a mass shell. For a shell with inner radius $l$, outer radius $L$, the dephasing rate due to the redshift is given by

$$\mathcal{D} = \frac{\Gamma_z}{2} + \frac{\pi G\hbar\omega^2}{2c^4}(l^{-1} - L^{-1}). \tag{3.8}$$

Form this expression we see that it is only close-by masses in a thick ($L \gg l$) shell that significantly contribute to the dephasing rate. Thus in a laboratory experiment, the dephasing will be dominated by the immediate environment of the clock, even though all particles contribute to the systematic redshift.

Alternatively, the macroscopic particle could be treated as a single degree of freedom; the dephasing on the clock is then simply given by eq. (3.6) with a single term in the sum,

$$\mathcal{D} = \frac{\Gamma_z}{2} + \frac{G^2M^2\omega^2}{8c^4d^4\Gamma_i} \tag{3.9}$$

where $M = Nm$ is the total mass of the macroscopic object with a single measurement rate $\Gamma_i$. For $M$ the mass of the earth and $d$ as the mean separation between the earths and clocks center of mass, we can use atomic clock experiments [170, 167] to bound $\Gamma_i > 10$ Hz m$^{-2}$ and $\Gamma_z < 0.1$ mHz. These bounds are set as such experiments have not observed anomalous dephasing. From this result we conclude that any dephasing from a classical channel model of gravity would not be identifiable in any gravitational redshift measurements, and despite their precision, quantum clocks are not a desirable system to observe consequences of CCG.

## 3.5 Discussions

In this chapter we have studied the consequences of the CCG model when treating time operationally, that is by using two level systems as idealized clocks than an observer must

use in order to define the rate of external dynamics. Two such clocks will couple gravitationally and in the Newtonian limit this can be understood from mass-energy equivalence. In this context we derive the rate at which they will decohere under CCG, and show that the minimum rate is fixed by the post-Newtonian interaction. We have also extended this analysis to optical lattice clocks in one, two and three spatial dimensions, computing how the minimum dephasing rate scales as the number of independent two level systems in the lattice. Finally we have studied a clock coupled to the earth's gravitational field and analyzed in detail the position-spin interaction in the context of the CCG model. However, due to the asymmetry between the mass-clock system we were not able to meaningfully minimize the dephasing rate. Nevertheless, we showed that the gravitational redshift must be accompanied by some dephasing with the dominant contribution being due to close by atoms. Although the model considered in this work for clocks predict dephasing, the weakness of the gravitational interaction and the sub-linear scaling with the number of particles (Table 3.1) give a prediction thirty-seven orders of magnitude away from the current experiments. However, note that the dephasing rates computed in this work are the minimum and it is not clear that nature will saturate this bound. This shows that despite quantum clocks being the most precise measurement devices to date and therefore seem like a natural candidate to look for deviations of standard quantum mechanics, these are not the best devices to test the CCG model.

Let us emphasize that the dephasing present in our model is fundamental to each clock and cannot be avoided as it is a consequence of reproducing the Newtonian force using only classical information. In particular, the dephasing on one clock does not depend on the quantum state of the surrounding clocks, which is consistent with the clocks being in a separable state. Therefore, this decoherence is to be understood as a fundamental limit to temporal resolution for any clock and cannot be reduced by including measurements of other clocks. For unitary evolution of a system under the Newtonian potential, as considered in ref. [59], the decoherence appears as a result of entanglement of a single clock with a global system; if an observer has access to the full quantum system, there is no decoherence and therefore no limit to the temporal resolution. In contrast, each clock dephasing individually in CCG means that even access to the global quantum system is not enough to resolve time with zero uncertainty.

# Chapter 4

# Testing the Classical Channel model of Gravity

## 4.1 Introduction

In this chapter we show that the information-theoretic notion of classicality of gravity[1] is incompatible with the results of recent atom interference experiments [2, 7], heavily constraining the possibility that gravity acts as pairwise classical channels effectively inducing Newtonian force at low energies. While current experiments do not directly prove that gravity does entangle massive particles, they provide a strong argument for the physical relevance of gravity-mediated entanglement, and constrain the same model that would be tested in experiments proposed in refs [75, 76, 77]. Furthermore, we show that decoherence resulting from the CCG approach is conceptually and quantitatively different from decoherence in the Diosi-Penrose (DP) and related models [52, 5, 68, 51, 67], not refuted by the same experimental data.
While considering the CCG framework we are going to build a multiparticle extension in the pairwise sense we discussed in ch. 3. While for the noise minimization we decide to minimize decoherence rate[2].

[1] We remind the reader that the notion of classicality we refer to is that it can not generate entanglement – this is one of the 'features' of the CCG model.

[2] There are other options to proceed for the multiparticle extension and, on the other hand, noise minimization for the 2 particle case, but we postpone we discussion to the Outlook chapter 8. In this sense the aim of the chapter is not to show that the whole CCG framework is rule out, but rather a particular extension/noise minimization.

### 4.1.1 Composite systems

Having review the CCG model in chapter 1.3 we shall apply now the CCG approach to a pair of systems comprising an atom in an interferometer and the Earth. We first demonstrate that upon extending the CCG model to macroscopic systems the lower bound on decoherence (1.14) remains unchanged up to a factor related to the geometry of the bodies (see Appendix C.1).

Let $s_1$, $s_2$ be rigid bodies with total masses $M_1$, $M_2$, comprising $N_1$, $N_2$ elementary constituents, respectively, with masses $m_i$, $i = 1, ..., N_1 + N_2$. We take the minimum of the decoherence rates, as in eq. (1.14), for each pair, whose evolution is described by eq. (1.13). We consider $s_1$ to be a test mass, in a superposition of different radial distances from the body $s_2$ which describes all the remaining matter (Earth, $\sim$ 500 kg of tungsten [1], etc) and is thus considered initially well localised. The resulting dynamics of the centre-of-mass (CM) of $s_1$, in the radial direction, is described by

$$\dot{\rho}_{s_1} = -\frac{i}{\hbar}[\hat{H}_0 + V, \rho_{s_1}] - \mathcal{D}_{min}[\hat{r}_1, [\hat{r}_1, \rho_{s_1}]], \tag{4.1}$$

where $V \approx -G\frac{M_1 M_2}{|d+r_1+r_2|}$, with $r_k$ the displacement of the CM of $s_k$ and

$$\mathcal{D}_{min} := \frac{1}{2\hbar}\left(\sum_{i\neq j\in s_1} |K_{ij}| + \sum_{i\in s_1}\sum_{j\in s_2} |K_{ij}|\right), \tag{4.2}$$

where $K_{ij}$ is the Newtonian force gradient between the masses $m_i$, $m_j$ in three dimensions. The non-unitary term is simply the sum of pairwise contributions from all constituents of the bodies. The corresponding minimal decoherence rate reads

$$\tilde{\Gamma}^{min}_{\text{CCG}} = \mathcal{D}_{min}\Delta x^2. \tag{4.3}$$

The sum of the unitary contributions approximates Newtonian interactions between all constituents – which is the gravitational potential energy between two point masses $M_1, M_2$. However, the decoherence rate (4.2) in general differs from that for two elementary masses: first, it contains terms connecting constituents of $s_1$ (first sum), and $s_1$ with $s_2$ (second sum). Second, for non-convex bodies the rate (4.3) might be smaller than the rate given by the original model, eq. (1.14) applied to the CMs of $s_1, s_2$ (e.g. when $s_2$ is a spherical shell of matter with $s_1$ at the centre). For an elementary test mass $m$ near the surface of a homogeneous ball of mass $M$ and radius $R$, the CCG decoherence rate is at least as large as (see Appendix C.1)

$$\Gamma^{min}_{\text{CCG}} \geq \tilde{\Gamma}^{C}_{\text{CCG}} = C\frac{GMm}{\hbar R^3}\Delta x^2, \tag{4.4}$$

with $C \simeq 0.47$ for this particular geometry. For $C = 1$ the above reduces to the original CCG model applied directly to the CMs of the two systems.

Note that in general one cannot here approximate the mass distributions to be continuous, since contributions from the body's own constituents diverge and an explicit definition of the *fundamental* constituents is needed. We propose that these should be the smallest constituents between which the binding energy contribution to the total mass can be neglected (since the total mass of the system is here the sum of the masses of its constituents). We hereafter consider atoms as such fundamental constituents.

## 4.2 CCG vs Atomic Fountains

Atomic fountains send a cloud of atoms against the gravitational field of earth that subsequently free fall. By using a sequence of interferometers, both in the up and down trajectories, one can measure with good accuracy interference fringes that can be used to test gravitational effects.
We now confront our extension to the CCG proposal against two interferometric tests with atoms that use large momentum transfer (LMT) [2, 7] whitin atomic fountains. We treat the interfering atom as a test mass $s_1$ and Earth as the massive ball $s_2$ in eq. (4.4).

In LMT interferometers a sequence of $N$ $\frac{\pi}{2}$ laser pulses implements a beam splitter, preparing the atoms in a superposition of wave packets with momentum difference $2N\hbar k$ in the vertical direction, where $k$ is the laser wave-number. For time $T$ the wave packets propagate freely and thus spatially separate; then a sequence of $\pi$-pulses exchanges their momenta and at time $2T$ the wave packets interfere at a final beam splitter ($N$ $\frac{\pi}{2}$-pulses). For an atom of mass $m$ the vertical separation between the wave packets is $\Delta x(t) = 2N\hbar kt/m$ for $t < T$, it then symmetrically decreases until $t = 2T$. eq. (4.1) entails that the magnitude of the off-diagonal elements of the atom $V(t) := |\langle r_1 |\rho_{s_1}| r_2\rangle(t)|$ at the end of the interferometric sequence reads $V(2T) = |\langle r_1 |\rho_{s_1}| r_2\rangle(0)| e^{-\int_0^{2T} dt \mathcal{D}_{min} \Delta x^2(t)}$. Since $V(2T)$ describes the visibility of the interference pattern attainable in the experiment, the maximal visibility allowed by the classical channel framework for atom fountains on Earth is estimated as $e^{-2\int_0^T dt\, \tilde{\Gamma}^C_{\mathrm{CCG}}}$, which for the above $\Delta x(t)$ reads:

$$V^{max}_{CCG} = e^{-\frac{2}{3} C \frac{G\hbar M_\oplus}{m R^3_\oplus} (2Nk)^2 T^3}. \tag{4.5}$$

In fig. 4.1 we compare this prediction for $C = 1$ (the original CCG model), $C = 0.47$ (our multi particle correction), and $C = 0.1$ (arbitrary down-scaling of the decoherence rate) against measured visibilities [2] and [7] (noting at this point the controversy [177] regarding

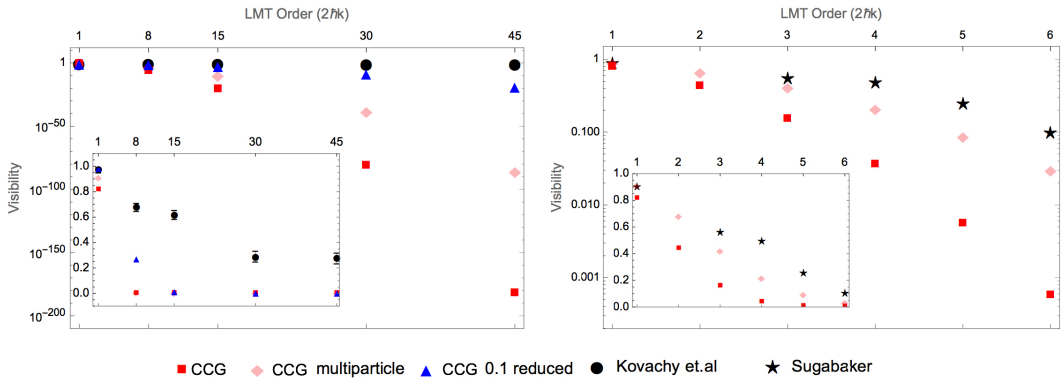


Figure 4.1: Logarithm of the interferometric visibility as a function of the superposition size (LMT order) reported in ref. [2] (black dots, left panel – including the reported error bars) and in ref. [7] (black stars, right panel) vs the prediction of the CCG model eq. (4.5) for $C = 1$ (red squares), its multi particle correction $C = 0.47$ (pink diamonds), reduced CCG correction $C = 0.1$ (blue triangles). (The insets represent the same data in a linear scale.) Both experiments used $^{87}$Rb; the reported superpositions were up to 8.2 cm in [7] and 54cm in [2]. Both experiments contravene the CCG model (including its multi-particle formulation).

ref. [2]). The values of the relevant parameters are $M_\oplus = 6 \cdot 10^{24}$ kg; $R_\oplus = 6 \cdot 10^3$ km, $\frac{\hbar k}{m} = 5.8\ \frac{\text{mm}}{\text{s}}$, $m = 1.4 \cdot 10^{-25}$ kg ($^{87}$Rb); $T = 1.15$ s in ref. [7] and $T = 1.04$ s in ref. [2].

Both the CCG model ($C = 1$)[3] and the multi particle correction ($C = 0.47$) predict maximal visibilities that are well below the measured ones. Taking into account finite duration of light-atom interactions would introduce a correction to the path separation. In the insets of fig. 4.1 we show that even if this resulted in a reduction of the decoherence rate to $C = 0.1$, the resulting visibilities would still be smaller than the measured ones by factors ranging from $\sim 2.5$ to $\sim 10^{18}$.

## 4.3 Comparison to the Diosi-Penrose model

The experiments refuting the classical-channel model of gravity do not constrain the DP model, see Table 4.1. The key difference is that in the DP model decoherence is quantified

[3]We shall emphasize a crucial difference between the original CCG proposal and our comparison: the two masses we use in our analysis have very different mass and it remains to construct a model which takes this into consideration (see ch. 8).

Table 4.1: Comparison of decoherence times $1/\Gamma_{\rm DP}$ and $1/\Gamma^{min}_{\rm CCG}$ predicted by DP and CCG models for matter-wave interference experiments [1, 2, 3, 4]. For all tests $1/\Gamma^{min}_{\rm CCG}$ contains the contribution from Earth $M_\oplus \sim 6\times10^{24}$ kg, $R_\oplus \sim 6\times10^{3}$ km, and for experiment [1] additionally from 24 bars of tungsten each with mass $\sim$ 21.5 kg, and 6 of each at approximate distances of 107.6 mm, 177.6 mm, 279.5 mm and 313.1 mm from the atoms. For $\Gamma_{\rm DP}$ we took $\delta = 10^{-15}$. Labels denote: $m$ – mass of the interfering particles; $M$ – "source" mass/masses; $d$ – distance between the source and the test mass (both relevant only for $\Gamma_{\rm CCG}$); $\Delta x$ – superposition size. For simplicity we treat all test masses as single particles.

| Experiment | m [Kg] | M [Kg] | $d$ [m] | $\Delta x$ [m] | $1/\Gamma_{\rm DP}$ [s] | $1/\Gamma^{min}_{\rm CCG}$ [s] |
|---|---|---|---|---|---|---|
| 10 m atomic fountain with $^{87}$Rb [2] | $1.4\times10^{-25}$ | $M_\oplus$ | $R_\oplus$ | 0.54 | $3\times10^{10}$ | $2\times10^{-3}$ |
| two atomic fountains with $^{87}$Rb [1] (operating as gravity-gradiometer) | $1.4\times10^{-25}$ | $M_\oplus$<br>$4\times129$ | $R_\oplus$<br>0.11,<br>0.18,<br>0.28,<br>0.31 | $1.86\times10^{-3}$ | $3\times10^{10}$ | $2\times10^{1}$ |
| large-molecule interferometry [3] | $1.6\times10^{-23}$ | $M_\oplus$ | $R_\oplus$ | $2.7\times10^{-7}$ | $3\times10^{6}$ | $6\times10^{7}$ |
| $PcH_2$ diffraction on alga skeleton [4] | $8.2\times10^{-25}$ | $M_\oplus$ | $R_\oplus$ | $2\times10^{-7}$ | $1\times10^{9}$ | $2\times10^{9}$ |

essentially by a "self-interaction" between the superposed amplitudes of a system: for a rigid body (and in particular for an elementary mass) $\Gamma_{DP} = \frac{1}{2\hbar}[U(XX)+U(YY)-2U(XY)]$, where $U(XY) = -G\int d^3r \int d^3r' \frac{f_X(r)f_Y(r')}{|r-r'|}$ is a gravitational energy between two mass-distributions $f_X, f_Y$ which are here associated with two superposed configurations $X, Y$ of *the same system* [5]. By contrast, in the CCG approach decoherence depends on the gravitational interaction between *different systems*. As a result, both frameworks predict decoherence in the position basis, whose magnitude is related to gravity, but differ both quantitatively (Table 4.1) and conceptually (Table 4.2) as follows:

For a point particle $\Gamma_{DP}$ diverges and requires a cut-off $\delta$ in the *coherent spread* of the particle's wave-function [5], whereas the CCG approach is well-defined for point particles.

A single elementary particle in an otherwise empty universe decoheres in the DP model, but does not decohere in the CCG approach: if other systems are removed far from the particle $\tilde{\Gamma}^{min}_{CCG} \to 0$, Table 4.2 row (i). This is an important feature since for a single particle in an otherwise empty universe the notion of "location" has no physical meaning. Thus, arguing that the particle is – or is not – in a superposition of "two different locations" has no physical meaning either – and the scenario cannot give rise to any physical effect.

Table 4.2: General form of the decoherence rates $\Gamma_{\rm DP}$ (Diosi-Penrose) and $\tilde{\Gamma}^{min}_{\rm CCG}$ (Kafri-Taylor-Milburn) (4.3) for spherical mass distributions [5, 6]. $\delta$ denotes the cut-off of the DP model, and $\Delta x$ is the superposition size. Case (iii) considers decoherence of the CM of a body comprising $N_1$ constituents of mass $m$ in the presence of another body comprising $N_2$ masses $m$. Whereas $\tilde{\Gamma}^{min}_{\rm CCG}$ depends on the gravitational force gradients between *different* particles, $\Gamma_{\rm DP}$ depends on the *self-interaction* between superposed amplitudes of the same particle.

| | **Scenario:** | $\Gamma_{\rm DP}$ | $\tilde{\Gamma}^{min}_{\rm CCG}$ |
|---|---|---|---|
| $(i)$ | **single particle**<br>mass $m$ | $\frac{Gm^2\Delta x^2}{2\delta^3\hbar}$ for $\delta \gg \Delta x$<br>$\frac{2Gm^2}{\delta\hbar}\left(\frac{6}{5}-\frac{\delta}{\Delta x}\right)$ for $\delta \ll \Delta x$ | 0 |
| $(ii)$ | **two particles**<br>masses $m, M$; distance $d$ | same as (i) | $\frac{GmM\Delta x^2}{d^3\hbar} = \begin{cases} 0, \ d\to\infty \\ \frac{mc^2}{\hbar}(\frac{\Delta x}{R_S})^2, \ d\to R_S := \frac{2GM}{c^2} \end{cases}$ |
| $(iii)$ | **two composite bodies;**<br>masses $N_1 m$, $N_2 m$; dist. $d_{ij}$ | $N_1\frac{Gm^2\Delta x^2}{2\delta^3\hbar}$; $\delta \gg \Delta x$<br>$N_1\frac{2Gm^2}{\delta\hbar}\left(\frac{6}{5}-\frac{\delta}{\Delta x}\right)$ for $\delta \ll \Delta x$ | $\frac{\Delta x^2}{2\hbar}\left(\sum_{i\neq j=1}^{N_1}\lvert K_{ij}\rvert + \sum_{i=1}^{N_1}\sum_{j=N_1+1}^{N_1+N_2}\lvert K_{ij}\rvert\right)$ |

CCG decoherence crucially depends on the distance $d$ between the test particle and other masses: For fixed $M$ and $\Delta x$: $0 < \Gamma^{min}_{\rm CCG} < \frac{mc^2}{\hbar}(\frac{\Delta x}{R_S})^2$ where the lower bound holds for $d \to \infty$ and the upper for $d = R_S = 2GM/c^2$ (the Schwarzschild radius of $M$), Table 4.2 row (ii). In contrast, $\Gamma_{DP}$ for a single particle is independent of its gravitational environment.

The CCG "self interaction" terms – first sum in eq. (4.2), Table 4.2 row (iii) – are purely classical: They connect *different constituents* of a composite system, not different points of a single system wave-function.

The CCG proposal predicts vanishing decoherence when all force gradients $K_{ij}$ are negligible, i.e. the sum of the homogeneous field contributions is induced without decoherence. It is thus compatible (to a limited extent) with the equivalence principle, as it does not predict any decoherence in the above case as well as for an accelerating particle.

## 4.4 Discussion

While we have shown that an LOCC gravity framework is strongly constrained by experiments, our result depends on auxiliary assumptions. One such assumption concerns the mass distribution of the earth; another is that all $N$ laser pulses comprising each $\pi$ and $\pi/2$ atom-light interaction are applied effectively simultaneously. This could open potential "loopholes" that call for additional experimental scrutiny of classical channel gravity. To improve on here presented analysis one could use an atom-fountain gravity-gradiometer (two interferometers with vertical separation $L$) and a large mass $M$ (in the plane of, say, the lower interferometer), whose horizontal distance $d_h$ to the atoms can be varied [1, 84, 85], cf. Table 4.1. A continuous mode of operation could be considered for improved sensitivity [178]. The CCG proposal predicts a different phase noise in the two interferometers as a function of $d_h$. With $M = 252$ kg and $0.25 < d_h < 0.5$ m, an experiment at LMT order $10\hbar k$ and $T = 0.5$ s would see the lower interferometer's contrast varying between 0.5—0.65, while the upper – between 0.62—0.64.

Thus far, tests of the CCG framework were suggested with optomechanical or torsion balance setups. However, even including Earth into the analysis, as in the present work, such tests would still face a formidable challenge. For an optomechanical experiment, in order to detect CCG decoherence on top of the thermal noise, the mechanical frequency $\Omega$, quality factor $Q$ and the temperature $T$ of the mechanical oscillator must satisfy $T\Omega/Q < G\hbar M_\oplus/2k_B R_\oplus^3 \sim 10^{-18}$ K/s, where $k_B$ is the Boltzmann constant; a state of the art setup [179] with $Q = 2 \times 10^7$, $\Omega/2\pi = 1$ Hz, $T = 4$ K yields $T\Omega/Q \sim 10^{-6}$ K/s. For the original CCG model to be discernible from measurement noise, the measurement frequency $\omega$ must satisfy $\omega^2 < GM_\oplus/R_\oplus^3 \sim 10^{-6}$ Hz$^2$, whereas the value considered in [179] (at the standard quantum limit) gives $\omega^2 \sim 10^6$ Hz$^2$. Current optomechanical sensitivities thus still need to be improved in order to test CCG assumptions. From a theoretical perspective, an immediate question is how much entanglement (what channel capacity) suffices to reproduce the experimental results. To address this question it would be desirable to first formulate a fully covariant, relativistic version of the classical channel gravity. In this context, we note that the experimental constraints on the CCG proposal mean that any "complete" dynamical theory that has Newtonian gravity as its low-energy limit cannot be fundamentally classical, as this would require its Newtonian limit to be classical as well, which contradicts experiments. Any relativistic version of the CCG framework would correspondingly need to allow for some entanglement to be transmitted, at least in the regime of small masses.

## 4.5 Conclusion

Results of the recent atom interference experiments strongly constrain the worldview in which gravity does reduce to the Newtonian pair potential at low energies *and* is also fundamentally classical: mediated by LOCC channels acting pairwise between atoms. We have further shown that – contrary to current belief – the CCG framework is not equivalent to the DP model. It is noteworthy that the same experiments do not constrain other alternative models (gravity-related or not) including DP, continuous spontaneous localisation, or Schrödinger-Newton theory [180, 181, 51]. This raises a question about the notion of classicality of gravity in these models and their information-theoretic aspects.

Indeed, our understanding of the classical vs quantum properties of gravity is far from clear [182] and needs further work. However, the fact that the CCG framework can be empirically tested opens a novel route of investigation, one that focuses on a robust information-theoretic characterization of channels implied by alternative approaches to quantizing (or not quantizing) gravity. From a broader perspective, our work demonstrates that general frameworks as well as specific models for gravitational decoherence previously thought to be out of reach can be experimentally tested.

Finally, we note that generalizations of classical channel gravity, resulting in an increased channel capacity, can be constructed e.g. by relaxing the assumption of local system-ancilla interactions or constraining the amount of energy introduced to the system by the ancilla 3. Empirically constraining such models and understanding their ramifications for the gravitationally induced entnaglement remains an interesting subject for further investigation.

# Part III

# CCG for cosmology

# Chapter 5

# Fundamentals of CCG for cosmology

So far we have studied dynamic emergent form collisional markovian models and the CCG model in the context of the Newtonian and post-Nextonian context. In this part we take the first steps towards a CCG model in the relativistic regime. The question we want to answer is how to apply the CCG model when one has quantum metric degrees of freedom, and what are its consequences. We do this by considering a gravitational system with the fewest number of degrees of freedom possible, namely a canonically quantized empty Friedmann Robertson Walker (FRW) universe in ch. 6 and add primordial dust in ch. 7.

In the Newtonian case, the trajectory of a test particle depends on the masses and configuration of the source, whereas in the GR description the dynamics are given solely by the metric components, i.e. the scale factor in an FRW spacetime. In CCG, the source necessarily experiences decoherence, and we will show that in the FRW context, CCG introduces decoherence of the spacetime. We will show that for an observer in such a universe this decoherence is manifested as a time dependent dark fluid.

The goal now is to describe in detail the relativistic description of CCG. We do this by comparing unitary Newtonian gravity with the Wheeler de Witt equation, and show how the CCG model fundamentally differs from unitary dynamics. In particular we explain how the presence of a test particle in the Newtonian model of CCG results in decoherence of any object that sources a (gravitational) potential for that test particle. We then argue analogously that in relativistic CCG the presence of a test particle in an FRW universe leads to decoherence in the scale factor, and therefore non-unitary evolution of the universe.

*Unitary Newtonian Interaction.* Consider a quantum Newtonian interaction between a source and a test particle (fig. 5.1 top left). Under unitary evolution the two (perhaps

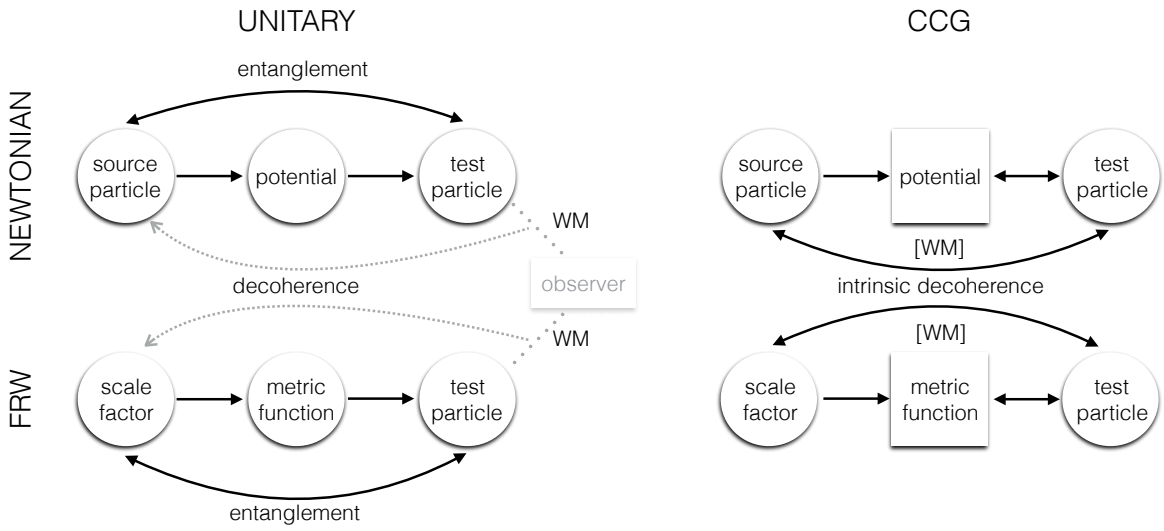


Figure 5.1: GRAVITATIONAL MODELS. Cartoon of the four models. We describe them by considering a source particle, a potential (top – Newtonian) or metric (bottom – cosmological) and a test particle reacting to the potential or metric. The circles represent quantum degrees of freedom whereas the squares represent classical degrees of freedom. For the unitary cases (left) the joint system source-potential (metric)-test particle evolve unitarily. In this case the source/test particle may become entangled and an observer making measurements on the test particle results in a weak measurement (WM) of the source, including the associated decohere. On the other hand, the CCG model (right) assumes that the only way a test particle can respond to the source is through classical information, which is mathematically equivalent to weak measurement and feedback control [8]. This process results in decoherence for the source and classical fluctuations on the potential (metric) and therefore is fundamentally a non-unitary evolution for either quantum systems.

distant) particles may become entangled, where such entanglement implicitly assumes a quantum "force carrier" (potential) — analogous to the photon in electrodynamics; i.e. if the source particle is in a quantum superposition, the test particle will feel a coherent superposition of potentials, and thus follow two trajectories in superposition. Any observer who makes a projective measurement of the position of the test particle is effectively making a weak measurement of the source particle, and this weak measurement induces decoherence of the source particle [89, 183]. This is an example of how two fundamental postulates of quantum mechanics (unitary evolution and the Born rule) lead to decoherence of a quantum state. In particular a projective measurement, i.e. an observer, is required for this type of decoherence and the fundamental evolution is unitary.

*Newtonian Classical Channel Gravity.* The CCG model postulates that there is no quantum description for gravity and that the non-local interactions emerge from local interactions between a quantum particle and a classical potential. In this case, the gravitational interaction between a source and a test particle is mediated by a classical (as opposed to quantum) information channel (fig. 5.1 top right). The question is now how a quantum particle can source a classical potential and how a test particle responds to it. In ref. [8] it was shown that such a classical information channel is equivalent to an agent performing weak measurements of the position of the source and using the measurement outcome to control a potential for the test particle. Consequently the test particle does not respond to a quantum potential generated by the source but rather to a classical estimate of this potential. In CCG the existence of a test particle responding to the potential necessarily results in decoherence and subsequent non-unitary evolution of the source, even in the absence of an observer making any measurements of the test particle. Finally, we mention that this model goes beyond the standard postulates of quantum mechanics.

The discussion so far has focused on the Newtonian description. Our goal is to understand how this same procedure can be carried out in a relativistic context. In the following we give a relativistic formulation of CCG in the cosmological context and compare it to the Wheeler-DeWitt equation.

*Wheeler-deWitt.* The Wheeler-DeWitt equation, $\hat{H}|\psi\rangle = 0$ where $\hat{H}$ is the Hamiltonian operator of the spacetime including any matter and $|\psi\rangle$ is the quantum state of the universe, is the standard approach to quantum cosmology. In general relativity the least action principle always forces the classical Hamiltonian to vanish, and the Wheeler-DeWitt equation is the quantum implementation of this constraint. We will restrict the following discussion to an empty FRW universe so the only spacetime observables are the scale factor $\hat{a}$ and its canonical conjugate momentum $\hat{\pi}$. If we now consider a quantum test particle moving in such a universe, we would expect the particle to become entangled with the state of the universe, exactly analogous to how a test particle becomes entangled with a source

particle in unitary quantum mechanics (fig. 5.1 bottom left). By test particle we mean a particle whose contribution to the mass/energy of spacetime can be neglected, but is (in principle) able to become entangled with the spacetime state. In this context, we can view the scale factor as acting like a source that influences the dynamics of a test particle via the metric. Analogous to the unitary Newtonian case, in this scenario the presence of an observer making a measurement on the test particle is needed in order to get decoherence in the quantum state of the universe, but othwerwise the evolution is entirely unitary. In the following we will use the analogy: source $\rightarrow$ scale factor and potential $\rightarrow$ metric to explain the main idea of this paper: the relativistic version of CCG.

*Relativistic Classical Channel Gravity.* So far we have shown the interpretational similarity between unitary Newtonian gravity and the Wheeler-DeWitt equation: both are mediated by a *quantum potential* (metric). We are interested in understanding how CCG applies to the relativistic gravity: how a quantum spacetime can influence the dynamics of a test particle via a classical metric (fig. 5.1 bottom right). Our interpretation in the empty FRW case is to view the quantum scale factor as a 'source' of the classical metric, analogous to the way that a quantum particle sources a classical potential in Newtonian CCG. A test particle in an FRW spacetime will follow a trajectory that solely depends on the scale factor, and thus the scale factor generates an effective potential for the test particle. Therefore, in analogy with the Newtonian CCG description, the scale factor-test particle interaction can be understood in terms of weak measurements and feedback control, and therefore there must be intrinsically non-unitary evolution of the quantum state.

Using the same language of measurement and feedback from ref. [8] we posit that the quantum state of the universe is subject to weak continuous measurement of the variable $\hat{a}^2$. The measurement is of $\hat{a}^2$, as opposed to $\hat{a}$, since classically it is the factor $a^2$ that appears in the metric function, and therefore the trajectory of any test particle can only depend explicitly on $a^2$. The measurement process forces the gravitational influence of spacetime on the test particle to be mediated by classical information. In other words, the test particle responds to a classical estimate of the scale factor (the measurement results) analogous to the way that a test particle responds to the Newtonian potential in CCG.

The presence of the weak measurement on the quantum scale factor changes the evolution of the quantum state of the universe, resulting in a master equation for the ensemble averaged state that we shall describe in detail in the next section. An observer who tries to recover the dynamics of the scale factor, must measure the trajectories of many test particles and so cannot distinguish which sequence of measurement histories took place [156, 184]; hence they observe an ensemble averaged (i.e. averaged over all possible measurement histories) spacetime.
We shall denote $\mathsf{a}^2$ as the classical scale factor experienced by any observer in the Universe.

We will define the relationship between $\mathtt{a}^2$ and $\hat{a}^2$ shortly. In our model, the evolution of $\mathtt{a}$ is different from the standard Friedmann evolution and we will show that this is consistent with a dark energy fluid. Note that the effective measurement process avoids defining the classical scale factor as $\langle\hat{a}\rangle^2$ or $T_{\mu\nu} = \langle\hat{T}_{\mu\nu}\rangle$ where the expectation value is calculated with the quantum state given by the Wheeler-DeWitt equation.

We have described the relevant properties of unitary evolution in both the Newtonian regime and in the cosmological scenario. These two models share the feature that interactions are mediated by quantum potentials that are able to entangle the interacting constituents. On the other hand, CCG postulates that the gravitational interaction should be mediated by a classical potential, i.e. the interacting constituents (assumed to be quantum) will *communicate* with each other by exchanging classical information. Such an interaction induces noise in the dynamics of the quantum constituents, and such noise can be modelled by a measurement feedback channel. The fundamental distinction between the unitary approach and CCG is studied in the next section for the cosmological case.

## 5.1 Model and strategy

In the next two chapters we are considering an empty universe and a universe filled with dust $\rho_p$. Since the model is the same for both we are going to present a discussion for a universe with dust and in ch. 6 we will set $\rho_p = 0$.

### 5.1.1 Hamiltonian density

We consider an homogeneous and isotropic universe filled with dust described by the FRW metric:

$$ds^2 = -n^2 dt_{\mathtt{d}}^2 + a_p^2(t_{\mathtt{d}})\left(\frac{dr^2}{1-kr^2} + r^2 d\Omega\right) , \tag{5.1}$$

where $N$ is the lapse function, $a_p(t_{\mathtt{d}})$ denotes the physical scale factor– from now on a subscript $p$ will denote a *physical* quantity, $k = -1, 0, 1$ is the spatial curvature, and $t_{\mathtt{d}}$ is the proper time associated with a dust fluid filling the universe – here one a subscript $d$ denotes *dust*. The action Einstein-Hilbert for a spacetime filled with a pressureless perfect fluid (or dust) is [185]:

$$\mathcal{S} = \int d^4x\,\sqrt{-\mathrm{g}}\left[\frac{1}{2\kappa}\mathrm{R} - \rho_p\right] , \tag{5.2}$$

where g is the determinant of the metric $g_{\mu\nu}$, R is the Ricci scalar, $\rho$ the energy density of the fluid and $\kappa = 8\pi G c^{-4}$. The dust fluid is characterized by its energy momentum tensor

$$T^{ab}_{\mathtt{d}} = \rho\, U^a_{\mathtt{d}} U^b_{\mathtt{d}}\,, \qquad U^a_{\mathtt{d}} = \left(\frac{\partial}{\partial t_{\mathtt{d}}}\right)^a\,, \tag{5.3}$$

where $U^a_{\mathtt{d}}$ is the four velocity of the dust. The dynamics of the fluid are determined by the conservation of the stress-energy

$$\nabla_a\, T^{ab}_{\mathtt{d}} = 0\,. \tag{5.4}$$

Eqs.(5.3) and (5.4) allow as to write the energy density as a function of the scale factor

$$\rho(t_{\mathtt{d}}) = \frac{\rho_{0p}}{a_p(t_{\mathtt{d}})^3}\,, \tag{5.5}$$

where $\rho_{0p}$ is the energy density at a reference time $t_0$ such that $a_p(t_0) = 1$.
By rewriting the metric in conformal time

$$ds^2 = a_p^2[n^2(\tau)d\tau^2 + \frac{dr^2}{\sqrt{1-kr^2}} + r^2 d\theta^2 + r^2\sin^2(\theta)d\phi^2]\,, \tag{5.6}$$

we can compute the Lagrangian density

$$\mathcal{L} = \frac{3a_p^2 n(\tau)k}{\kappa} - \frac{3a_p'^2}{n(\tau)\kappa c^2} - \rho_p a_p^4 n(\tau)\,, \tag{5.7}$$

where $a_p'$ denotes derivative with respect to the conformal time. In order to compute the Hamiltonian density we define the momentum density as

$$\pi = \frac{\partial\mathcal{L}}{\partial a_p'} = -\frac{6a_p'}{n(\tau)\kappa c^2}\,, \tag{5.8}$$

and we obtain

$$\mathcal{H} = \pi\, a_p' - \mathcal{L} = -\frac{\pi^2\kappa c^2}{12} - 3\frac{a_p^2 k}{\kappa} - \rho_p a_p^4\,. \tag{5.9}$$

Upon defining the physical momentum $p_p = \int \pi d^3x$ we can compute the Hamiltonian for the system

$$H = -\frac{p_p^2\kappa c^2}{12V_0} - 3\frac{a_p^2 k V_0}{\kappa} - \rho_p a_p V_0\,, \tag{5.10}$$

where $V_0 = \int d^3x$ is a fiducial volume which in the coordinates we have chosen is $V_0 = \int \frac{r^2}{\sqrt{1-kr^2}}\sin(\theta)drd\theta d\phi$. We now rescale the scale factor and the momentum in the following way

$$a = \sqrt{\frac{3V_0}{\kappa}}a_p\,, \qquad p = \sqrt{\frac{\kappa}{3V_0}}p_p\,. \tag{5.11}$$

Note that with this definitions $a$ and $p$ are still canonical conjugate variables since their Poisson bracket is equal to one. Finally, we have also rescaled $\rho_0 = \rho_{0p}\sqrt{\kappa\, V_0/3}$ to find

$$H = -\frac{p^2 c^2}{4} - ka^2 + \rho_0 a^{1}\,. \tag{5.12}$$

The standard procedure in quantum cosmology is to canonically quantize the degrees of freedom $a$ and $p$ and solve the Wheeler-deWitt equation $\hat{H}\Psi(\hat{a},\rho) = 0$ for the wave function of the universe $|\Psi(\hat{a},\rho)\rangle$. This process is the quantum analog of imposing the classical Hamiltonian constraint $\mathcal{H} = 0$, which indeed reduces to the first Friedman equation. Note that the Wheeler-deWitt equation can be reformulated in terms of the density matrix $\hat{\varrho}$ associated with the wave function $|\Psi\rangle$ as

$$\frac{d\hat{\varrho}}{d\tau} = -\frac{i}{\hbar}[\hat{H},\hat{\varrho}]\,. \tag{5.13}$$

The Wheeler De-Witt equation, (5.13), can also be written in terms of the von-Neumann equation for the quantum density matrix $\hat{\varrho} = |\Psi(a,\rho)\rangle\langle\Psi(a,\rho)|$

$$\frac{d\hat{\varrho}}{d\tau} = -\frac{i}{\hbar}[\hat{\mathcal{H}},\hat{\varrho}] = 0\,, \tag{5.14}$$

where $\tau$ is the time flow used to define the operator $\pi$ in the Legendre transformation. Different interpretations of the meaning of $|\Psi\rangle$ lead either to single patch models (where the whole universe is thought of as a collection of interacting homogeneous patches) or to minisuperspace models (where the patch is the whole universe at early times when no inhomogeneities had formed). Either approach leads to the well-known problems of time and interpretation of the wavefunction in quantum cosmology [186], and efforts to solve them have led to a range of different models [187, 188, 189, 190]. In either case one then is left with the problem of both computing the wavefunction (or density matrix) of the universe and of interpreting it in such a manner that admits a reasonable classical limit.

### 5.1.2 Master equation

We are now going to derive the master equations covering dynamics for CCG applied to cosmology. At this point we diverge slightly from the discussion in ref. [8] and in Sec. 1.3, and instead of treating each particle symmetrically, we consider $\hat{x}_1$ as a 'source' particle

[1] In the next chapters we will use $c = 1$.

and $\hat{x}_2$ as a 'test' particle, although the distinction is made arbitrarily. Since we now have a 'test' particle, we are not concerned with the back reaction from the test onto the source, and therefore the effective feedback Hamiltonian to consider is $H_{fb} = K\bar{x}_1\hat{x}_2$ to generate the dynamics of the test particle. In this case $H_{fb}$ does not affect the Hilbert space of the source, and the measurement of the source (required for $H_{fb}$), does not affect the Hilbert space of the test particle. Therefore if the joint state is initially separable, $\hat{\rho}_0 = \hat{\rho}_1 \otimes \hat{\rho}_2$, and there is no other interaction present, then the joint state will remain separable at all times, $\hat{\rho}(t) = \hat{\rho}_1(t) \otimes \hat{\rho}_2(t)$. However, the introduction of the measurement of the source implies fundamental decoherence in its quantum state and is required by the simple existence of the test particle (see fig. 5.1 top-right). In this asymmetric treatment between the two particles, there is no way to minimize the decoherence rate, but we can conclude that there must be a non-zero decoherence rate, $\Gamma_1 > 0$, of the source particle to determine the dynamics of the test particle.

This one sided description is analogous to what we consider in the cosmological case. The dynamics of the test particle depends on classical information from the scale factor state. We therefore suggest, that in CCG there is some fundamental, observer independent decoherence. Since we do not consider the back reaction from the presence of a test particle on the scale factor the decoherence rate cannot be minimized, and is left as a free, but strictly positive parameter. Further exploration should include the back reaction and thus introduce a noise minimization procedure.

Following Sec. 1.3 we derive the master equation for the cosmological system. We propose that the state is subject to weak continuous measurement of the variable $a_p^2$[2]. The way a test particle responds to the influence of the quantum scale factor through a classical metric function is via the result of a weak measurement. In this case the metric function is given by, $ds^2 = \bar{a}^2(-d\tau^2 + dx^2)$ where $\bar{a}^2 = \langle \hat{a}_p^2 \rangle_c + \sqrt{\frac{\hbar}{\gamma}} dW/d\tau$, relabeling $\Gamma \to \gamma$ from (1.9). This is analogous to the way a test particle responds to the Newtonian potential though $H_{fb} = K\bar{x}_1\hat{x}_2$. The presence of the weak measurement on the quantum scale factor changes the evolution of the quantum state $\hat{\varrho}$, resulting in the stochastic master equation

$$d\hat{\varrho}_c \;=\; -\frac{i}{\hbar}[\hat{H}(a_p, p_p), \hat{\varrho}]d\tau - \frac{\gamma_p}{8\hbar}[\hat{a}_p^2, [\hat{a}_p^2, \hat{\varrho}]d\tau - \sqrt{2\hbar}dW\mathcal{H}[\hat{a}_p^2]\hat{\varrho}_c\,, \tag{5.15}$$

where we have assumed a continuous Gaussian measurement of $\hat{a}_p^2$, and the subscript $c$ refers to fact that the change in $\hat{\varrho}$ is conditioned on the measurement result $\bar{a}_p^2$. Any observer who is unaware of the measurement outcome $\bar{a}_p^2$, will describe the state as an ensemble average over the measurement process, $d\hat{\varrho}_c \to \mathcal{E}(d\hat{\varrho}_c) = d\hat{\varrho}$, with the corresponding ensemble

[2]This is because (classically) it is exactly the factor $a_p^2$ that appears in the metric function, and therefore the trajectory of any test particle explicitly can only depend on $a^2$.

averaged metric, $\bar{a}^2 \to \mathcal{E}(\bar{a}^2) = \langle \hat{a}_p^2 \rangle \equiv \mathsf{a}_p^2$ . Consequently the corresponding dynamics are given by

$$\frac{d\hat{\varrho}}{d\tau} = -\frac{i}{\hbar}[\hat{H}(a_p, p_p), \hat{\varrho}] - \frac{\gamma_p}{8\hbar}[\hat{a}_p^2, [\hat{a}_p^2, \hat{\varrho}]]\,, \tag{5.16}$$

where $\gamma_p$ is the decoherence parameter which has units of $1/T$. Upon normalization of the quantities we can write the master equation as

$$\frac{d\hat{\varrho}}{d\tau} = -\frac{i}{\hbar}[\hat{H}(a, p), \hat{\varrho}] - \frac{\gamma}{8\hbar}[\hat{a}^2, [\hat{a}^2, \hat{\varrho}]]\,, \tag{5.17}$$

where $\gamma = \gamma_p \frac{\kappa^2}{9V_0^2}$ . Eq. (5.17) is the master equation we employ in the next chapters. In addition the spacetime dynamics are given by

$$ds^2 = \langle \hat{a}_p^2(\tau) \rangle [-d\tau^2 + \frac{1}{1-kr^2}dr^2 + r^2 d\Omega^2] = \mathsf{a}_p^2(\tau)[-d\tau^2 + \frac{1}{1-kr^2}dr^2 + r^2 d\Omega^2]\,, \tag{5.18}$$

where the evolution of $\langle \hat{a}_p^2 \rangle$ is given by eq. (5.15) using $\langle \dot{\hat{A}} \rangle = \mathrm{Tr}[\hat{A}\dot{\hat{\varrho}}]$ for any operator $\hat{A}$. The condition $\gamma \neq 0$ is required in order for the test particle to feel the presence of the scale factor in the classical metric function, and $\gamma \geq 0$ is required preserve the positivity of $\hat{\rho}$ [191, 80]. Therefore $\gamma > 0$ is a requirement for the model to be physical. Fluctuations in the measurement record (of order $dW\sqrt{\hbar/\gamma}$) induce fluctuations in the metric function. However, any observer making multiple measurements would average over all fluctuations, and only see the ensemble averaged dynamics [156], i.e. eq. (5.17) for the quantum system. The latter term in (5.17) takes into account both the non-unitary evolution of the scale factor due to the presence of test particle(s) and the ensemble average of an observer when making measurements on multiple test particles. It can be derived from a collisional model in which the quantum degrees of freedom are continuously interacting with the external test particles as discussed in ch. 2. This process introduces a new fundamental constant $\gamma$ that emerges as a consequence of the interaction between the test particle and the scale factor via the metric function. The form of equation (5.17) have been previously used in different scenarios, in particular to account for modifications of quantum mechanics such as collapse models [51] and with a focus on cosmological consequences of metric theories with non conservation of energy momentum tensor [192]. Here we go a step further, and analyze the consequences in the cosmological scenario of (5.17) when emergent form Quantum-classical interactions as the master equation for observables measured by a classical observer.

We emphasize that the interpretation of this model is fundamentally different from that of the standard Wheeler-DeWitt approach in (5.14). Here the evolution of the universe is obtained by solving the master equation (5.17), for the time dependence of $\mathsf{a}^2 = \langle \hat{a}^2(\tau) \rangle$ as in equation (5.18). The resulting spacetime will behave very differently compared to that

of an empty universe, particularly at early times. As we shall demonstrate, the universe described by (5.18) will evolve as though there were a form of time-dependent dark energy present. In the next chapters we shall present the solutions to these equations and analyze the various resulting behaviours. However, before doing so, we first analyze the behaviour of the Hamiltonian operator in our model. We find

$$\frac{d\langle \hat{H} \rangle}{d\tau} = -\frac{\gamma}{4}(c\hbar)^2 \left\langle \hat{a}^2 \right\rangle \,, \tag{5.19}$$

which is only equal to zero if $\gamma = 0$. Note that the Wheeler-DeWitt equation will indeed conserve the quantity $\langle \hat{H} \rangle$ since the Hamiltonian operator commutes with itself at all times. If $\langle \hat{H} \rangle$ is regarded as a measure of the classical energy emergent from a quantum theory of gravity, we see that CCG predicts the existence of additional energy. In this sense it is another example of energy non-conservation theories as unimodular gravity (see [193] and references therein) that might present interesting observable consequences [192]. We emphasize that any observer unaware of the quantum nature of spacetime and describing its dynamics via the Einstein equations will see this extra energy manifest as a dark energy fluid.

## 5.2 Measured quantitates and notation

Before we move on to present the results let us clarify and organize our notation. As discussed before the observed scale factor of an observer unaware of the underlying quantum mechanism will be

$$\mathtt{a}_p \equiv \sqrt{\langle \hat{a}_p^2 \rangle} \,. \tag{5.20}$$

On the other hand we will compute all quantities and show plots of quantities involving $a$ which is related with $a_p$ via eq. (5.11). This implies that is

$$\mathtt{a} \equiv \sqrt{\langle \hat{a}^2 \rangle} = \sqrt{\frac{3V_0}{\kappa}}\mathtt{a}_p \,. \tag{5.21}$$

Upon solving the system of equations (7.6)–(7.8) we will get an expression for $\mathtt{a}(\tau)$ and we will use the relation $a(\tau)d\tau = dt$ to find the functional form of $a(t)$. With this relations we also find that the observed proper time is

$$t_p \equiv \int \mathtt{a}_p(\tau) d\tau = \sqrt{\frac{\kappa}{3V_0}} t \,. \tag{5.22}$$

Note that in the case where $\mathtt{a}(\tau) \propto \exp(\omega\tau)$ (we find this behaviour for late times in CCG regardless of the value of $k$) we have $\mathtt{a}(t) = \mathtt{a}_p(t_p)$ with no explicit dependence in $V_0$ of the observed scale factor. Nonetheless, the time $\bar{t}$ after which the behaviour of $\mathtt{a}$ is well approximated by a linear function implies that the observed scale factor is well approximated by the same linear function only for $t_p > \bar{t}_p = \sqrt{\frac{\kappa}{3V_0}}\bar{t}$.

Through the next chapters we use different notation to indicate the difference between underlaying physical quantities, observed physical quantities and fiducial quantities (that were defined after physical quantities for convenience):

Physical quantities: $a_p, p_p, \rho_{0p}$.

Observed quantities: $\mathtt{a}_p, \gamma_p, t_p, H_p, \rho_{\mathrm{CCG}}, w_p, \Omega_{\mathrm{CCG}}$.

Fiducial quantities: $a, p, \rho_0, \hat{a}, \hat{p}, \mathtt{a}, t, \gamma, H_u, \rho, w$.

The relation between the fiducial quantities and the physical and observed quantities is summarized in Table 5.1.

Table 5.1: Relation between physical, observed and fiducial quantities where $\eta = \sqrt{\frac{\kappa}{3V_0}}$. Note that the time derivatives denoted by an upper dot are with respect of $t_p/t$ if applied to physical/fiducial quantities.

| Name | Description | Definition | Properties |
|---|---|---|---|
| $a_p$ | underlying scale factor | | |
| $p_p$ | canonical conjugate momentum | | $\{a_p, p_p\} = 1$ |
| $\hat{a}_p$ | scale factor operator | | |
| $\hat{\pi}$ | momentum density operator | | |
| $\hat{p}_p$ | physical momentum operator | $p = \int dV \pi$ | $[\hat{a}_p, \hat{p}_p] = i\hbar$ |
| $\gamma_p$ | physical decoherence parameter | See (5.16) | |
| $\rho_{0p}$ | primordial dust | | |
| $\mathtt{a}_p$ | observed scale factor | $\sqrt{\langle \hat{a}_p^2 \rangle}$ | |
| $t_p$ | observed comoving time | $\mathtt{a}_p d\tau = dt_p$ | |
| $H_p$ | observed Hubble parameter | $\frac{\dot{\mathtt{a}}_p}{\mathtt{a}_p}$ | $H_p^2 + \frac{k}{\mathtt{a}_p^2} = \frac{\kappa}{3}\rho_{\rm ccg}$ |
| $\rho_{\rm ccg}$ | observed dark energy density | | $\rho_{\rm ccg} = \frac{3}{\kappa}(\frac{\dot{\mathtt{a}}_p^2 + k}{\mathtt{a}_p^2})$ |
| $w_p$ | observed equation of state | $P_{\rm ccg} = w_p \rho_{\rm ccg}$ | $w_p = \frac{\dot{\rho}_{\rm ccg}}{3H_p\rho_{\rm ccg}} - 1$ |
| $\Omega_{\rm ccg}$ | | $\frac{\rho_{\rm ccg}\kappa}{3H_p^2}$ | |
| $a$ | fiducial scale factor | $a_p/\eta$ | |
| $p$ | fiducial momentum | $\eta\, p_p$ | $\{a, p\} = 1$ |
| $\rho_0$ | fiducial primordial dust | $\rho_{0p}\, \eta\, V_0$ | |
| $\hat{a}$ | fiducial scale factor operator | $\hat{a}_p/\eta$ | |
| $\hat{p}$ | fiducial momentum operator | $\hat{p}_p\, \eta$ | $[\hat{a}, \hat{p}] = i\hbar$ |
| $\gamma$ | fiducial decoherence parameter | $\gamma_p\, \eta^4$ | See (5.17) |
| $\mathtt{a}$ | fiducial observed scale factor | $\mathtt{a}_p/\eta$ | $\sqrt{\langle \hat{a}^2 \rangle}$ |
| $t$ | fiducial comoving time | $t_p/\eta$ | $\mathtt{a} d\tau = dt$ |
| $H_u$ | fiducial Hubble parameter | $\eta\, H_p$ | $\frac{\dot{\mathtt{a}}}{\mathtt{a}}$ |
| $\rho$ | fiducial dark energy density | $\eta^2 \rho_{\rm ccg}$ | $\rho = \frac{3}{\kappa}(\frac{\dot{\mathtt{a}}^2 + k}{\mathtt{a}^2})$ |
| $w$ | fiducial equation of state | $w = w_p$ | $w_p = \frac{\dot{\rho}}{3H\rho} - 1$ |

# Chapter 6

# Emergent dark energy via decoherence in quantum interactions

## 6.1 Organization

In this chapter we study the effect of the model described above in an empty universe. This chapter is organized as follows: we analyze the solutions of the equations of motion in section 6.2 and compute the effective energy momentum tensor arising from this model. We then analyze the effective form of dark energy that emerges and consider how it affects the evolution of the spacetime. We close with some final remarks in section 6.3 and discuss future directions for this approach. Through all this work we are considering units $G = 1 = c$.

## 6.2 Dark Energy from Decoherence

The evolution of $\mathsf{a}^2$ is solved by using the master equation (5.17) and computing time derivatives of the first and second order moments of the quantum operators $(\hat{a}, \hat{\pi})$. We

need to solve the following coupled equations

$$\frac{d}{d\tau}\langle\hat{a}\rangle = -\langle\hat{\pi}\rangle/2\,, \tag{6.1}$$

$$\frac{d}{d\tau}\langle\hat{\pi}\rangle = 2k\langle\hat{a}\rangle\,, \tag{6.2}$$

$$\frac{d}{d\tau}\langle\hat{a}^2\rangle = -\langle\hat{a}\hat{\pi}+\hat{\pi}\hat{a}\rangle/2\,, \tag{6.3}$$

$$\frac{d}{d\tau}\langle\hat{\pi}^2\rangle = 2k\langle\hat{a}\hat{\pi}+\hat{\pi}\hat{a}\rangle+\gamma\langle\hat{a}^2\rangle\,, \tag{6.4}$$

$$\frac{d}{d\tau}\langle\hat{a}\hat{\pi}+\hat{\pi}\hat{a}\rangle = -\langle\hat{\pi}^2\rangle+4k\langle\hat{a}^2\rangle\,. \tag{6.5}$$

We see from equations (6.1)–(6.5) that only the second order moments are required to obtain the evolution of (5.18). Solving for these yields the evolution of the spacetime metric, and our subsequent task is to solve this set of equations for a variety of initial conditions for different values of the curvature constant $k$. We find there is always one exponentially growing mode, which makes the universe expand and two modes that either yield exponential decay or decaying oscillation of the scale factor. A general solution is a linear combination of these eigen-solutions, and so will in general asymptote to one that grows exponentially with time.

We now proceed to interpret these solutions from the perspective of an observer who only has access to to the trajectories of test particles to back out the metric (5.18).
As noted above, an observer can in principle determine the temporal evolution of the observable $\mathsf{a}^2$. Having no direct access to the underlying quantum observables, this observer can compute the Einstein tensor associated with the metric (5.18) and then use Einstein's equations to determine the effective stress-energy tensor governing the observed evolution of spacetime.

The solution for $\mathsf{a}^2(\tau)$ depends on the six variables $\{\tau, k, \gamma, \mathsf{a}_0^{(2)}, \pi_0^{(2)}, \zeta_0\}$, where $\tau$ is the conformal time and $\{\mathsf{a}_0^{(2)}, p_0^{(2)}, \zeta_0\}$ are the second order moments of the quantum state $\{\langle\hat{a}^2\rangle, \langle\hat{p}^2\rangle, \langle\hat{a}\hat{p}+\hat{p}\hat{a}\rangle\}$ at $\tau = 0$. These quantities can be constrained using a variety of physical criteria, as we shall discuss in the next section.

To see the general dependence of $\mathsf{a}^2$ on $\gamma$, we set $\mathsf{a}_0^{(2)} = 1 + 1/4$, $\pi_0^{(2)} = 1$ , $\zeta_0 = 0$, describing displaced ground state of the quantum state and plot the results in comoving time in fig. 6.1 for each value of $k$. To better understand the dynamics of the scale factor, and indeed the general physics of our model (anticipating a comparison with data), it is useful to analyze relevant physical quantities in terms of the comoving time $t$

$$t(\tau) = \int_0^\tau \mathsf{a}(\tau')d\tau'\,, \tag{6.6}$$

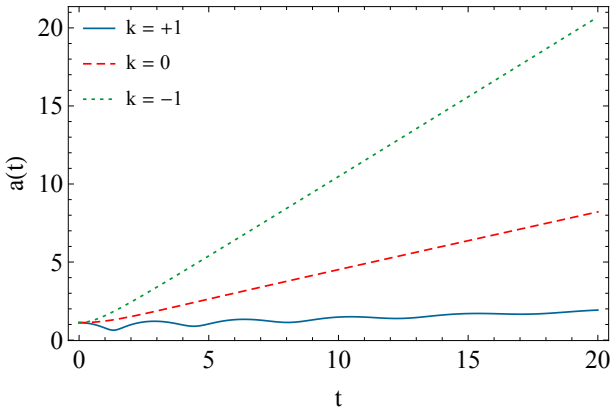


Figure 6.1: Scale factor behaviour for $\gamma = 0.1$ and different values of $k$ as a function of comoving time. The quantum is system initially in a coherent state centered at $a_0 = 1$. The relative behavior remains qualitatively the same as the decoherence parameter $\gamma$ is varied.

with $\tau$ being the conformal time. We see that in the case $k > 0$ for small $\gamma$ the scale factor undergoes damped oscillations. Furthermore, there exists a time scale that is half the e-folding time associated with the positive root $\lambda_+$, after which the scale factor grows linearly in comoving time (exponentially in conformal time) without oscillations as noted above. This growth, while present, is not visible for the most oscillatory curve in figure 6.1. For the $k \leq 0$ cases there is exponential growth but no oscillations for this choice of parameters. We also note that the growth of the scale factor is faster for $k > 0$ and slower for $k = 0$.

From the point of view of an observers will infer from the motion of test particles the metric (5.18), and describe the resultant spacetime dynamics with the Einstein equations

$$G_{\mu\nu}(\mathsf{a}^2) = 8\pi T_{\mu\nu}\,, \tag{6.7}$$

where $G_{\mu\nu} = R_{\mu\nu} - \frac{1}{2}Rg_{\mu\nu}$ is the Einstein tensor. The Ricci tensor $R_{\mu\nu}$ and Ricci scalar $R$ are constructed with second derivatives of the metric tensor $g_{\mu\nu}$ which is given by (5.18). Such an observer will infer that the expansion is driven by a form of *dark energy*, whose effective stress-energy is $T_{\mu\nu}$, and which we shall now compute.

The symmetries of the FRW metric (homogeneity and isotropy) tell us that the energy-

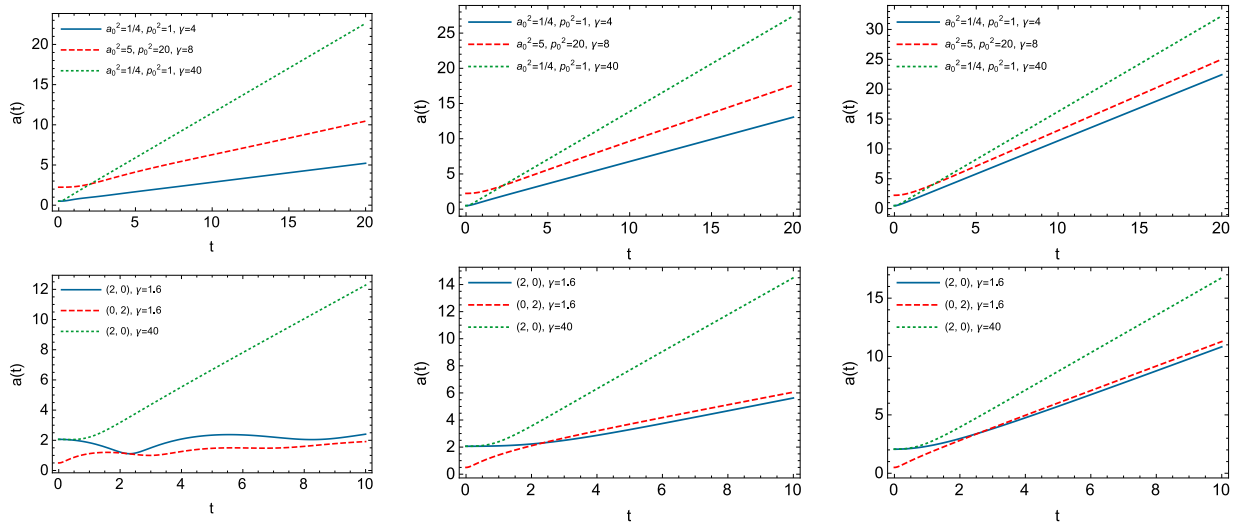


Figure 6.2: Evolution of the scale factor in comoving time for initial thermal (top) and coherent (bottom) states, for $k = 1$ (left), $k = 0$ (middle) and $k = -1$ (right). In each case the steady state gradient is determined by $\gamma$. The oscillation in the $k = 1$ case can be understood by considering the equations of motion (Eqs. (6.1)–(6.5)) as $\gamma \to 0$. The equations are then that of a Harmonic oscillator, with the amplitude of the oscillations defined by the Euclidean sum of the coherent amplitude $(a_0, p_0)$, where $\tan^{-1}(a_0/p_0)$ defines the initial phase.

momentum tensor must have the form of a perfect fluid

$$T^{\nu}_{\mu} = \begin{pmatrix} -\rho & 0 & 0 & 0 \\ 0 & P & 0 & 0 \\ 0 & 0 & P & 0 \\ 0 & 0 & 0 & P \end{pmatrix}, \tag{6.8}$$

where $\rho$ and $P$ are the energy density and pressure of our perfect fluid. The type of matter is characterized by $w$ in the equation of state $P = w\rho$.

We must also choose the free parameters $\{a_0, p_0, \mathsf{a}_0^{(2)}, \pi_0^{(2)}, \zeta_0, \gamma\}$ where $a_0$ and $\pi_0$ are the initial means of $\hat{a}$ and $\hat{p}$ respectively. This is a rather large parameter space, and constraining it to obtain useful information is a bit of a challenge. We will consider two kinds of Gaussian states: coherent states saturating the uncertainty inequality, characterized by their mean amplitude $(a_0, p_0)$ (with $\zeta_0 = a_0\pi_0$), and thermal states for which $4a_0^{(2)} = \pi_0^{(2)}$ with $\zeta_0 = a_0 = \pi_0 = 0$. Note that the spacetime

only depends on $\mathtt{a}^2 = \langle \hat{a}^2 \rangle$, which in turn is governed by equations (6.1)–(6.5). Consequently, initial values of $a_0 = \pi_0 = 0$ result in a spacetime driven by noise from either a quantum (for minimum uncertainty states), or quantum and statistical (for mixed states) source. Additionally we can impose the following physical conditions on the spacetime

- Strong Energy Condition: $\rho > 0$ and $w(t) > -1$ .
- Weak Energy Condition: $\rho > 0$ and $|w(t)| < 1$ .
- A non-singular spacetime: $K < \infty$, where $K$ is the Kretschmann scalar $K = R^{abcd}R_{abcd}$.

Finally, a more sophisticated model would have to be observationally constrained by early-universe data from the CMB, as well as from information on structure formation, but this is beyond the scope of this toy model.

We now concentrate in the description of the perfect fluid and an analysis of singularities. We find that the Kretschmann scalar

$$K = \frac{12}{\mathtt{a}^4}\left[(k + \mathtt{a}'^2)^2 + \mathtt{a}^2\mathtt{a}''^2\right], \tag{6.9}$$

does not diverge, since we must have $\mathtt{a} > 0$ to have a physical quantum state. The expression for the effective density is

$$\rho(t) = \frac{3}{8\pi}\frac{\mathtt{a}'^2 + k}{\mathtt{a}^2}, \tag{6.10}$$

and the equation of state is described by the function $w(t)$, defined via

$$P(t) = w(t)\rho(t), \tag{6.11}$$

where we find

$$w(t) = -\frac{2}{3}\frac{\mathtt{a}''\mathtt{a}}{\mathtt{a}'^2 + k} - \frac{1}{3}, \tag{6.12}$$

where we have used Einstein equations (6.7) for $\mathtt{a}^2$ assuming a perfect fluid (6.8), and where $a' = \frac{da}{dt}$.

We plot the behavior of the scale factor as a function of comoving time for different parameters. The results are depicted in figure 6.2. We see that the cosmic evolution has low sensitivity to the initial conditions indeed at late times, the different curves become indistinguishable for all values of $k$. However there is rather high sensitivity to the choice

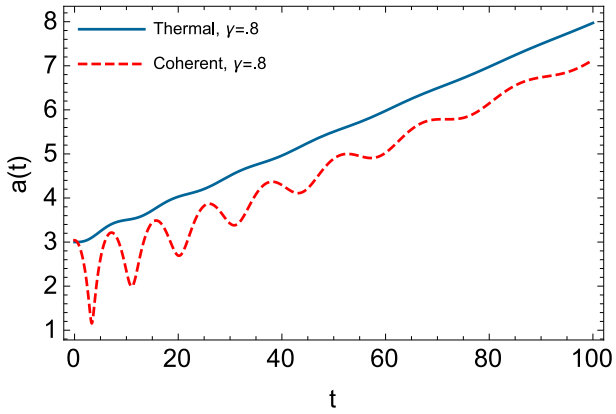


Figure 6.3: Evolution of the scale factor for $k = 1$. The large initial amplitude causes many oscillations before the transient behavior becomes dominated by the decoherence. The initial coherent state begins with an amplitude of $(3, 0)$ and is compared to a thermal state of $a_0^{(2)} = 9$. Without decoherence, the thermal state would remain constant in time.

of $\gamma$, particularly at early times, as is clear from figure 6.2. For small $\gamma$ the coherent behavior is resolvable for a longer time. This is clearly visible in the case of a large coherent amplitude, shown in figure 6.3, where the large initial coherent amplitude causes many visible oscillations before the spacetime is dominated by the decoherence.

The behaviour of the Hubble parameter $H = \frac{a'}{a}$ as a function of comoving time (not plotted) displays considerable sensitivity for various choices of $\pi$ and $\gamma$ at early times, but convergence at late times. We also find that the effective energy density $\rho$ is always positive, and that at early times its behavior can be quite oscillatory for small values $\gamma$ when $k = +1$, but for all values of $k$ it tends to grow initially for various choices of $\pi$ and $\gamma$. At late times, regardless of these choices and values of $k$, the energy density is a monotonically decreasing function of time.

An interesting feature of the model is that for large times, depicted in fig. 6.4, the system asymptotes to the relation $P(t) = -\frac{1}{3}\rho(t)$. Although at early times the strong energy condition is generally (but not always) violated, at late times it is satisfied, with the equation of state settling down to the zero-acceleration case of $w = -1/3$. This is a rather striking feature of our model that is robust to any changes in initial conditions as long as $\gamma > 0$, and occurs for all values of $k$. It is a consequence of the existence of the growing mode, which ensures at late conformal times exponential growth of the scale factor, which translates into asymptotic linear growth in comoving time. From the Friedmann equations, if $w(t) > -1/3$ then the universe undergoes an decelerating expansion whereas

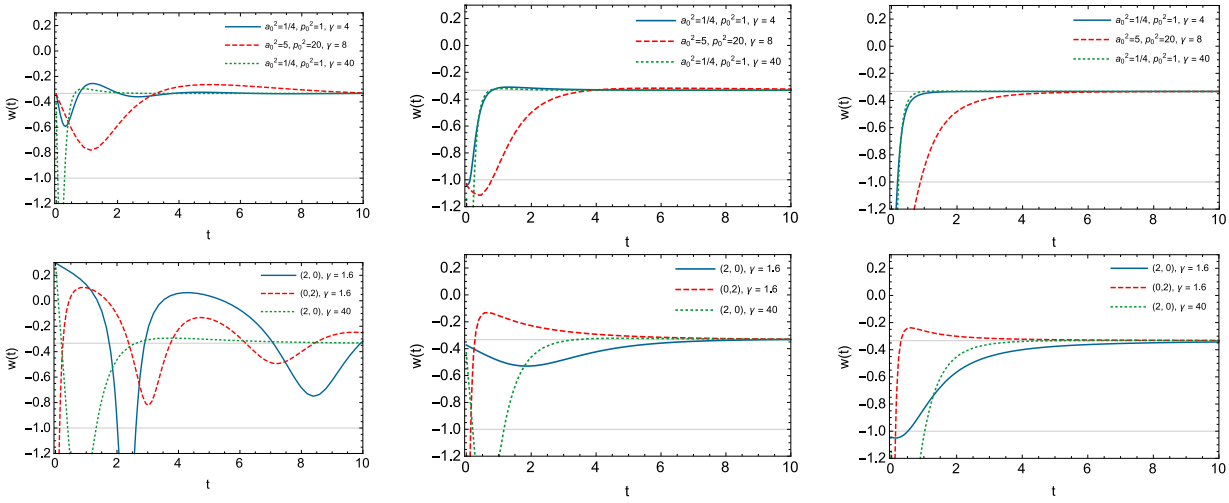


Figure 6.4: Behaviour of the equation of state parameter in comoving time for thermal initial states (top) and coherent initial states (bottom), for each value of $k = 1$ (left), $k = 0$ middle, $k = -1$ (right). In each case $w(t) \to -1/3$ regardless of the initial conditions or curvature. For late times $t > 5$ both the strong and weak energy conditions hold. Furthermore in all case $w(t)$ approaches the asymptote faster for large $\gamma$.

if $w(t) < -1/3$ we have an accelerated expansion which is a necessary condition for inflating universes. A closer analysis of the behaviour of the different quantities involved in eq. (6.12) shows that $\mathsf{a}'(t)$ asymptotes to a constant finite value and, as shown in fig. 6.2, the scale factor as a function of comoving time grows linearly with time. We thus conclude that the asymptotic behavior of the equation of state is governed by the acceleration $\mathsf{a}''(t)$ which goes to zero for large times. This crucially depends on the positivity of $\gamma$, whose effects are most pronounced in the $k = 1$ case. In the limit $\gamma \to 0$, this case becomes purely oscillatory. Increasingly large values of $\gamma$ both damp the oscillations and cause a more rapid growth in the scale factor, which asymptotes to a linear function of conformal time for all values of $k$. The fact that there are times for which the universe is expanding in an accelerated fashion suggests that our model can be used as an alternative to inflationary models, but the complete investigation of this aspect is beyond the scope of the present work.

## 6.3 Conclusions

We have explored the first implementation of CCG in a relativistic setting, showing how it can be implemented in an FRW spacetime. We found that this yields an alternative model for quantum cosmology, one in which the dynamical variables are quantum, and source a classical metric that influences test particles. By construction the evolution of the spacetime in the presence of such test particles is fundamentally non-unitary and results in an unavoidable decoherence of the quantum system and an arrow of time. The non-unitarity is required in order for a test particle to be influenced by the scale factor in the CCG model. This results in an arrow of time and unavoidable decoherence of the quantum system. Furthermore, the big-bang singularity is removed, since the scale factor is now interpreted as the mean of a positive quantum variable which is constrained by the uncertainty relations.

The net effect of this interaction is manifest in a form of time-dependent dark energy as our subsequent investigation of the evolution of the metric (as seen by an observer that measures the trajectories of test particles) indicated. For positive curvature $k > 0$ we found that the cosmological evolution is generally characterized by oscillatory behaviour of the scale factor (consistent with the Friedmann solutions) that is eventually dominated by exponential growth in conformal time. Transforming to comoving coordinates, the equation of state parameter $w(t)$ initially undergoes oscillations that damp out, with this parameter reaching the asymptotic value of $-1/3$ at late times. This condition, present for all values of $k$, is robust to initial conditions and is a consequence of the aforementioned exponential growth, which in turn is driven by the constraint of the decoherence rate of the quantum system.

We have thus shown than an observer in the universe will see the presence of a dark fluid as a consequence of test particles interacting with the metric. This form of fluid is characterized by $\gamma$, the fundamental parameter in our model. However the energy conditions are generically not satisfied at early times, with $|w(t)| > 1$, although two notable exceptions are illustrated in the upper left of figure 6.4 (the solid and dashed curves) for thermal initial states. This suggests that a more sophisticated model could generically satisfy the energy conditions. Furthermore $\rho > 0$ for $k \leq 0$. Of course the model we have presented here is overly simplistic, ignoring matter contributions and possible spatial inhomogeneities and anisotropies. A more realistic cosmology must take such factors into account.

The model discussed in this chapter can be extended to consider perhaps more realistic scenarios. In particular we are interested in how a matter source interacting with the scale factor will modify the equations. In this scenario, there is no need to introduce the

notion of a test particle to account for non unitary evolution. In fact, the CCG model states that in order for two quantum systems to interact gravitationally (in this case scale factor and matter) both subsystems need to continuously have knowledge of the other subsystem properties, and this can be achieved by a classical communication channel or weak measurements. This (effective) weak measurements will break unitary evolution and an observer in that universe that measure the matter field in order to describe its dynamics will induce decoherence on the joint system scale factor- matter therefore changing the dynamics as of a universe that behaves according to the Wheeler-deWitt equation.

Let us comment on the covariance properties of the CCG model as presented in this work. As formulated here, the model explicitly brakes unitary evolution in the frame where the weak measurements performed by the test particles are held and therefore the master equation for the scale factor was computed in the proper frame of the test particles. In this exploratory work we decided to work in conformal time, and thus both the test particles and the observers have the conformal time as their proper time. A more careful extension of the model should have this feature taken into account. For example, when matter is introduced one should look at its associated energy momentum tensor and in particular to its proper time. The proper time of the matter is then the frame in which the matter will interact with the metric and thus is in this frame where unitarity is broken. One should in principle write the master equation as a function of a the proper time of the matter. A similar description that we presented in this work will therefore hold for an observer whose proper time is the proper time of matter. For any other observer, that does not share the same proper time as the matter, one will need to perform a change of reference to described the emergent dark fluid. We postpone this extension to the next chapter.

# Chapter 7

# Emergent dark energy from quantum interactions with matter

## 7.1 Introduction

If CCG is to be regarded as the fundamental description of classical gravity it is then also fundamental in describing the interplay between gravity and matter. This work presented in this chapter is the first attempt in investigating this aspect of CCG: we consider a universe filled with dust, which serves as the effective stress-energy of some primordial weakly interacting matter. Even though dust is not the most general matter source, this chapter sheds light on the interplay of matter with a universe dominated by quantum variables that is still fully classical for any observer. For the analysis, we choose to adopt a model in which all the noise is in the scale factor (similar to the description presented in the last chapter); the primordial dust acts as a *spectator*, modifying the initial Hamiltonian governing the equations of motion of the scale factor. This is not the only option nor is it the most general, and we will discuss other possibilities for how to treat the primordial dust in the concluding section of our paper.

In this chapter we analyze the behaviour of both the emergent fluid and the primordial perfect fluid focusing on the differences with respect to the empty universe model. Extending this study, we provide an improved description of the emergent dark fluid and find that it can be characterized as emergent curvature in the universe. We organize our material as follows. In Sec. 7.2 we derive the equations of motion for our system and give a discussion about the conservation of the Hamiltonian. Section 7.3 is devoted to the results, where we present the behaviour for the scale factor, the emergent fluid and the behaviour and

consequences of the primordial dust. We conclude this work in sections 7.4 and 7.5, giving a discussion about the observable consequences of CCG and future directions.

## 7.2 Equations of motion

In order to find the equations of motion we make use of the formula $\langle \hat{A} \rangle = \mathrm{Tr}(\hat{A}\hat{\varrho})$ together with the master equation (5.17) to find:

$$\frac{d\langle \hat{a} \rangle}{d\tau} = -\frac{\langle \hat{p} \rangle}{2} c^2 \,, \tag{7.1}$$

$$\frac{d\langle \hat{p} \rangle}{d\tau} = 2k \langle \hat{a} \rangle - \rho_0 \,, \tag{7.2}$$

$$\frac{d\langle \hat{a}^2 \rangle}{d\tau} = -\frac{\langle \hat{p}\hat{a} + \hat{a}\hat{p} \rangle}{2} c^2 \,, \tag{7.3}$$

$$\frac{d\langle \hat{p}^2 \rangle}{d\tau} = 2k \langle \hat{p}\hat{a} + \hat{a}\hat{p} \rangle + \gamma \hbar^2 \langle \hat{a}^2 \rangle - 2\rho_0 \langle \hat{p} \rangle \tag{7.4}$$

$$\frac{d\langle \hat{p}\hat{a} + \hat{a}\hat{p} \rangle}{d\tau} = -c^2 \langle \hat{p}^2 \rangle + 4k \langle \hat{a}^2 \rangle - 2\rho_0 \langle \hat{a} \rangle \,. \tag{7.5}$$

These five equations form a closed coupled system of differential equations. By comparing with the equations of motion found in the previous chapter we note that the presence of dust in the background couples Eqs.(7.3)-(7.5) with Eqs.(7.1)-(7.2). Nevertheless, Eqs.(7.3)-(7.5) decouple from each other at third order:

$$\langle \hat{a}^2 \rangle''' + 4kc^2 \langle \hat{a}^2 \rangle' - \frac{\gamma \hbar^2 c^4}{2} \langle \hat{a}^2 \rangle = -\frac{3}{2} c^4 \rho_0 \langle \hat{p} \rangle \,, \tag{7.6}$$

$$\langle \hat{p}^2 \rangle''' + 4kc^2 \langle \hat{p}^2 \rangle' - \frac{\gamma \hbar^2 c^4}{2} \langle \hat{p}^2 \rangle = \rho_0 \gamma \hbar^2 c^2 \langle \hat{a} \rangle \,, \tag{7.7}$$

$$\langle \hat{\Gamma} \rangle''' + 4kc^2 \langle \hat{\Gamma} \rangle' - \frac{\gamma \hbar^2 c^4}{2} \langle \hat{\Gamma} \rangle = 3c^2 \rho_0 (2k \langle \hat{a} \rangle - \rho_0) \,, \tag{7.8}$$

where we have renamed $\hat{a}\hat{p} + \hat{p}\hat{a} = \hat{\Gamma}$ and make use of the notation $d/d\tau = '$.

## 7.3 Results

In this section we present the result of our analysis, in particular for the scale factor and the emergent dark energy fluid due to the modification of the Wheeler-DeWitt equation

(5.17). To this end we are going to solve for the scale factor $\mathsf{a} = \sqrt{\langle a^2 \rangle}$ in conformal time $\tau$ using the coupled system of equations (7.6)-(7.7) and convert to proper time $t$ using the relation $\mathsf{a}(\tau)d\tau = dt$. Note that for $\rho_0 = 0$ the solution for the scale factor can be written as

$$\mathsf{a}^2 = \sum_{i=1}^{3} A_i \exp(\omega_i \tau)\,, \tag{7.9}$$

where the coefficients $A_i$ depend on the initial conditions, $k$ and $\gamma$, and where the characteristic equation

$$\omega_i^3 + 4kc^2\omega_i - \frac{\gamma\hbar^2 c^4}{2} = 0 \tag{7.10}$$

yields the solution for $\omega_i$.

In our case, because the system of equations is inhomogeneous, our solution for the scale factor will be the homogenous solution plus a particular solution of (7.6)

$$\begin{aligned} \mathsf{a}^2 = &\sum_{i}^{3} A_i^{(k)} \exp(\omega_i \tau) \\ &+ \begin{cases} -\frac{3}{\gamma}\rho_0^2\tau + 3\frac{p_0\rho_0}{\gamma}, & k = 0 \\ 3\tilde{A}\cos(\sqrt{k}\tau) - \tilde{B}\frac{3}{\sqrt{k}}\sin(\sqrt{k}\tau), & k = \pm 1 \end{cases} \end{aligned} \tag{7.11}$$

where we have used units where $c = \hbar = 1$ and

$$\tilde{A} = \frac{\rho_0}{36k^3 + \gamma^2}(12k^2 a_0 + \gamma p_0 - 6k\rho_0)\,, \tag{7.12}$$

$$\tilde{B} = \frac{\rho_0}{36k^3 + \gamma^2}(6k^2 p_0 - 2a_0 k\gamma + \gamma\rho_0)\,. \tag{7.13}$$

Here $A_i^{(k)} = A_i^{(k)}[k, \gamma, a_0, p_0, \rho_0, a_{20}, p_{20}, \Gamma_0]$ is a function of the physical parameters and initial conditions, where $a_0 = \langle \hat{a} \rangle(0)$, $p_0 = \langle \hat{p} \rangle(0)$, $a_{20} = \langle \hat{a}^2 \rangle(0)$, $p_{20} = \langle \hat{p}^2 \rangle(0)$ and $\Gamma_0 = \langle \hat{\Gamma} \rangle(0)$. The initial conditions must be chosen in such a way that the uncertainty principle holds

$$\left(\langle \hat{a}^2 \rangle - \langle \hat{a} \rangle^2\right)\left(\langle \hat{p}^2 \rangle - \langle \hat{p} \rangle^2\right) \geq \left(\frac{1}{2}\langle \hat{\Gamma} \rangle - \langle \hat{a} \rangle\langle \hat{p} \rangle\right)^2 + \frac{1}{4}\,. \tag{7.14}$$

In the sequel we choose to work with $a_0 = p_0 = \gamma_0 = 0$, $p_{20} = 1$ and choose $a_{20} = 1/4$ in order to saturate the uncertainty principle. This states are called coherent states with minimum uncertainty.

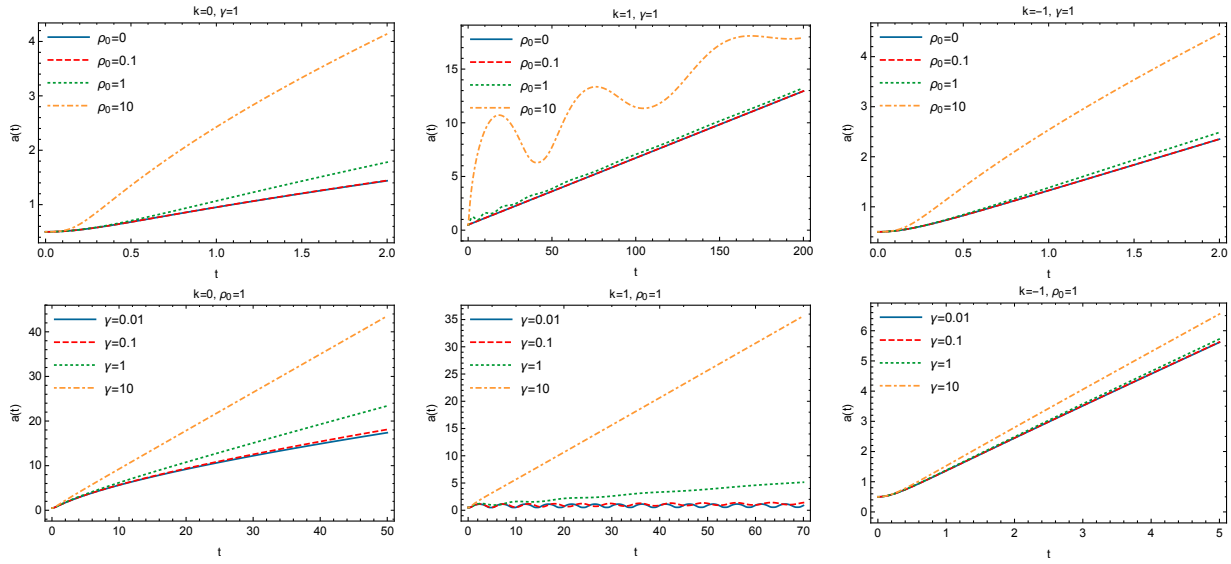


Figure 7.1: Evolution of the scale factor in comoving time for $k = 0$ (left), $k = 1$ (middle ) and $k = -1$ (right). We show results for coherent states with minimal uncertainty, varying $\rho_0$ (top) and $\gamma$ (bottom). In all cases we find that the late time behaviour asymptotes to linear growth; for $k = 1$ the universe is oscillatory at early times that are dominated by small $\gamma$ and/or large $\rho_0$.

### 7.3.1 Scale Factor

In this section we present the results for the behaviour of the scale factor under the classical channel gravity when varying $\gamma$ and $\rho_0$ for the three different values of $k$. In figure 7.1 we depict the scale factor `a` as a function of proper time for fixed $\gamma$ (first row) and $\rho_0$ (second row).

We find for $k = 1$ that the early time behaviour of the scale factor is dominated by oscillations that become sharper for small $\gamma$ or large $\rho_0$. At late times, the scale factor behaves linearly in $t$ in all cases, suggesting an exponential expansion as a function of conformal time. The characteristic equation (7.10) always admits a positive real root for any positive value of $\gamma$ and indeed the solution associated with this root dominates the homogeneous solution. The behaviour of the three different frequencies as a function of gamma is shown in Fig 7.2. Showing in solid lines the pure real root and in dashed the real part of complex roots.

In addition, for $k = 0$ and $k = 1$ the inhomogeneous solution is subdominant at late times since it grows either linearly or oscillates respectively. The case $k = -1$ is different:

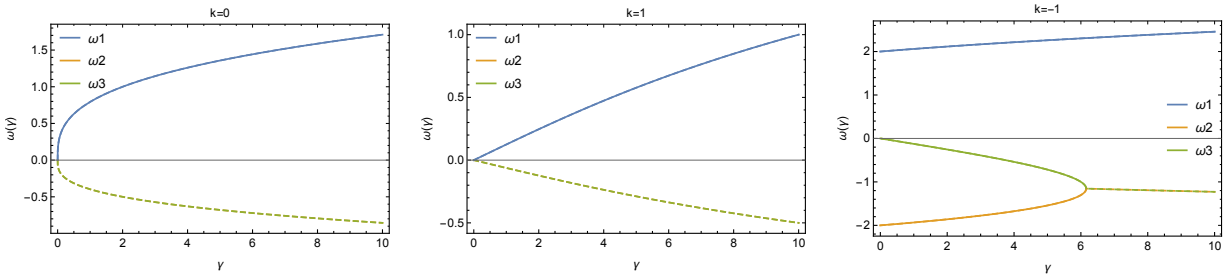


Figure 7.2: Behaviour of the roots of the characteristic equation (7.10) for the three different values of $k$. For all cases the characteristic equation admits a positive real root (solid, blue line). In dashed lines we show the real part of the imaginary solutions and for the cases $k = 0$ and $k = 1$ it coincides for both roots $\omega_1$ and $\omega_2$ (dashed green line – Note that the orange dashed curve is superposed). For the case $k = -1$ the characteristic equation admits two negative real solutions for $\gamma < 6$. The fact that there always exists a positive real solution means that for late time the scale factor will be dominated by this solution.

the inhomogeneous solution is exponential in conformal time $\sim \exp\tau$. This inhomogeneous solution competes with the exponential growth of the homogenous part. However, the rightmost diagram in fig. 7.2 shows that the real root for $k = -1$ is always bigger than 2, which implies an exponential growth of at least $\sim \exp 2\tau$. This analysis shows that for all curvatures the homogenous part of the solution for the scale factor dominates the late time behaviour and thus the late time universe predicted by the classical channel model with matter will behave comparably to the previously studied empty case.

This translates into linear behaviour of the scale factor as a function of comoving time, which in turn indicates a curvature dominated universe. Indeed, for $k = 0$ there exists one positive real root of the characteristic equation (7.10) ($\omega_1$ shown in fig. 7.2 with solid lines) while the other two are complex roots with real part negative (dashed lines). This means that for late conformal times we can write

$$\mathsf{a}^2(\tau) = A_1^{(0)} \exp(\omega_1 \tau)\,, \tag{7.15}$$

which yields a scale factor in proper time

$$\mathsf{a}(t) = \frac{\omega_1}{2} t\,, \tag{7.16}$$

where $\omega_1 = 0.793(\gamma\hbar^2 c^4)^{1/3}$. By use of the Friedmann equation $H^2 = \frac{\kappa}{3}\rho(t)$, where $H = \dot{\mathsf{a}}/\mathsf{a}$ (and the dot denotes the derivative with respect to comoving time $t$), we realize that $\rho(t) \propto \mathsf{a}^{-2}$ which is equivalent to a universe dominated by a positive effective *curvature like* fluid ($K_{\text{eff}} = \omega_1^2/4$). From now on, when we refer to $K_{\text{eff}}$ we mean at the level of

Friedmann equations — the topology of spacelike surfaces does not change and is fixed by $k$. This also implies that for late times the equation of state parameter $w$, defined as $P = w\rho$, is $w = -1/3$. One can see this with use of the second Friedmann equation $\dot{\rho} + 3H(P + \rho) = 0$ and the fact that $\rho(t) \propto \mathsf{a}^{-2}$. We will make a deeper analysis of the equation of state in the next section. Note that because of the exponential behaviour of eq. (7.15) the expression (7.16) for the observed scale factor as a function of the observed proper time $t_p$ is the same i.e. $a_p = \frac{\omega_1}{2} t_p$.

### 7.3.2 Emergent Dark Fluid

For an classical observer unable to access the quantum nature of the scale factor, the universe will be described by Einstein equations

$$G_{ab}(\mathsf{a}_p) = \kappa T_{ab}\,, \tag{7.17}$$

where $G_{ab}$ is the Einstein tensor and $T_{ab}$ is the energy momentum tensor. As noted above, because CCG does not break the homogenous and isotropic symmetries the effective metric for the observer is still of the form (5.18) while the energy momentum tensor is the one associated with a perfect fluid

$$T^{ab} = (\rho + P)U^a U^b + P g^{ab}\,, \tag{7.18}$$

where $\rho$ is the energy density, $P$ the pressure, $U^a = (\frac{\partial}{\partial t})^a$ the 4-velocity of the fluid and $g^{ab}$ the metric. On the other hand, a perfect fluid can be characterized by its equation of state $w$ defined as $P = w\rho$. The Einstein equations guarantee the conservation of the energy momentum tensor $\nabla_a T^{ab} = 0$ and reducing the the two Friedman equations

$$H_u^2 + \frac{k}{\mathsf{a}^2} = \frac{\kappa}{3}\rho\,, \tag{7.19}$$

$$\dot{\rho} - 3H\rho(1 + w) = 0\,, \tag{7.20}$$

where $H_u = \frac{\dot{\mathsf{a}}}{\mathsf{a}}$ is the fiducial Hubble parameter. The above equations can be solved to find

$$\rho(t) = \frac{3}{\kappa}\left(\frac{\dot{\mathsf{a}}^2 + k}{\mathsf{a}^2}\right), \tag{7.21}$$

$$w(t) = -\frac{1}{3}\left(1 + 2\frac{\ddot{\mathsf{a}}\mathsf{a}}{\dot{\mathsf{a}}^2 + k}\right). \tag{7.22}$$

Note that Eqs. (7.19)-(7.22) are for the fiducial quantities and the expression for the physical quantities can be read of Table 5.1. In particular we have that $w = w_p$ where $w_p$ is the

physical observed equation of state. As previously advertised in the last section, for late times the scale factor grows linearly with time, and so has $\ddot{\mathtt{a}} = 0$ and $\dot{\mathtt{a}} = \alpha = \text{constant}$, reducing the above equations to

$$\rho = \frac{3}{\kappa}\frac{1}{\mathtt{a}^2}(\alpha^2 + k)\,, \qquad w = -\frac{1}{3}\,. \tag{7.23}$$

We illustrate the behaviour of the equation of state as a function of comoving time for all values of $k$ and different values of $\rho_0$ in fig. 7.3 (first row) where we see the late time asymptote to $w = -1/3$ for all cases. This implies that the first Friedman equation (7.19) can be written as

$$H_u^2 - \frac{1}{\mathtt{a}^2}(k + \alpha^2) = 0\,, \tag{7.24}$$

giving a universe dominated by curvature with an effective curvature constant $K_{\text{eff}} = 2k + \alpha^2$.

We emphasize that this *curvature domination* is at the level of the Friedmann equations; $K_{\text{eff}}$ does not change the topology of the universe. For $k = 0$ and $k = 1$ the effective curvature is always positive. For $k = -1$ the universe could be hyperbolic if $\alpha^2 < 2$. In the second row of fig. 7.3 we present $K_{\text{eff}}$ for the three different values of $k$ as a function of $\gamma$. As expected, $K_{\text{eff}}$ is insensitive to the value of $\rho_0$ and it is consistent with the analysis that at late times the homogenous part of the solution of the scale factor dominates.

### Separation

As outlined in Sec. 7.3.2 the classical emergent fluid is composed of a purely emergent part due to CCG and a part due to the primordial dust $T^{ab}_{\mathtt{d}}$. Here we outline the strategy for analyzing the classical perfect fluid $T^{ab}$ and how the primordial dust $T^{ab}_{\mathtt{d}}$ affects it.

To this end, note that in CCG the comoving time $t$ is defined *a posteriori* once we have solved eq. (5.17) for the scale factor $\mathtt{a}$. Also note that $t$ is in general different from the proper time $t_{\mathtt{d}}$ of the primordial dust. These two coordinates are respectively defined as

$$\mathtt{a}(\tau)d\tau = dt\,, \qquad a(\tau)d\tau = dt_{\mathtt{d}}\,, \tag{7.25}$$

where $a(\tau)$ is the scale factor entering in eq. (5.5) and $\mathtt{a}(\tau)$. With these definitions we can write the energy-momentum tensor of the dust defined by eq. (5.3) in terms of the classical scale factor $\mathtt{a}$ and its associated comoving time

$$T^{ab}_{\mathtt{d}} = \rho\, U^a_{\mathtt{d}} U^b_{\mathtt{d}} = \rho\,\frac{\mathtt{a}^2}{a^2}\,U^a U^b = \rho_N\, U^a U^b \qquad U^a = \left(\frac{\partial}{\partial t}\right)^a\,, \tag{7.26}$$

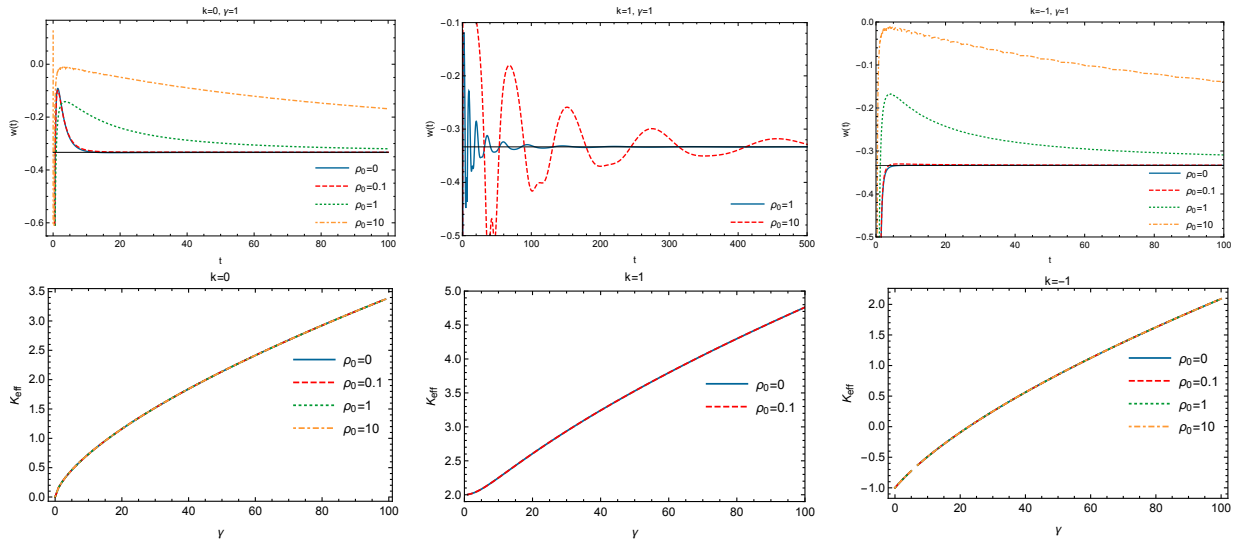


Figure 7.3: Behaviour of the equation of state (top) and $K_{\text{eff}}$ (bottom) for the three different topologies. For large times the equation of state converges to the value $-1/3$ making the universe to be dominated by curvature. The value of the curvature parameter is shown in the bottom part and it does not depend on the value of $\rho_0$. This is because for late time the scale factor is dominated by the homogenous solution that is where the effect of CCG is much stronger than the initial matter content. The case $k = -1$ is the only case that admits a change in sign of $K_{eff}$, $K_{eff} = 0$ (effectively flat - empty universe) can be fine tuned for $\gamma \sim 25$.

where $\rho_N = \rho \frac{\mathtt{a}^2}{a^2}$ and $U^a$ is the four-velocity of the classical fluid $T^{ab}$. We are now interested in whether the dust energy-momentum tensor defined with the previous equation is conserved or not. The divergence of $T^{ab}_{\mathtt{d}}$ in terms of the covariant derivative associated with the metric (5.18) yields

$$\nabla_a T^{ab}_{\mathtt{d}} = \frac{d\rho_N}{dt} - 3H_u\rho_N = \rho\frac{\mathtt{a}}{a^2}\left(\frac{d\,a}{d\,t_{\mathtt{d}}} - \frac{d\mathtt{a}}{dt}\right). \tag{7.27}$$

The right-hand side of (7.27) is generically non-zero. Hence the original dust fluid $T^{ab}_{\mathtt{d}}$ will not be conserved in the classical observed spacetime.

In other words, CCG implies rather naturally a perfect fluid *emergent* from eq. (5.17) that we denote by $T^{ab}$ (since it is the perfect fluid a classical observer will detect) and that is conserved under the covariant derivative associated with the metric (5.18). This emergent fluid has a component that is intrinsic to CCG and another contribution from the primordial dust $T^{ab}_{\mathtt{d}}$. We have shown that we cannot treat $T^{ab}_{\mathtt{d}}$ as a conserved disjoint fluid but we can still describe its properties using

$$T^{ab} = T^{ab}_D + T^{ab}_{\mathtt{d}}\,, \tag{7.28}$$

where $T^{ab}$ was studied in the previous section and $T^{ab}_{\mathtt{d}}$ is defined by equation (7.26). By use of this equation we can write the relation between energy densities and pressures

$$\rho = \rho_D + \rho_o\,, \qquad P = P_D\,, \tag{7.29}$$

where $\rho_o$ denotes the energy density of the primordial dust in the new coordinates (7.26)

$$\rho_o = \rho_0\frac{\mathtt{a}^2}{a^5}\,. \tag{7.30}$$

In the last expression all the quantities are functions of the new comoving time $t$. Note that $a(\tau)$ as a function of conformal time is the solution to a Friedman universe filled with dust and thus

$$a(\tau) = \frac{\kappa}{3}\rho_0 \begin{cases} \sin(\tau/2)^2, & k=1 \\ \tau^2/4, & k=0 \\ \sinh(\tau/2)^2, & k=-1 \end{cases} \tag{7.31}$$

Since an observer in the universe will only infer from measurement one conserved fluid, he/she will not be able to distinguish between the parts ($\rho_{\mathtt{d}}$ , $\rho_o$) that form it. Nevertheless, as shown in fig. 7.1 the presence of $\rho_o$ imparts a quantitative difference to the evolution of the universe as compared to the $\rho_o = 0$ case.

## 7.4 Discussion

Perhaps, the most striking feature of our CCG model with matter is the fact that if the primordial dust is treated as a classical fluid, its influence in the universe will be *washed out* for late times – where the decoherence (dominated by $\gamma$) takes over. An observer at late times will be unable to discern whether or not the universe had some primordial classical matter. On the other hand, the primordial fluid does not have the same consequences as dust has in classical General Relativity. As seen in fig. 7.2 (top), the primordial dust makes the universe expand faster, contrary to the intuition one has from GR – the dust makes the universe contract. In CCG there is an interplay between the value of the primordial dust and the decoherence parameter $\gamma$ conspiring to produce such an effect. Note, however, that in the limit where $\gamma = 0$ (which in turns correspond to a fully classical description) we recover the Friedman equations with dust. Nonetheless, this is not fully satisfactory, since Friedman evolution has been very well constrained by data [18], questioning the necessity to introduce CCG in the first place.

This leaves open the question of how to include matter in the model. Phenomenologically, one could argue that the observed energy momentum tensor (7.18) is indeed composed of cold dark matter and a cosmological constant plus a CCG contribution. The first Friedman equation for the values today can be written as

$$1 = \Omega_b^0 + \Omega_{\rm cdm}^0 + \Omega_{\rm rad}^0 + \Omega_\Lambda^0 + \Omega_k^0 + \Omega_{\rm CCG}^0 \,, \tag{7.32}$$

where $\Omega_i^0 = \frac{\rho_i(t_0)}{\rho_c^0}$ for the respective baryon, cold dark matter, radiation, vacuum, curvature, and CCG contributions, with $\rho_c^0$ the value of the critical density today. Using the results for the cosmological parameters given by Planck [18] we can constrain

$$0 \leq \Omega_k^0 + \Omega_{\rm CCG}^0 \leq 0.001 \pm 0.004 \,, \tag{7.33}$$

In a universe where $k = 0$, since $\mathsf{a}_p = \frac{\omega_1}{2} t_p$ for late times, this implies (upon use of Friedmann equation) that $\rho_{\rm CCG} = 3\omega_1^2/(4\kappa \mathsf{a}_p^2)$, where $\omega_1 = 0.7(\hbar^2 c^4 \gamma)^{1/3}$. With this we can write eq. (7.33) as

$$\Omega_{ccg} = \frac{\omega_1^2}{4(\mathsf{a}_p^0)^2 (H_p^0)^2} < 0.001 \,, \tag{7.34}$$

where the superscript 0 denotes the values today. We finally find

$$\gamma_p < 0.1 (\mathsf{a}_p^0 H_p^0)^3 \left( \frac{V_0}{\kappa \hbar c^2} \right)^2 \sim \frac{10^{66}}{m^6 s} V_0^2 \,. \tag{7.35}$$

Taking the fiducial volume to be the order of the Hubble volume, one finds that $\gamma_p < 10^{266}$!!. This implies that present cosmological observations are far from ruling out this model.

Conversely, one could also conclude that the cosmological effects of the CCG model are of negligible observational consequence.

Is this a game stopper? As discussed above there is still work to be done in trying to understand how to include the presence of classical and quantum matter in CCG in a way that i) is able to reproduce the strongly constrained behaviour of the ΛCDM model and ii) gives a possible resolution to the unsolved problems of this standard model of cosmology.

## 7.5 Conclusion

We have studied the cosmological consequences of the CCG model in a universe containing primordial dust. We found that for late times the homogenous solution dominates, meaning that the fundamental CCG modification is stronger than that of a primordial perfect fluid. Extending the analysis in the previous chapter, we have furthermore found that the equation of state asymptotes to $w = -1/3$, yielding a universe that is curvature-dominated, and computed the effective 'curvature fluid'. This shows that the emergent dark fluid behaves as a curvature parameter in the Einstein equations at late times.

More realistic extensions of this model would include incorporating both vacuum energy and primordial radiation, which should correspond to the effective stress energy of the elementary particles of the standard model. More generally one could add a conserved energy momentum tensor representing different matter components of the universe, analyzing the effect that each has on the evolution of the scale factor in the CCG context. Constrained by current observations [18], the curvature of the observable universe is close to zero suggesting that CCG modifications to Friedman equations must be small enough to i) predict a vacuum-dominated universe and ii) give $\Omega_k \sim 0$. Finally, it would be interesting to study CCG in the context of theories of gravity that violate energy conservation to better understand the observable consequences of CCG and construct a comparison background of theories of modified gravity.

# Chapter 8

# Outlook

## 8.1 Future directions

In this thesis we have studied in detail the Classical Channel Gravity (CCG) model that posits that the gravitational interaction is fundamentally classical, in the sense that it can not transmit quantum information. Starting from a deep analysis of collisional Markovian interactions we have shown that many emergent dynamics can emerge as a result of short weak interactions. Under certain circumstances the dynamics are equivalent to those proposed by gravitational decoherence models. Since the reasearch field is relatively young we are still to find out a fundamentally broad description of gravitational decoherence. Nevertheless this seams a promising path to study the interplay between quantum mechanics and gravity in limits that are (or are soon going to be) reachable. As we showed in this thesis, there are available experiments that can test the predictions of CCG and it remains as a theoretical task to produce a concrete, and physically motivated, extension of CCG to particles of different masses.

Along these lines, with Jamie Breault we are investigating the possibility that instead of minimizing the decoherence rate, one minimizes the heating rate when two particles of different masses are involved in the interaction. Starting with the master equation for two particles interacting under the CCG framework (1.11)

$$\frac{d\hat{\rho}}{dt} = -\frac{i}{\hbar}[\hat{H}_0 + \hat{H}_I, \rho] - \left(\frac{1}{4D_2} + \frac{K^2 D_1}{4\hbar^2}\right)[\hat{x}_2, [\hat{x}_2, \rho]] - \left(\frac{1}{4D_1} + \frac{K^2 D_2}{4\hbar^2}\right)[\hat{x}_1, [\hat{x}_1, \rho]]\,, \quad (8.1)$$

a crucial assumption we have made in ch. 4 is that $D_1 = D_2 = D$ meaning that all the measurement strengths for both particles are the same. Under this assumption the minimization of the decoherence rate gives $\mathcal{D}^{DR}_{min} = \frac{K}{2\hbar}$ for both particles. The $DR$ superscript

denotes decoherence rate. Physically, this means that the noise added to each of this particles is the same regardless of their mass.

The heating rate $R_h$ is defined as the average rate of change of the system's kinetic energy with respect to time due to energy being introduced into the system. The kinetic energy of the system is described by $\hat{H}_0 = \frac{\hat{p}_1^2}{2m_1} + \frac{\hat{p}_2^2}{2m_2}$, the free Hamiltonian for the particles. Using the master equation (8.1) we can compute the heating rate as

$$R_h = \mathrm{Tr}[\hat{H}_0 \dot{\rho}] = \frac{\hbar^2}{m_1}\left(\frac{1}{4D_1} + \frac{K^2 D_2}{4\hbar^2}\right) + \frac{\hbar^2}{m_2}\left(\frac{1}{4D_2} + \frac{K^2 D_1}{4\hbar^2}\right). \tag{8.2}$$

Notice that minimizing heating rate wrt. $D_1$ and $D_2$ is equivalent to minimizing decoherence rate, however, if $D_1 \neq D_2$ we get

$$D_1 = \frac{\hbar}{K}\sqrt{\frac{m_2}{m_1}} \qquad \& \qquad D_2 = \frac{\hbar}{K}\sqrt{\frac{m_1}{m_2}}\,, \tag{8.3}$$

which yields a master equation

$$\frac{d\hat{\rho}}{dt} = -\frac{i}{\hbar}[\hat{H}_0 + \hat{H}_I, \rho] - \frac{K}{2\hbar}\left[\sqrt{\frac{m_2}{m_1}}[\hat{x}_2, [\hat{x}_2, \rho]] + \sqrt{\frac{m_1}{m_2}}[\hat{x}_1, [\hat{x}_1, \rho]]\right]. \tag{8.4}$$

Note that if $m_1 = m_2$ minimizing heating rate yields the same result as minimizing decoherence rate. In addition, note that the most massive particle will decohere much faster than its lighter counterpart, which, in our opinion, is a more physical mechanism for a system with different masses. It remains to compare this with experiments and show that this extension is still a classical channel; in the sense that it can not entangle the particles.

In this thesis we have also studied the cosmological extension of CCG and showed that it predicts the emergence of a perfect fluid acting as a dark fluid filling the universe. We have shown that current observations do not put tight constraints on the model, however future efforts should be directed into trying to understand the testability of this model with current cosmological observations such as the CMB and pulsar timing.

We now discuss a fun fact about our model. In chapters 6 and 7 we have studied the master equation for a universe that has effectively its scale factor constantly being measured by the test particles sitting on spacetime. Now we can ask the question of what happens if the backreaction of these test particles is taken into account? Following the same procedure as in sec. 1.3 and ch. 2 we can show that feedback on the same observable that was measured ($\hat{a}^2$) with a strength $\alpha$ is

$$d\hat{\rho} = \frac{i}{\hbar}[H_0 + \frac{\alpha}{2}a_p^4, \rho]d\tau - \left(\frac{\gamma}{8} + \frac{\alpha}{2\gamma\hbar^2}\right)[a_p^2, [a_p^2, \rho]]d\tau\,. \tag{8.5}$$

The decoherence is minimized by choosing $\gamma = \frac{2\alpha}{\hbar}$. By renaming

$$\alpha = 2\frac{V_0}{\kappa}\Lambda_p\,, \tag{8.6}$$

the master equation is

$$d\rho = -\frac{i}{\hbar}[H_0 + \frac{V_0}{\kappa}\Lambda_p a_p^4]d\tau - \frac{V_0}{\kappa\hbar}\Lambda_p[a_p^2,[a_p^2,\rho]]d\tau\,. \tag{8.7}$$

Note that the feedback mechanism produces an extra unitary term of the form

$$\frac{V_0}{\kappa}\Lambda_p a_p^4\,, \tag{8.8}$$

on top of the usual decoherence term. In a universe dominated by eq. 8.7 an observer will not only see a dark fluid characterized by the decoherence term in (8.7), but will also see a cosmological constant term produced by the extra unitary term. We see this since the term $\frac{V_0}{\kappa}\Lambda_p a_p^4$ is the same appearing in the Hamiltonian produced by the following action

$$S = \frac{1}{2\kappa}\int d^4x\sqrt{-g}[R - 2\Lambda_p]\,. \tag{8.9}$$

Using $\kappa = 8\pi\mathrm{G}\mathrm{c}^{-4}$, $\Lambda_p = 1.1\times10^{-52}\mathrm{m}^{-2}$ and $V_0 = 3.58\times10^{80}\mathrm{m}^3$ to be the Hubble volume we get $\gamma_p \approx 10^{105}$ which is very well within the constraint found in ch. 7, $\gamma_p < 10^{226}$.

Finally we mention that a full extension of CCG for the the full GR construction is missing. Following the ideas developed in this thesis, a possibility to extend to CCG is explore the Hamiltonian of full GR with all its degrees of freedom coupled with matter and think how this matter will decohere the spacetime. An option could be to implement CCG decoherence to all those degrees of freedom that couple with matter degrees of freedom at the level of the Hamiltonian[1]. However, this idea is still 'under construction', and there is still no agreement in the community on how to include gravitational decoherence in the full GR framework.

## 8.2 Final words

Congratulations! You've made it to the end of this thesis. Thank you very much for your interest and for taking the time for reading this. If you have any comments, suggestions or criticisms (constructive ones) feel free to reach me, I'll be happy to hear them.

[1] With Kiran Khosla and Matthew Robbins we are exploring this area.

# References


[1] G. Rosi, F. Sorrentino, L. Cacciapuoti, M. Prevedelli, and G. Tino, "Precision measurement of the Newtonian gravitational constant using cold atoms," *Nature* **510**, 518–521 (2014).

[2] T. Kovachy, P. Asenbaum, C. Overstreet, C. Donnelly, S. Dickerson, A. Sugarbaker, J. Hogan, and M. Kasevich, "Quantum superposition at the half-metre scale," *Nature* **528**, 530–533 (2015).

[3] S. Eibenberger, S. Gerlich, M. Arndt, M. Mayor, and J. Tüxen, "Matter–wave interference of particles selected from a molecular library with masses exceeding 10000 amu," *Physical Chemistry Chemical Physics* **15**, 14696–14700 (2013).

[4] M. Sclafani, T. Juffmann, C. Knobloch, and M. Arndt, "Quantum coherent propagation of complex molecules through the frustule of the alga Amphipleura pellucida," *New Journal of Physics* **15**, 083004 (2013).

[5] L. Diosi, "Notes on certain Newton gravity mechanisms of wavefunction localization and decoherence," *Journal of Physics A: Mathematical and Theoretical* **40**, 2989 (2007).

[6] I. Pikovski, "On Quantum Superpositions in an Optomechanical System," diploma thesis, Freie Universität Berlin, 2009.

[7] A. Sugarbaker, " Atom interferometry in a 10 m fountain, Stanford, 2014,".

[8] D. Kafri, J. M. Taylor, and G. J. Milburn, "A classical channel model for gravitational decoherence," *New J. Phys.* **16**, 065020 (2014).

[9] **Particle Data Group** Collaboration, J. Beringer *et al.*, "Review of Particle Physics (RPP)," *Phys. Rev.* **D86**, 010001 (2012).

[10] **LIGO Scientific Collaboration and Virgo Collaboration** Collaboration, B. P. Abbott and *et.al*, "Observation of Gravitational Waves from a Binary Black Hole Merger," *Phys. Rev. Lett.* **116**, 061102 (2016). https://link.aps.org/doi/10.1103/PhysRevLett.116.061102.

[11] **LIGO Scientific Collaboration and Virgo Collaboration** Collaboration, B. P. Abbott and *et.al*, "GW170814: A Three-Detector Observation of Gravitational Waves from a Binary Black Hole Coalescence," *Phys. Rev. Lett.* **119**, 141101 (2017). https://link.aps.org/doi/10.1103/PhysRevLett.119.141101.

[12] **LIGO Scientific Collaboration and Virgo Collaboration** Collaboration, B. P. Abbott and *et.al*, "GW170817: Observation of Gravitational Waves from a Binary Neutron Star Inspiral," *Phys. Rev. Lett.* **119**, 161101 (2017). https://link.aps.org/doi/10.1103/PhysRevLett.119.161101.

[13] T. Baker, D. Psaltis, and C. Skordis, "Linking Tests of Gravity on All Scales: from the Strong-field Regime to Cosmology," *The Astrophysical Journal* **802**, 63 (2015). http://stacks.iop.org/0004-637X/802/i=1/a=63.

[14] J. Polchinski, *String theory. Vol. 1: An introduction to the bosonic string*. Cambridge University Press, 2007.

[15] C. Rovelli, "Loop quantum gravity: the first twenty five years," *Class. Quant. Grav.* **28**, 153002 (2011), arXiv:1012.4707 [gr-qc].

[16] R. Penrose, "On the Gravitization of Quantum Mechanics 1: Quantum State Reduction," *Foundations of Physics* **44**, 557–575 (2014).

[17] R. D. Sorkin, "Light, links and causal sets," *Journal of Physics: Conference Series* **174**, 012018 (2009). http://stacks.iop.org/1742-6596/174/i=1/a=012018.

[18] **Planck** Collaboration, P. A. R. Ade *et al.*, "Planck 2015 results. XIII. Cosmological parameters," *Astron. Astrophys.* **594**, A13 (2016), arXiv:https://arxiv.org/abs/1502.01589 [astro-ph.CO].

[19] W. G. Unruh, "Notes on black-hole evaporation," *Phys. Rev. D* **14**, 870–892 (1976). https://link.aps.org/doi/10.1103/PhysRevD.14.870.

[20] S. W. HAWKING, "Black hole explosions?," *Nature* **248**, 30 EP – (1974). http://dx.doi.org/10.1038/248030a0.

[21] S. W. Hawking, "Particle creation by black holes," *Communications in Mathematical Physics* **43**, 199–220 (1975). https://doi.org/10.1007/BF02345020.

[22] J. Polchinski, "The Black Hole Information Problem," in *Proceedings, Theoretical Advanced Study Institute in Elementary Particle Physics: New Frontiers in Fields and Strings (TASI 2015): Boulder, CO, USA, June 1-26, 2015*, pp. 353–397. 2017. arXiv:1609.04036 [hep-th]. https://inspirehep.net/record/1486509/files/arXiv:1609.04036.pdf.

[23] O. Lunin and S. D. Mathur, "Statistical Interpretation of the Bekenstein Entropy for Systems with a Stretched Horizon," *Phys. Rev. Lett.* **88**, 211303 (2002). https://link.aps.org/doi/10.1103/PhysRevLett.88.211303.

[24] O. Lunin and S. D. Mathur, "AdS/CFT duality and the black hole information paradox," *Nuclear Physics B* **623**, 342 – 394 (2002). http://www.sciencedirect.com/science/article/pii/S0550321301006204.

[25] U. Leonhardt, I. Griniasty, S. Wildeman, E. Fort, and M. Fink, "Classical analogue of the Unruh effect," arXiv:1709.02200 [gr-qc].

[26] J. Abedi, H. Dykaar, and N. Afshordi, "Echoes from the abyss: Tentative evidence for Planck-scale structure at black hole horizons," *Phys. Rev. D* **96**, 082004 (2017). https://link.aps.org/doi/10.1103/PhysRevD.96.082004.

[27] J. Abedi and N. Afshordi, "Echoes from the Abyss: A highly spinning black hole remnant for the binary neutron star merger GW170817," arXiv:1803.10454 [gr-qc].

[28] S. B. Giddings, "Possible observational windows for quantum effects from black holes," *Phys. Rev. D* **90**, 124033 (2014). https://link.aps.org/doi/10.1103/PhysRevD.90.124033.

[29] S. B. Giddings and D. Psaltis, "Event Horizon Telescope observations as probes for quantum structure of astrophysical black holes," *Phys. Rev. D* **97**, 084035 (2018). https://link.aps.org/doi/10.1103/PhysRevD.97.084035.

[30] R. C. Ritter, C. E. Goldblum, W.-T. Ni, G. T. Gillies, and C. C. Speake, "Experimental test of equivalence principle with polarized masses," *Phys. Rev. D* **42**, 977–991 (1990). https://link.aps.org/doi/10.1103/PhysRevD.42.977.

[31] S. Gerlich, L. Hackermüller, K. Hornberger, A. Stibor, H. Ulbricht, M. Gring, F. Goldfarb, T. Savas, M. Müri, M. Mayor, and M. Arndt, "A Kapitza–Dirac–Talbot–Lau interferometer for highly polarizable molecules," *Nature Physics* **3**, 711 EP – (2007). http://dx.doi.org/10.1038/nphys701.

[32] S. Gerlich, S. Eibenberger, M. Tomandl, S. Nimmrichter, K. Hornberger, P. J. Fagan, J. Tüxen, M. Mayor, and M. Arndt, "Quantum interference of large organic molecules," *Nature Communications* **2**, 263 EP – (2011). http://dx.doi.org/10.1038/ncomms1263.

[33] S. Eibenberger, S. Gerlich, M. Arndt, M. Mayor, and J. Tuxen, "Matter-wave interference of particles selected from a molecular library with masses exceeding 10 000 amu," *Phys. Chem. Chem. Phys.* **15**, 14696–14700 (2013). http://dx.doi.org/10.1039/C3CP51500A.

[34] C. Pfister, J. Kaniewski, M. Tomamichel, A. Mantri, R. Schmucker, N. McMahon, G. Milburn, and S. Wehner, "A universal test for gravitational decoherence," *Nature Communications* **7**, 13022 (2016).

[35] P. H. Kim, B. D. Hauer, C. Doolin, F. Souris, and J. P. Davis, "Approaching the standard quantum limit of mechanical torque sensing," *Nature Communications* **7**, 13165 EP – (2016). http://dx.doi.org/10.1038/ncomms13165.

[36] A. Peters, K. Y. Chung, and S. Chu, "High-precision gravity measurements using atom interferometry," *Metrologia* **38**, 25 (2001). http://stacks.iop.org/0026-1394/38/i=1/a=4.

[37] S.-w. Chiow, T. Kovachy, H.-C. Chien, and M. A. Kasevich, "102$\hbar k$ Large Area Atom Interferometers," *Phys. Rev. Lett.* **107**, 130403 (2011). https://link.aps.org/doi/10.1103/PhysRevLett.107.130403.

[38] G. Tino, F. Sorrentino, D. Aguilera, B. Battelier, A. Bertoldi, Q. Bodart, K. Bongs, P. Bouyer, C. Braxmaier, L. Cacciapuoti, N. Gaaloul, N. Gürlebeck, M. Hauth, S. Herrmann, M. Krutzik, A. Kubelka, A. Landragin, A. Milke, A. Peters, E. Rasel, E. Rocco, C. Schubert, T. Schuldt, K. Sengstock, and A. Wicht, "Precision Gravity Tests with Atom Interferometry in Space," *Nuclear Physics B - Proceedings Supplements* **243-244**, 203 – 217 (2013). http://www.sciencedirect.com/science/article/pii/S0920563213005471. Proceedings of the IV International Conference on Particle and Fundamental Physics in Space.

[39] D. J. Kapner, T. S. Cook, E. G. Adelberger, J. H. Gundlach, B. R. Heckel, C. D. Hoyle, and H. E. Swanson, "Tests of the Gravitational Inverse-Square Law below the Dark-Energy Length Scale," *Phys. Rev. Lett.* **98**, 021101 (2007). https://link.aps.org/doi/10.1103/PhysRevLett.98.021101.

[40] J. Schmöle, M. Dragosits, H. Hepach, and M. Aspelmeyer, "A micromechanical proof-of-principle experiment for measuring the gravitational force of milligram masses," *Classical and Quantum Gravity* **33**, 125031 (2016). http://stacks.iop.org/0264-9381/33/i=12/a=125031.

[41] A. Bassi, A. Großardt, and H. Ulbricht, "Gravitational decoherence," *Classical and Quantum Gravity* **34**, 193002 (2017). http://stacks.iop.org/0264-9381/34/i=19/a=193002.

[42] S. anchez G omez J L, "Stochastic Evolution of Quantum States in Open Systems and in Measurement Processes," *(Singapore: World Scientific) chap Decoherence Through Stochastic Fluctuations of the Gravitational Field, pp 88–93* (1993).

[43] E. Göklü and C. Lämmerzahl, "Metric fluctuations and the weak equivalence principle," *Classical and Quantum Gravity* **25**, 105012 (2008). http://stacks.iop.org/0264-9381/25/i=10/a=105012.

[44] H.-P. Breuer, E. Göklü, and C. Lämmerzahl, "Metric fluctuations and decoherence," *Classical and Quantum Gravity* **26**, 105012 (2009). http://stacks.iop.org/0264-9381/26/i=10/a=105012.

[45] Z. Haba, "Decoherence by Relic Gravitons," *Modern Physics Letters A* **15**, 1519–1527 (2000).

[46] B. L. Hu and E. Verdaguer, "Stochastic Gravity: Theory and Applications," *Living Reviews in Relativity* **11**, 3 (2008). https://doi.org/10.12942/lrr-2008-3.

[47] M. P. Blencowe, "Effective Field Theory Approach to Gravitationally Induced Decoherence," *Phys. Rev. Lett.* **111**, 021302 (2013). https://link.aps.org/doi/10.1103/PhysRevLett.111.021302.

[48] C. Anastopoulos and B. Hu, "A master equation for gravitational decoherence: probing the textures of spacetime," *Classical and Quantum Gravity* **30**, 165007 (2013).

[49] P. Kok and U. Yurtsever, "Gravitational decoherence," *Phys. Rev. D* **68**, 085006 (2003). https://link.aps.org/doi/10.1103/PhysRevD.68.085006.

[50] G. J. Milburn, "Intrinsic decoherence in quantum mechanics," *Phys. Rev. A* **44**, 5401–5406 (1991). https://link.aps.org/doi/10.1103/PhysRevA.44.5401.

[51] A. Bassi, K. Lochan, S. Satin, T. P. Singh, and H. Ulbricht, "Models of Wave-function Collapse, Underlying Theories, and Experimental Tests," *Rev. Mod. Phys.* **85**, 471–527 (2013), arXiv:1204.4325 [quant-ph].

[52] L. Diósi, "Models for universal reduction of macroscopic quantum fluctuations," *Phys. Rev. A* **40**, 1165 (1989).

[53] L. Diósi, "The gravity-related decoherence master equation from hybrid dynamics," *Journal of Physics: Conference Series* **306**, 012006 (2011).

[54] A. S. L. C. C. U. Press), "Gravitation and the noise needed in objective reduction models Quantum Nonlocality and Reality: 50 Years of Bell's Theorem ed Bell M and Gao S," *Cambridge: Cambridge University Press* (2016).

[55] F. Karolyhazy, "Gravitation and quantum mechanics of macroscopic objects," *Nuov Cim A* **42**, 390–402 (1966).

[56] L. Diosi, "Gravitation and quantummechanical localization of macroobjects," *Phys. Lett.* **A105**, 199–202 (1984), arXiv:1412.0201 [quant-ph].

[57] R. Penrose, "On Gravity's role in Quantum State Reduction," *Gen Relat Gravit* **28**, 581–600 (1996).

[58] I. Pikovski, M. Zych, F. Costa, and C. Brukner, "Universal decoherence due to gravitational time dilation," *Nat Phys* **advance online publication**, (2015).

[59] E. Castro Ruiz, F. Giacomini, and Č. Brukner, "Entanglement of quantum clocks through gravity," *Proceedings of the National Academy of Sciences* **114**, E2303–E2309 (2017).

[60] E. Nelson, "Quantum decoherence during inflation from gravitational nonlinearities," *Journal of Cosmology and Astroparticle Physics* **2016**, 022 (2016). http://stacks.iop.org/1475-7516/2016/i=03/a=022.

[61] C. P. Burgess, R. Holman, G. Tasinato, and M. Williams, "EFT beyond the horizon: stochastic inflation and how primordial quantum fluctuations go classical," *Journal of High Energy Physics* **2015**, 90 (2015). https://doi.org/10.1007/JHEP03(2015)090.

[62] P. Martineau, "On the decoherence of primordial fluctuations during inflation," *Classical and Quantum Gravity* **24**, 5817 (2007). http://stacks.iop.org/0264-9381/24/i=23/a=006.

[63] M. Franco and E. Calzetta, "Decoherence in the cosmic background radiation," *Classical and Quantum Gravity* **28**, 145024 (2011). http://stacks.iop.org/0264-9381/28/i=14/a=145024.

[64] M. J. Hall and M. Reginatto, "Interacting classical and quantum ensembles," *Physical Review A* **72**, 062109 (2005).

[65] M. Albers, C. Kiefer, and M. Reginatto, "Measurement analysis and quantum gravity," *Phys. Rev. D* **78**, 064051 (2008).

[66] M. J. Hall and M. Reginatto, *Ensembles on Configuration Space: Classical, Quantum, and Beyond*, vol. 184. Springer, 2016.

[67] A. Tilloy and L. Diósi, "Sourcing semiclassical gravity from spontaneously localized quantum matter," *Phys. Rev. D* **93**, 024026 (2016).

[68] "On gravity's role in quantum state reduction," *General Relativity and Gravitation* **28**, 581–600 (1996).

[69] T. Jacobson, "Thermodynamics of spacetime: the Einstein equation of state," *Physical Review Letters* **75**, 1260 (1995).

[70] D. N. Page and C. D. Geilker, "Indirect Evidence for Quantum Gravity," *Phys. Rev. Lett.* **47**, 979–982 (1981).

[71] C. J. Isham, "Canonical quantum gravity and the problem of time," in *Integrable systems, quantum groups, and quantum field theories*, pp. 157–287. Springer, 1993.

[72] K. Eppley and E. Hannah, "The necessity of quantizing the gravitational field," *Foundations of Physics* **7**, 51 (1977).

[73] C. Marletto and V. Vedral, "Why we need to quantise everything, including gravity," *NPJ Quantum Information* **3**, (2017).

[74] C. Kiefer, *Quantum Gravity*. Oxford University Press, Oxford, 2012.

[75] C. Marletto and V. Vedral, "Witness gravity's quantum side in the lab," *Nature* **547**, 156–158 (2017).

[76] C. Marletto and V. Vedral, "Gravitationally Induced Entanglement between Two Massive Particles is Sufficient Evidence of Quantum Effects in Gravity," *Phys. Rev. Lett.* **119**, 240402 (2017).

[77] S. Bose, A. Mazumdar, G. W. Morley, H. Ulbricht, M. Toroš, M. Paternostro, A. A. Geraci, P. F. Barker, M. S. Kim, and G. Milburn, "Spin Entanglement Witness for Quantum Gravity," *Phys. Rev. Lett.* **119**, 240401 (2017).

[78] C. Anastopoulos and B.-L. Hu, "Comment on "A Spin Entanglement Witness for Quantum Gravity" and on "Gravitationally Induced Entanglement between Two Massive Particles is Sufficient Evidence of Quantum Effects in Gravity"," arXiv:1804.11315 [quant-ph].

[79] D. Kafri and J. M. Taylor, "A noise inequality for classical forces," *ArXiv e-prints* (2013), arXiv:1311.4558 [quant-ph].

[80] H. M. Wiseman and G. J. Milburn, *Quantum measurement and control*. Cambridge University Press, 2009.

[81] K. Jacobs, *Quantum measurement theory and its applications*. Cambridge University Press, 2014.

[82] R. Colella, A. W. Overhauser, and S. A. Werner, "Observation of gravitationally induced quantum interference," *Physical Review Letters* **34**, 1472 (1975).

[83] V. V. Nesvizhevsky, H. G. Börner, A. K. Petukhov, H. Abele, S. Baeßler, F. J. Rueß, T. Stöferle, A. Westphal, A. M. Gagarski, G. A. Petrov, *et al.*, "Quantum states of neutrons in the Earth's gravitational field," *Nature* **415**, 297–299 (2002).

[84] G. Rosi, L. Cacciapuoti, F. Sorrentino, M. Menchetti, M. Prevedelli, and G. M. Tino, "Measurement of the Gravity-Field Curvature by Atom Interferometry," *Phys. Rev. Lett.* **114**, 013001 (2015).

[85] P. Asenbaum, C. Overstreet, T. Kovachy, D. D. Brown, J. M. Hogan, and M. A. Kasevich, "Phase Shift in an Atom Interferometer due to Spacetime Curvature across its Wave Function," *Phys. Rev. Lett.* **118**, 183602 (2017).

[86] D. Kafri, G. J. Milburn, and J. M. Taylor, "Bounds on quantum communication via Newtonian gravity," *New J. Phys.* **17**, 015006 (2015).

[87] G. Baym and T. Ozawa, "Two-slit diffraction with highly charged particles: Niels Bohr's consistency argument that the electromagnetic field must be quantized," *PNAS* **106**, 3035–3040 (2009). http://www.pnas.org/content/106/9/3035.

[88] M. A. Nielsen, "Conditions for a Class of Entanglement Transformations," *Phys. Rev. Lett.* **83**, 436–439 (1999). http://link.aps.org/doi/10.1103/PhysRevLett.83.436.

[89] Y. Aharonov, D. Z. Albert, and L. Vaidman, "How the result of a measurement of a component of the spin of a spin- \textit{1/2} particle can turn out to be 100," *Phys. Rev. Lett.* **60**, 1351–1354 (1988). http://link.aps.org/doi/10.1103/PhysRevLett.60.1351.

[90] C. W. Gardiner and M. J. Collett, "Input and output in damped quantum systems: Quantum stochastic differential equations and the master equation," *Phys. Rev. A* **31**, 3761–3774 (1985). http://link.aps.org/doi/10.1103/PhysRevA.31.3761.

[91] L. Diósi, "Quantum dynamics with two Planck constants and the semiclassical limit," *arXiv:quant-ph/9503023* (1995). http://arxiv.org/abs/quant-ph/9503023.

[92] L. Diósi, N. Gisin, and W. T. Strunz, "Quantum approach to coupling classical and quantum dynamics," *Phys. Rev. A* **61**, 022108 (2000). http://link.aps.org/doi/10.1103/PhysRevA.61.022108.

[93] M. A. Nielsen and I. L. Chuang, *Quantum Computation and Quantum Information*. ambridge University Press, Cambridge, 2000.

[94] C. M. Caves and G. J. Milburn, "Quantum-mechanical model for continuous position measurements," *Phys. Rev. A* **36**, 5543–5555 (1987).

[95] N. Altamirano, P. Corona-Ugalde, R. B. Mann, and M. Zych, "Unitarity, Feedback, Interactions – Dynamics Emergent from Repeated Measurements," *New J. Phys.* **19**, 013035 (2017), arXiv:https://arxiv.org/abs/1605.04312 [quant-ph].

[96] K. Khosla and N. Altamirano, "Detecting gravitational decoherence with clocks: Limits on temporal resolution from a classical channel model of gravity," *Phys. Rev.* **A95**, 052116 (2017), arXiv:https://arxiv.org/abs/1611.09919 [quant-ph].

[97] N. Altamirano, P. Corona-Ugalde, R. B. Mann, and M. Zych, "Gravity is not a Pairwise Local Classical Channel," arXiv:1612.07735 [quant-ph].

[98] N. Altamirano, P. Corona-Ugalde, K. Khosla, R. B. Mann, and G. Milburn, "Emergent dark energy via decoherence in quantum interactions," *Class. Quant. Grav.* **34**, 115007 (2017), arXiv:https://arxiv.org/abs/1605.05980 [gr-qc].

[99] R. Pascalie, N. Altamirano, and R. B. Mann, "Emergent Dark Energy in Classical Channel Gravity with Matter," *ArXiv e-prints* (2017), arXiv:1706.02312 [gr-qc].

[100] J. VonNeumann, *Mathematical Foundations of Quantum Mechanics*. Princeton University Press, 1955.

[101] G. Lüders, "Concerning the state-change due to the measurement process," *Ann. Phys.* **8**, 322 (1951).

[102] K. Kraus, *States, Effects and Operations: Fundamental Notions of Quantum Theory*. Lecture Notes in Physics (190). Spring-Verlag, Berlin, 1983.

[103] H.-P. Breuer and F. Petruccione, *The theory of open quantum systems*. Oxford Univ. Press, 2002.

[104] W. Stinespring, "Positive Functions on C*-algebras," *Proceedings of the American Mathematical Society* **6**, 211–216 (1955).

[105] S. Lloyd, "Universal quantum simulators," *Science* **273**, 1073 (1996).

[106] T. D. Ladd, F. Jelezko, R. Laflamme, Y. Nakamura, C. Monroe, and J. L. O/'Brien, "Quantum computers," *Nature* **464**, 45–53 (2010).

[107] J. Du, X. Rong, N. Zhao, Y. Wang, J. Yang, and R. B. Liu, "Preserving electron spin coherence in solids by optimal dynamical decoupling," *Nature* **461**, 1265–1268 (2009).

[108] L. Viola, E. Knill, and S. Lloyd, "Dynamical Decoupling of Open Quantum Systems," *Phys. Rev. Lett.* **82**, 2417–2421 (1999).

[109] S. Weinberg, *The quantum theory of fields*, vol. 2. Cambridge University Press, 1996.

[110] L. Diósi, "A Universal Master Equation for the Gravitational Violation of Quantum Mechanics," *Phys. Lett. A* **120**, 377 (1987).

[111] J. Rau, "Relaxation Phenomena in Spin and Harmonic Oscillator Systems," *Phys. Rev.* **129**, 1880–1888 (1963).

[112] R. Alicki and K. Lendi, *Quantum Dynamical Semigroups and Applications*, vol. 717 of *Lecture Notes in Physics*. Springer-Verlag, Berlin Heidelberg, 1987.

[113] M. Ziman and V. Bužek, "All (qubit) decoherences: Complete characterization and physical implementation," *Phys. Rev. A* **72**, 022110 (2005).

[114] M. Ziman, P. Štelmachovič, and V. Bužek, "Description of Quantum Dynamics of Open Systems Based on Collision-Like Models," *Open Syst. Inf. Dyn.* **12**, 81–91 (2005).

[115] D. Layden, E. Martín-Martínez, and A. Kempf, "Universal scheme for indirect quantum control," *PRA* **93**, 040301 (2016).

[116] D. Layden, E. Martín-Martínez, and A. Kempf, "Perfect Zeno-like effect through imperfect measurements at a finite frequency," *PRA* **91**, 022106 (2015).

[117] D. Grimmer, D. Layden, R. B. Mann, and E. Martín-Martínez, "Open dynamics under rapid repeated interaction," *Phys. Rev. A* **94**, 032126 (2016).

[118] D. A. Lidar and K. Birgitta Whaley, *Irreversible Quantum Dynamics*, ch. Decoherence-Free Subspaces and Subsystems, pp. 83–120. Springer Berlin Heidelberg, Berlin, Heidelberg, 2003.

[119] B. Misra and E. C. G. Sudarshan, "The Zeno's Paradox in Quantum Theory," *J. Math. Phys.* **18**, 756 (1977).

[120] P. Facchi and S. Pascazio, "Quantum Zeno Subspaces," *Phys. Rev. Lett.* **89**, 080401 (2002).

[121] S. Lloyd, "Coherent quantum feedback," *Phys. Rev. A* **62**, 022108 (2000).

[122] M. B. Plenio, V. Vedral, and P. L. Knight, "Quantum error correction in the presence of spontaneous emission," *Phys. Rev. A* **55**, 67–71 (1997).

[123] A. Napoli, M. Guccione, A. Messina, and D. Chruściński, "Interaction-free evolving states of a bipartite system," *Phys. Rev. A* **89**, 062104 (2014).

[124] G. J. Milburn, "Decoherence and the conditions for the classical control of quantum systems," *Phil. Trans. R. Soc. A* **370**, 4469–4486 (2012).

[125] P. Busch, *Quantum Reality, Relativistic Causality, and Closing the Epistemic Circle: Essays in Honour of Abner Shimony*, ch. "No Information Without Disturbance": Quantum Limitations of Measurement, pp. 229–256. Springer Netherlands, Dordrecht, 2009.

[126] E. W. Streed, J. Mun, M. Boyd, G. K. Campbell, P. Medley, W. Ketterle, and D. E. Pritchard, "Continuous and Pulsed Quantum Zeno Effect," *Phys. Rev. Lett.* **97**, 260402 (2006).

[127] M. J. Gagen and G. J. Milburn, "Quantum Zeno effect induced by quantum-nondemolition measurement of photon number," *Phys. Rev. A* **45**, 5228–5236 (1992).

[128] P. Facchi, H. Nakazato, S. Pascazio, and S. Tasaki, "Control of decoherence via quantum Zeno subspaces," *International Journal of Modern Physics B* **20**, 1408–1420 (2006).

[129] N. Syassen, D. M. Bauer, M. Lettner, T. Volz, D. Dietze, J. J. García-Ripoll, J. I. Cirac, G. Rempe, and S. Dürr, "Strong Dissipation Inhibits Losses and Induces Correlations in Cold Molecular Gases," *Science* **320**, 1329–1331 (2008).

[130] A. J. Daley, J. M. Taylor, S. Diehl, M. Baranov, and P. Zoller, "Atomic Three-Body Loss as a Dynamical Three-Body Interaction," *Phys. Rev. Lett.* **102**, 040402 (2009).

[131] M. Roncaglia, M. Rizzi, and J. I. Cirac, "Pfaffian State Generation by Strong Three-Body Dissipation," *Phys. Rev. Lett.* **104**, 096803 (2010).

[132] C.-E. Bardyn, M. A. Baranov, C. V. Kraus, E. Rico, A. İmamoğlu, P. Zoller, and S. Diehl, "Topology by dissipation," *New Journal of Physics* **15**, 085001 (2013).

[133] J. Zhang, Y.-x. Liu, R.-B. Wu, K. Jacobs, and F. Nori, "Quantum feedback: theory, experiments, and applications," *arXiv preprint arXiv:1407.8536* (2014).

[134] N. Yamamoto, "Coherent versus Measurement Feedback: Linear Systems Theory for Quantum Information," *Phys. Rev. X* **4**, 041029 (2014).

[135] K. Jacobs, X. Wang, and H. M. Wiseman, "Coherent feedback that beats all measurement-based feedback protocols," *New Journal of Physics* **16**, 073036 (2014).

[136] M. Poggio, C. L. Degen, H. J. Mamin, and D. Rugar, "Feedback Cooling of a Cantilever's Fundamental Mode below 5 mK," *Phys. Rev. Lett.* **99**, 017201 (2007).

[137] P. Bushev, D. Rotter, A. Wilson, F. m. c. Dubin, C. Becher, J. Eschner, R. Blatt, V. Steixner, P. Rabl, and P. Zoller, "Feedback Cooling of a Single Trapped Ion," *Phys. Rev. Lett.* **96**, 043003 (2006).

[138] M. Koch, C. Sames, A. Kubanek, M. Apel, M. Balbach, A. Ourjoumtsev, P. W. H. Pinkse, and G. Rempe, "Feedback Cooling of a Single Neutral Atom," *Phys. Rev. Lett.* **105**, 173003 (2010).

[139] H.-A. Bachor and T. C. Ralph, *A guide to experiments in quantum optics*, vol. Physics textbook. Wiley-VCH, 2004.

[140] W. Bowen and G. Milburn, *Quantum Optomechanics*. Taylor & Francis, 2015.

[141] K. Hammerer, A. S. Sørensen, and E. S. Polzik, "Quantum interface between light and atomic ensembles," *Rev. Mod. Phys.* **82**, 1041–1093 (2010).

[142] J. Wang, H. M. Wiseman, and G. J. Milburn, "Dynamical creation of entanglement by homodyne-mediated feedback," *Phys. Rev. A* **71**, 042309 (2005).

[143] A. R. R. Carvalho, M. Busse, O. Brodier, C. Viviescas, and A. Buchleitner, "Optimal Dynamical Characterization of Entanglement," *Phys. Rev. Lett.* **98**, 190501 (2007).

[144] A. S. Sørensen and K. Mølmer, "Measurement Induced Entanglement and Quantum Computation with Atoms in Optical Cavities," *Phys. Rev. Lett.* **91**, 097905 (2003).

[145] C. W. Chou, H. de Riedmatten, D. Felinto, S. V. Polyakov, S. J. van Enk, and H. J. Kimble, "Measurement-induced entanglement for excitation stored in remote atomic ensembles," *Nature* **438**, 828–832 (2005).

[146] N. Roch, M. E. Schwartz, F. Motzoi, C. Macklin, R. Vijay, A. W. Eddins, A. N. Korotkov, K. B. Whaley, M. Sarovar, and I. Siddiqi, "Observation of Measurement-Induced Entanglement and Quantum Trajectories of Remote Superconducting Qubits," *Phys. Rev. Lett.* **112**, 170501 (2014).

[147] H. Bernien, B. Hensen, W. Pfaff, G. Koolstra, M. Blok, L. Robledo, T. Taminiau, M. Markham, D. Twitchen, L. Childress, *et al.*, "Heralded entanglement between solid-state qubits separated by three metres," *Nature* **497**, 86–90 (2013).

[148] F. A. Pollock, C. Rodriguez-Rosario, T. Frauenheim, M. Paternostro, and K. Modi, "Non-Markovian quantum processes: Complete framework and efficient characterization," *Physical Review A* **97**, (2018), `arXiv:1512.00589`.

[149] H.-P. Breuer, E.-M. Laine, J. Piilo, and B. Vacchini, "*Colloquium* : Non-Markovian dynamics in open quantum systems," *Rev. Mod. Phys.* **88**, 021002 (2016).

[150] T. Rybár, M. Ziman, P. Štelmachovič, and V. Bužek, "Simulation of indivisible qubit channels in collision models," *J. Phys. B: At. Mol. Opt. Phys.* **45**, 154006 (2012).

[151] F. Ciccarello, G. M. Palma, and V. Giovannetti, "Collision-model-based approach to non-Markovian quantum dynamics," *Phys. Rev. A* **87**, 040103 (2013).

[152] K. Modi, "Operational approach to open dynamics and quantifying initial correlations," *Sci. Rep.* **2**, 581 (2012).

[153] N. D. Birrell and P. C. W. Davies, *Quantum fields in curved space*. No. 7. Cambridge university press, 1984.

[154] R. Gambini and J. Pullin, "Free will, undecidability, and the problem of time in quantum gravity," *arXiv:0903.1859* (2009), arXiv:0903.1859.

[155] D. N. Page and W. K. Wootters, "Evolution without evolution: Dynamics described by stationary observables," *Phys. Rev. D* **27**, 2885–2892 (1983).

[156] T. G. Downes, G. J. Milburn, and C. M. Caves, "Optimal Quantum Estimation for Gravitation," arXiv:1108.5220.

[157] M. Zych, F. Costa, I. Pikovski, and C. Brukner, "Quantum interferometric visibility as a witness of general relativistic proper time," *Nature Communications* **2**, 505 (2011).

[158] J. Schmole, M. Dragosits, H. Hepach, and M. Aspelmeyer, "A micromechanical proof-of-principle experiment for measuring the gravitational force of milligram masses," *Class. Quantum Grav.* **33**, 125031 (2016).

[159] S.-Y. Lin, "Radiation by an Unruh-DeWitt Detector in Oscillatory Motion," arXiv:1601.07006.

[160] I. Pikovski, M. R. Vanner, M. Aspelmeyer, M. S. Kim, and C. Brukner, "Probing Planck-scale physics with quantum optics," *Nature Physics* **8**, 393–397 (2012).

[161] Y. Li, A. M. Steane, D. Bedingham, and G. A. D. Briggs, "Detecting continuous spontaneous localisation with charged bodies in a Paul trap," arXiv:1605.01881.

[162] A. D. Ludlow, M. M. Boyd, J. Ye, E. Peik, and P. Schmidt, "Optical atomic clocks," *Rev. Mod. Phys.* **87**, 637–701 (2015).

[163] M. Zych and C. Brukner, "Quantum formulation of the Einstein Equivalence Principle," arXiv:1502.00971.

[164] M. Zych, "Quantum Complementarity and Time Dilation," in *Quantum Systems under Gravitational Time Dilation*. Springer, 2017. http://link.springer.com/book/10.1007%2F978-3-319-53192-2.

[165] M. Zych, I. Pikovski, F. Costa, and C. Brukner, "General relativistic effects in quantum interference of "clocks"," *J. Phys.: Conf. Ser.* **723**, 012044 (2016). http://stacks.iop.org/1742-6596/723/i=1/a=012044.

[166] M. Zych, F. Costa, I. Pikovski, T. C. Ralph, and C. Brukner, "General relativistic effects in quantum interference of photons," *Class. Quantum Grav.* **29**, 224010 (2012). http://stacks.iop.org/0264-9381/29/i=22/a=224010.

[167] C. W. Chou, D. B. Hume, J. C. J. Koelemeij, D. J. Wineland, and T. Rosenband, "Frequency Comparison of Two High-Accuracy ${\mathrm{Al}}^{+}$ Optical Clocks," *Phys. Rev. Lett.* **104**, 070802 (2010). http://link.aps.org/doi/10.1103/PhysRevLett.104.070802.

[168] T. Rosenband, D. B. Hume, P. O. Schmidt, C. W. Chou, A. Brusch, L. Lorini, W. H. Oskay, R. E. Drullinger, T. M. Fortier, J. E. Stalnaker, S. A. Diddams, W. C. Swann, N. R. Newbury, W. M. Itano, D. J. Wineland, and J. C. Bergquist, "Frequency Ratio of Al+ and Hg+ Single-Ion Optical Clocks; Metrology at the 17th Decimal Place," *Science* **319**, 1808–1812 (2008). http://science.sciencemag.org.ezproxy.library.uq.edu.au/content/319/5871/1808.

[169] N. Hinkley, J. A. Sherman, N. B. Phillips, M. Schioppo, N. D. Lemke, K. Beloy, M. Pizzocaro, C. W. Oates, and A. D. Ludlow, "An Atomic Clock with 10–18 Instability," *Science* **341**, 1215–1218 (2013). http://science.sciencemag.org/content/341/6151/1215.

[170] B. J. Bloom, T. L. Nicholson, J. R. Williams, S. L. Campbell, M. Bishof, X. Zhang, W. Zhang, S. L. Bromley, and J. Ye, "An optical lattice clock with accuracy and stability at the 10-18 level," *Nature* **506**, 71–75 (2014). http://www.nature.com/nature/journal/v506/n7486/full/nature12941.html#affil-auth.

[171] T. Akatsuka, M. Takamoto, and H. Katori, "Optical lattice clocks with non-interacting bosons and fermions," *Nat Phys* **4**, 954–959 (2008). http://www.nature.com/nphys/journal/v4/n12/abs/nphys1108.html.

[172] Y. D. Bayukov, A. V. Davydov, Y. N. Isaev, G. R. Kartashov, M. M. Korotkov, and V. V. Migachev, "Observation of the gamma resonance of a long-lived 109mAg isomer using a gravitational gamma-ray spectrometer," *Jetp Lett.* **90**, 499–503 (2009). http://link.springer.com.ezproxy.library.uq.edu.au/article/10.1134/S0021364009190011.

[173] J. C. Hafele and R. E. Keating, "Around-the-World Atomic Clocks: Predicted Relativistic Time Gains," *Science* **177**, 166–168 (1972). http://science.sciencemag.org/content/177/4044/166.

[174] G. C. Ghirardi, A. Rimini, and T. Weber, "Unified dynamics for microscopic and macroscopic systems," *Phys. Rev. D* **34**, 470–491 (1986). http://link.aps.org/doi/10.1103/PhysRevD.34.470.

[175] A. Smirne and A. Bassi, "Dissipative Continuous Spontaneous Localization (CSL) model," *Scientific Reports* **5**, 12518 (2015). http://www.nature.com/srep/2015/150805/srep12518/full/srep12518.html.

[176] S. Nimmrichter and K. Hornberger, "Stochastic extensions of the regularized Schr\"odinger-Newton equation," *Phys. Rev. D* **91**, 024016 (2015). http://link.aps.org/doi/10.1103/PhysRevD.91.024016.

[177] D. Stamper-Kurn, G. Marti, and H. Müller, "Verifying quantum superpositions at metre scales.," *Nature* **537**, E1 (2016).

[178] I. Dutta, D. Savoie, B. Fang, B. Venon, C. L. Garrido Alzar, R. Geiger, and A. Landragin, "Continuous Cold-Atom Inertial Sensor with 1 nrad/sec Rotation Stability," *Phys. Rev. Lett.* **116**, 183003 (2016).

[179] R. Schnabel, "Einstein-Podolsky-Rosen-entangled motion of two massive objects," *Phys. Rev. A* **92**, 012126 (2015).

[180] G. C. Ghirardi, P. Pearle, and A. Rimini, "Markov processes in Hilbert space and continuous spontaneous localization of systems of identical particles," *Phys. Rev. A* **42**, 78–89 (1990).

[181] D. Giulini and A. Großardt, "Gravitationally induced inhibitions of dispersion according to a modified Schrödinger–Newton equation for a homogeneous-sphere potential," *Classical and Quantum Gravity* **30**, 155018 (2013).

[182] M. J. W. Hall and M. Reginatto, "On two recent proposals for witnessing nonclassical gravity," *Journal of Physics A: Mathematical and Theoretical* **51**, 085303 (2018).

[183] K. Jacobs and D. A. Steck, "A straightforward introduction to continuous quantum measurement," *Contemporary Physics* **47**, 279–303 (2006).

[184] G. Kar, M. Sinha, and S. Roy, "Maxwell equations, nonzero photon mass, and conformal metric fluctuation," *Int J Theor Phys* **32**, 593–607 (1993). http://link.springer.com/article/10.1007/BF00673762.

[185] J. D. Brown, "Action functionals for relativistic perfect fluids," *Class. Quant. Grav.* **10**, 1579–1606 (1993), arXiv:gr-qc/9304026 [gr-qc].

[186] D. Wiltshire, "An introduction to quantum cosmology," *arXiv:gr-qc/0101003v2* (2010).

[187] P. MONIZ, "SUPERSYMMETRIC QUANTUM COSMOLOGY SHAKEN, NOT STIRRED," *International Journal of Modern Physics A* **11**, 4321–4382 (1996).

[188] G. Calcagni, "Fractal Universe and Quantum Gravity," *Phys. Rev. Lett.* **104**, 251301 (2010).

[189] R. Maartens and K. Koyama, "Brane-World Gravity," *Living Reviews in Relativity* **13**, 5 (2010). http://dx.doi.org/10.12942/lrr-2010-5.

[190] J. McGreevy and E. Silverstein, "The tachyon at the end of the universe," *JHEP* **0508**, 090 (2005).

[191] G. Lindblad, "On the generators of quantum dynamical semigroups," *Comm. Math. Phys.* **48**, 119–130 (1976). https://projecteuclid.org/euclid.cmp/1103899849.

[192] T. Josset, A. Perez, and D. Sudarsky, "Dark Energy from Violation of Energy Conservation," *Phys. Rev. Lett.* **118**, 021102 (2017), arXiv:https://arxiv.org/abs/1604.04183 [gr-qc].

[193] A. Padilla and I. D. Saltas, "A note on classical and quantum unimodular gravity," *Eur. Phys. J.* **C75**, 561 (2015), arXiv:https://arxiv.org/abs/1409.3573 [gr-qc].

# APPENDICES

# Appendix A

# Chapter II

## A.1 Exact unitarity

Here we sketch the proof of the conditions that guarantee exact unitary evolution of a system whose dynamics is given in eq. (2.9), discussed in Sec. 2.2.1. We repeat these conditions here for the convenience of the reader: The evolution of the system is *exactly* unitary if and only if $(i)$ the initial state of the ancillae is supported on a linear subspace $\mathcal{H}_M$ of eigenstates of $\hat{M}$ with a common eigenvalue and $(ii)$ the subspace $\mathcal{H}_M$ is invariant under $\hat{M}_0$.

It follows from $(i)$ that the total Hamiltonian (2.1) acting on the joint state of the system and ancilla can effectively be written as the sum of a term $\hat{H}_s(M) = \hat{S}_0 + \bar{g}M\hat{S}$ that acts only on the system (where $M$ denotes the common eigenvalue of $\hat{M}$ for states in $\mathcal{H}_M$), and a term $\hat{M}_0$ that acts only on the ancilla. From $(ii)$ we have that on the subspace $\mathcal{H}_M$ the operators $\hat{M}_0, \hat{M}$ commute. The evolution of the system thus factors out from the evolution of the ancilla, although it is described by an ancilla-dependent Hamiltonian $\hat{H}_s(M)$.

The proof of the necessary condition can be obtained as follows: A system evolves unitarily if its time evolution solves the Heisenberg equation

$$\dot{\rho} = -\frac{i}{\hbar}[\hat{h}, \rho] \tag{A.1}$$

for some Hermitian operator $\hat{h}$. In particular, this means that to all orders in $\tau$ eq. (2.9) must agree order by order with a corresponding expansion of an equation of the form $\rho(t_n) = \hat{U}_h(\tau)\rho(t_{n-1})\hat{U}_h^\dagger(\tau)$ with $\hat{U}_h(\tau) = \exp(-i\tau\hat{h}/\hbar)$. For this to be the case we must

have $(a)$: $\hat{h} = \hat{S}_0 + \bar{g}\langle\hat{M}\rangle\hat{S}$. Moreover, $(b)$ for all $k \in \mathbb{N}$ we must have $\langle\hat{M}^k\rangle = \langle\hat{M}\rangle^k$, which is equivalent to $(i)$ – the state of the ancilla must be in an eigensubspace of $\hat{M}$. Inspecting terms of order $\tau^3$, we obtain a further condition $(c)$: $\mathrm{Tr}\{(\hat{M}\hat{M}_0^2 - 2\hat{M}_0\hat{M}\hat{M}_0 + \hat{M}_0^2\hat{M})\rho_m\} = 0$. Using $(i)$ and denoting by $M$ the corresponding eigenvalue of $\hat{M}$, condition $(c)$ is equivalent to $M\mathrm{Tr}\{\hat{M}_0\rho_m\hat{M}_0\} = \mathrm{Tr}\{\hat{M}\hat{M}_0\rho_m\hat{M}_0\}$, that is $\hat{M}_0$ preserves $\mathcal{H}_M$. This completes the argument.

## A.2 Instantaneous position measurement and feedback-control

In this appendix we provide an example of eq. (2.30) with specific operators satisfying the limits (2.29). We take $\hat{S}_0 = \frac{\hat{p}^2}{2m}$ as the free Hamiltonian of the system and $\hat{M}_0 = 0$ (trivial evolution of the meters). We take the first interaction to be effectively a measurement performed by the meter over the system of some operator $\hat{S}_1$ for which we have $\hat{M}_1 = \hat{p}_m$ where $\hat{p}_m$ is the momentum operator of the meter. For the second interaction we choose $\hat{M}_2 = \hat{x}_m$ where $\hat{x}_m$ is the position operator of the meter. Finally, suppose we initially we prepare each meter in a Gaussian state $|\,\psi\rangle$ such that

$$\psi(x) = \langle\hat{x}\,|\,\psi\rangle = \frac{1}{(\pi\sigma)^{1/4}} e^{-\frac{x^2}{2\sigma}}, \tag{A.2}$$

for which the density matrix is $\hat{\rho}_m = |\,\psi\rangle\langle\psi\,|$ and the various expectation values are

$$\begin{aligned}
\langle\hat{M}_0\rangle &= 0\,, \\
\langle\hat{M}_2\rangle &= \langle\hat{x}_m\rangle = \int dx_m \langle x_m\,|\hat{x}_m\hat{\rho}_m|\,x_m\rangle = \int dx_m x_m \psi(x_m)^2 = 0 \\
\langle\{\hat{M}_1,\hat{M}_1\}\rangle &= \langle\{\hat{p}_m,\hat{p}_m\}\rangle = 2\int dx_m \langle x_m\,|\hat{p}_m^2\hat{\rho}_m|\,x_m\rangle = 2\int dx_m \left[\left(i\hbar\frac{\partial}{\partial x_m}\right)^2\psi(x_m)\right]\psi(x_m) = \frac{\hbar^2}{\sigma} \\
\langle\{\hat{M}_2,\hat{M}_2\}\rangle &= \langle\{\hat{x}_m,\hat{x}_m\}\rangle = 2\int dx_m \langle x_m\,|\hat{x}_m^2\hat{\rho}_m|\,x_m\rangle = \int dx_m x_m^2 \psi(x_m)^2 = \sigma \\
\langle\{\hat{M}_1,\hat{M}_2\}\rangle &= \langle\{\hat{x}_m,\hat{p}_m\}\rangle = \int dx_m \langle x_m\,|(\hat{x}_m\hat{p}_m + \hat{p}_m\hat{x}_m)\hat{\rho}_m|\,x_m\rangle = 0 \\
\langle i[\hat{M}_1,\hat{M}_2]\rangle &= \langle i[\hat{x}_m,\hat{p}_m]\rangle = -\hbar
\end{aligned} \tag{A.3}$$

With these expressions the limits (2.29) reduce to

$$\Xi_i = 0 \quad \forall i\,, \qquad \Gamma_{11} = \lim_{\tau'\to 0} \frac{1}{4}\tau' \bar{g}_1^2 \frac{\hbar^2}{\sigma}\,, \qquad \Gamma_{22} = \lim_{\tau'\to 0} \frac{1}{4}\tau' \bar{g}_2^2 \sigma\,, \qquad \tilde{M}_{12} = -\lim_{\tau'\to 0} \frac{\tau' \bar{g}_1 \bar{g}_2}{4}\,. \tag{A.4}$$

Let's now assume that the first interaction is an instantaneous measurement that can be modelled by choosing its interaction strength $\bar{g}_1 = \frac{1}{\tau'}$ – which results in an interaction of the form of a delta function in time. The strength of the second interaction is constant over the interval $\tau'$ and finite. The above limits are thus

$$\Gamma_{11} = \frac{1}{4}\lim_{\tau'\to 0} \frac{\hbar^2}{\tau'\sigma}\,, \qquad \Gamma_{22} = \frac{1}{4}\lim_{\tau'\to 0} \bar{g}_2^2\,\tau'\sigma\,, \qquad \tilde{M}_{12} = -\frac{\bar{g}_2}{4}\,. \tag{A.5}$$

We notice that in order to have a well defined master equation (2.30) we need to take an initial state for the meter such that $\sigma$ goes to infinity in a way that $\lim_{\tau'\to 0} \sigma\tau' = D$, where $D$ is a constant. This is equivalent to considering a measurement which is instantaneous and "infinitely" strong but also "infinitely" inaccurate. Finally, the master equation (2.30) for our example reads

$$\begin{aligned} \dot{\rho}(t) = & -\frac{i}{\hbar}[\hat{S}_0, \rho(t)] - \frac{i}{\hbar}\frac{\bar{g}_2}{4}[\hat{S}_2, \hat{S}_1\rho(t) + \rho(t)\hat{S}_1] \\ & - \frac{1}{8D}[\hat{S}_1, [\hat{S}_1, \rho(t)]] - \frac{D}{\hbar^2}\frac{\bar{g}_2^2}{8}[\hat{S}_2, [\hat{S}_2, \rho(t)]]\,. \end{aligned} \tag{A.6}$$

Note that choosing $\hat{S}_1 = \sqrt{2}\hat{x}_s$ to be the position operator of the system and $\bar{g}_2 = \sqrt{2}$ the last equation reduces to the unconditional master equation

$$\begin{aligned} \dot{\rho}(t) = & -\frac{i}{\hbar}[\hat{S}_0, \rho(t)] - \frac{i}{2\hbar}[\hat{S}_2, \hat{x}_s\rho(t) + \rho(t)\hat{x}_s] \\ & - \frac{1}{4D}[\hat{x}_s, [\hat{x}_s, \rho(t)]] - \frac{D}{4\hbar^2}[\hat{S}_2, [\hat{S}_2, \rho(t)]]\,. \end{aligned} \tag{A.7}$$

found by Milburn and Caves in ref. [94]. Those authors considered cycles of interaction, in which after an instantaneous position measurement a feedback control operation was introduced.

In general, feedback-control gates are applied to a system to control its behaviour after a measurement was performed. In the quantum information processing community, in the circuit framework, these are often approxiated as an instantaneous, non-infinitesimal transformations of the system depending on the measurement outcome. It is important to remark that contrary to this picture of feedback – where the state of the meter is not

modified – in the measurement/interaction approach applied here, the state of the meter will naturally get modified. For the example above, it will have the net effect of shifting the momentum of the meter. Finally notice that this will not affect the results of short interactions in our regime since each ancillae is discarded after the measurement – but it is an effect that needs to be taken into account when constructing measurement-based feedback gates. For completeness, recall that if $\hat{S}_2 = \alpha \hat{S}_1$, the second term in eq. (A.6) becomes a quadratic potential in $\hat{S}_1$.

## A.3 Emergent Newtonian-like interaction

Now we present a concrete application of Section 2.4 by introducing the gravitational example of ref. [8]. We first genralize our model to the symmetric case, where the total Hamiltonians during the first and the second sub-step correspondingly read

$$\hat{\mathcal{H}}^{(1)} = g_1(t)\hat{S}_1{}^{s_1} \otimes \hat{M}_1{}^{m_1} \otimes \hat{\mathcal{I}}^{s_2} \otimes \hat{\mathcal{I}}^{m_2} + g_2(t)\hat{\mathcal{I}}^{s_1} \otimes \hat{\mathcal{I}}^{m_1} \otimes \hat{S}_2{}^{s_2} \otimes \hat{M}_2{}^{m_2} \tag{A.8}$$

$$\hat{\mathcal{H}}^{(2)} = g_3(t)\hat{S}_3{}^{s_1} \otimes \hat{\mathcal{I}}^{m_1} \otimes \hat{\mathcal{I}}^{s_2} \otimes \hat{M}_3{}^{m_2} + g_4(t)\hat{\mathcal{I}}^{s_1} \otimes \hat{M}_4{}^{m_1} \otimes \hat{S}_4{}^{s_2} \otimes \hat{\mathcal{I}}^{m_2} \tag{A.9}$$

Following the same derivation as in the previous sections we obtain the master equation

$$\begin{aligned}
\dot{\rho}\quad (T) = &-\frac{i}{\hbar}[\hat{S}_0, \rho] + \lim_{\tau' \to 0} \\
- &\frac{i}{\hbar}\Big(\bar{g}_2\langle \hat{M}_2^{m_2}\rangle[\hat{S}_2^{s_2}, \rho] + \bar{g}_4\langle \hat{M}_4^{m_1}\rangle[\hat{S}_4^{s_2}, \rho] + \bar{g}_1\langle \hat{M}_1^{m_1}\rangle[\hat{S}_1^{s_1}, \rho] + \bar{g}_3\langle \hat{M}_3^{m_2}\rangle[\hat{S}_3^{s_1}, \rho]\Big) \\
- &\lim_{\tau \to 0} \frac{\tau}{4\hbar^2}\Big(\bar{g}_2^2\langle \hat{M}_2^{m_2{}^2}\rangle[\hat{S}_2^{s_2}, [\hat{S}_2^{s_2}, \rho]] + \bar{g}_4^2\langle \hat{M}_4^{m_1{}^2}\rangle[\hat{S}_4^{s_2}, [\hat{S}_4^{s_2}, \rho]] \\
+ &\bar{g}_1^2\langle \hat{M}_1^{m_1{}^2}\rangle[\hat{S}_1^{s_1}, [\hat{S}_1^{s_1}, \rho]] + \bar{g}_3^2\langle \hat{M}_3^{m_2{}^2}\rangle[\hat{S}_3^{s_1}, [\hat{S}_3^{s_1}, \rho]] \\
+ &\bar{g}_2\bar{g}_3\langle[\hat{M}_3^{m_2}, \hat{M}_2^{m_2}]\rangle[\hat{S}_3^{s_1}, \hat{S}_2^{s_2}\rho + \rho\hat{S}_2^{s_2}] + \bar{g}_1\bar{g}_4\langle[\hat{M}_4^{m_1}, \hat{M}_1^{m_1}]\rangle[\hat{S}_4^{s_2}, \hat{S}_1^{s_1}\rho + \rho\hat{S}_1^{s_1}] \\
+ &\bar{g}_2\bar{g}_3\langle\{\hat{M}_3^{m_2}, \hat{M}_2^{m_2}\}\rangle[\hat{S}_3^{s_1}, [\hat{S}_2^{s_2}, \rho]] + \bar{g}_1\bar{g}_4\langle\{\hat{M}_4^{m_1}, \hat{M}_1^{m_1}\}\rangle[\hat{S}_4^{s_2}, [\hat{S}_1^{s_1}, \rho]]\Big) \cdots
\end{aligned} \tag{A.10}$$

where $\rho$ denotes the state of both subsystems, $\hat{S}_0$ is the free part of the Hamiltonian, and we have suppressed the identity operators.

Since our main aim was to keep the terms in (2.36), which induce an interaction between the systems, we need the commutators $\langle[\hat{M}_4{}^{m_1}, \hat{M}_1{}^{m_1}]\rangle$ and $\langle[\hat{M}_3{}^{m_2}, \hat{M}_2{}^{m_2}]\rangle$ to be non vanishing. For simplicity, we choose:

$$\hat{M}_1{}^{m_1} = \hat{p}^{m_1} \quad \hat{M}_2{}^{m_2} = \hat{p}^{m_2} \quad \hat{M}_3{}^{m_2} = \hat{x}^{m_2} \quad \hat{M}_4{}^{m_1} = \hat{x}^{m_1} \tag{A.11}$$

and we use the ancillae initially prepared in a Gaussian state centered at zero as in eq. (A.2). Using Eqns. (A.3) and assuming instantaneous interactions for $\bar{g}_2$ and $\bar{g}_1$ (such that $\bar{g}_i = \frac{\chi_i}{\tau}$) and constant interactions for $\bar{g}_3$ and $\bar{g}_4$ (such that $\bar{g}_3 = \bar{g}_4 = 1$), then we get the following master equation:

$$\begin{aligned}\dot{\rho} = &-\frac{i}{\hbar}[\hat{S}_0, \rho] - \frac{i}{4\hbar}\left(\chi_2[\hat{S}_3^{s_1}, \hat{S}_2^{s_2}\rho + \rho\hat{S}_2^{s_2}] + \chi_1[\hat{S}_4^{s_2}, \hat{S}_1^{s_1}\rho + \rho\hat{S}_1^{s_1}]\right) \\ &- \frac{D}{8\hbar^2}\left([\hat{S}_3^{s_1}, [\hat{S}_3^{s_1}, \rho]] + [\hat{S}_4^{s_2}, [\hat{S}_4^{s_2}, \rho]]\right) \\ &- \frac{1}{8D}\left([\hat{S}_1^{s_1}, [\hat{S}_1^{s_1}, \rho]] + \hat{S}_2^{s_2}, [\hat{S}_2^{s_2}, \rho]]\right)\end{aligned} \tag{A.12}$$

If we choose the operators $\hat{S}_i^{s_k} = \hat{x}_k^{s_k}$, and set $\chi_1 = \chi_2 = K$, then this equation becomes

$$\begin{aligned}\dot{\rho} = &-\frac{i}{\hbar}[\hat{S}_0, \rho] - \frac{iK}{4\hbar}\left([\hat{x}_1, \hat{x}_2\rho + \rho\hat{x}_2] + [\hat{x}_2, \hat{x}_1\rho + \rho\hat{x}_1]\right) \\ &- \frac{D}{8\hbar^2}\left([\hat{x}_1, [\hat{x}_1, \rho]] + [\hat{x}_2, [\hat{x}_2, \rho]]\right) - \frac{1}{8D}\left([\hat{x}_1, [\hat{x}_1, \rho]] + [\hat{x}_2, [\hat{x}_2, \rho]]\right) \\ = &-\frac{i}{\hbar}[\hat{S}_0, \rho] - \frac{iK}{2\hbar}[\hat{x}_1\hat{x}_2, \rho] - \frac{D}{8\hbar^2}\left([\hat{x}_1, [\hat{x}_1, \rho]] + [\hat{x}_2, [\hat{x}_2, \rho]]\right) - \frac{1}{8D}\left([\hat{x}_1, [\hat{x}_1, \rho]] + [\hat{x}_2, [\hat{x}_2, \rho]]\right)\end{aligned}$$

which yields the quadratic potential for an induced gravitational interaction (with noise) studied in [8], taking $\hat{S}_0$ to be the sum of harmonic oscillator Hamiltonians for each subsystem.

# Appendix B

# Chapter III

## B.1 Dephasing Rate Minimization

The minimum dephasing rate for the multiparticle case cannot simply be obtained by considering only a single clock. For example the dephasing of a single clock $i$ in eq. (3.4) can be zero for $\Gamma_i \to 0$, and $\Gamma_{j\neq i} \to \infty$. However, this would result in each of the other $j \neq i$ clocks dephasing to a maximally mixed state instantly. Therefore, the minimization procedure must minimize each dephasing rate simultaneously to give a physically sensible result. We therefore minimize the sum of dephasing rates with respect to each of the $\Gamma_{ij}$'s (or $\Gamma_i$'s),

$$\frac{\mathrm{d}}{\mathrm{d}\Gamma_{kl}} \sum_i \left[ \sum_{j\neq i} \left( \frac{\Gamma_{ij}}{2} + \frac{g_{ij}^2}{8\Gamma_{ji}} \right) \right] = 0 \tag{B.1}$$

$$\text{or} \quad \frac{\mathrm{d}}{\mathrm{d}\Gamma_k} \sum_i \left[ \frac{\Gamma_i}{2} + \sum_{j\neq i} \frac{g_{ij}^2}{8\Gamma_j} \right] = 0. \tag{B.2}$$

For the pairwise feedback, the decoherence is minimized when $\Gamma_{ij} = \Gamma_{ji} = g_{ij}/2$, while for the global feedback the decoherence is minimized when $\Gamma_i^2 = \sum_{j\neq i} g_{ij}^2/4$ leading to minimum dephasing rates of (assuming $\omega_i = \omega_j = \omega$)

$$\mathcal{D}_{\mathrm{pw}}^{(i)} = \frac{G\hbar\omega^2}{2c^4} \sum_{j\neq i} \frac{1}{d_{ij}} \tag{B.3}$$

$$\mathcal{D}_{\mathrm{gl}}^{(i)} = \frac{G\hbar\omega^2}{2c^4} \sqrt{\sum_{j\neq i} d_{ij}^{-2}} \tag{B.4}$$

for pairwise and global feedback respectively. Alternatively, the measurement rates $\Gamma_{ij}$'s could be considered as some fundamental measurement rate that does not depend on the spatial distribution of the physical system. In this case, each of the $\Gamma$'s lose their $ij$ (or $j$) dependence. Nevertheless, there is still a dephasing on the clocks that can be bounded by current experiments. For a fixed $\Gamma$, the minimum dephasing on the $i$th particle is

$$\mathcal{G}_{\rm pw}^{(i)} = \sqrt{N-1}\frac{G\hbar\omega^2}{2c^4}\sqrt{\sum_{j\neq i} d_{ij}^{-2}} \tag{B.5}$$

$$\mathcal{G}_{\rm gl}^{(i)} = \frac{G\hbar\omega^2}{2c^4}\sqrt{\sum_{j\neq i} d_{ij}^{-2}}. \tag{B.6}$$

Although the dephasing from the measurement is assumed to be fixed, the total dephasing rate still depends on the local environment of the clock due to the feedback from all other clocks. For an arbitrary spatial distribution of clocks, the summations in $\mathcal{D}_{\rm pw}^{(i)}$ and $\mathcal{D}_{\rm gl}^{(i)}$ must be computed. However, for regular arrays of clocks the summations are well approximated by integrals and can be solved to find the dependence on the number of clocks $N$, and spatial distribution. If we consider a regular array of $N$ clocks with characteristic length $L_c$ between adjacent clocks, the sum can be written as,

$$\sum_j \frac{1}{d_{ij}^\alpha} \approx \frac{1}{L_c^D}\int_{V_D}\frac{dV_D}{r^\alpha} = \frac{S_D}{L_c^D}\int_{L_c}^{R} r^{D-1-\alpha}dr\,, \tag{B.7}$$

for a clock in the center of a D-dimensional array, e.g. linear ($1D$), circular planar ($2D$), or spherical ($3D$) lattices. The integral is over the macroscopic volume, (area in $2D$ or line in $1D$) of the array, and $S_D = 1,\ 2\pi,\ 4\pi$ for linear, planar and spherical geometries respectively. The integral is explicitly an approximation to the sum for the $i^{\rm th}$ clock in the center of an array of radius $R = N^{1/D}L_c$. However, by using symmetry, clocks on the sides/edge of an array would be expected to have the same scaling with $N$ (which is fixed by $D-1-\alpha$), and differ only by a constant factor of order unity. For linear arrays in $1D$ consider the following example:

$$\begin{aligned}\sum_{j\neq i}\frac{1}{d_{ij}} &\approx \int_{-N_L L_c}^{-L_c}\frac{1}{|x|}\frac{dx}{a} + \int_{L_c}^{N_R L_c}\frac{1}{|x|}\frac{dx}{a} \\ &= \frac{1}{L_c}\log(N_L N_R)\end{aligned} \tag{B.8}$$

where $N_L > 1$ ($N_R > 1$) are the number of clocks to the left (right) of the $i$th clock. As $N_L + N_R + 1 = N$, the sum scales as $\log(N)$ regardless of the physical position of the clock in the array.

# Appendix C

# Chapter IV

## C.1 CCG model for composite systems

Here we extend the CCG approach by constructing a model for composite systems in three dimensions relevant for the matter wave experiments we analyze in the main text. We consider two systems $s_1$ and $s_2$ respectively consisting of $N_1$ and $N_2$ elementary constituents – chosen to be atoms – with masses $m_i,\ i = 1, ..., N_1 + N_2$. Choosing atoms to be the basic constituents of a body ensures that (unlike the case for subatomic particles) the total mass of a body is equal to the sum of its individual constituents. Our aim is to describe the behaviour of the centres of mass of two objects in the CCG model, thereby allowing a more complete comparison between it and the Diosi-Penrose model. A multi-particle extension of the CCG model could also be used directly (though perhaps more cumbersomely) and the same final results would be obtained.

The classical gravitational potential energy between any two constituents $i, j$ reads

$$V_{ij} = \frac{Gm_i m_j}{|\vec{r}_{ij}|},$$

where $\vec{r}_{ij}$ is the vector joining the positions of the individual masses $m_i, m_j$. We write this as $\vec{r}_{ij} = \vec{d}_{ij} + \vec{x}_i + \vec{x}_j$, where $\vec{d}_{ij}$ is the vector joining their positions at the initial time and $\vec{x}_{i,j}$ is the displacement of the CM of a given body. We consider the case where $s_1$ and $s_2$ are rigid. In applications of interest here, $s_1$ will be a test mass (e.g. an atom in an interferometer) and $s_2$ will describe matter gravitationally interacting with $s_1$, (e.g. the Earth). We will thus assume that a) all constituents of a given body are in a superposition of equally distant locations (rigidity); b) there is one distinguished direction defined by the

superposition of the test mass (while the surrounding matter is well localised), see fig. C.1.

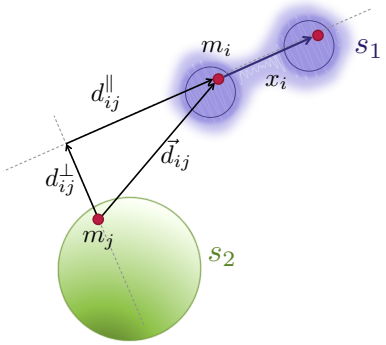


Figure C.1: Test body $s_1$ in a spatial superposition in the presence of a source mass $s_2$. For any pair of elementary masses $(m_i, m_j)$ forming the bodies, the distance $\vec{d}_{ij}$ between them can be decomposed into component $d_{ij}^{\parallel}$ along the direction of the spatial superposition of $s_1$ and a perpendicular component $d_{ij}^{\perp}$. $x_i$ is the displacement from the initial position of the mass $m_i$, whose values span all locations between which the particle can be superposed. Note that the assumption of rigidity implies that each constituent of $s_1$ is displaced by the same amount.

It is convenient to write $\vec{d}_{ij} = d_{ij}^{\parallel}\hat{e} + d_{ij}^{\perp}\hat{e}^{\perp}$ where $\vec{x}_i = x_i\hat{e}$ and thus $\hat{e}$ is a unit vector in the direction defined by the superposition and $\hat{e}^{\perp}$ is a unit vector in an orthogonal direction. With the above we can write

$$\begin{aligned} V_{ij} &= \frac{-Gm_im_j}{\sqrt{(d_{ij}^{\parallel}+x_i+x_j)^2+(d_{ij}^{\perp})^2}} \approx -Gm_im_j \times \\ &\times \left(\frac{1}{d_{ij}} - \frac{d_{ij}^{\parallel}}{d_{ij}^3}(x_i+x_j) + \frac{(d_{ij}^{\parallel})^2 - \frac{1}{2}(d_{ij}^{\perp})^2}{d_{ij}^5}(x_i+x_j)^2\right) \end{aligned} \tag{C.1}$$

where $d_{ij} = \sqrt{(d_{ij}^{\parallel})^2 + (d_{ij}^{\perp})^2}$.

For any pair $(i,j)$ the "measurement" part of the interaction can thus be taken as $\hat{x}_i \otimes \hat{p}_{m_i} + \hat{x}_j \otimes \hat{p}_{m_j}$ and the "feedback" as $K_{ij}\hat{x}_i \otimes \hat{x}_{m_j} + K_{ij}\hat{x}_j \otimes \hat{x}_{m_i} + \hat{Y}_i \otimes \hat{I}_{m_j} + \hat{Y}_j \otimes \hat{I}_{m_i}$, where $\hat{Y}_{i(j)}$ acts only on mass $m_{i(j)}$. The following master equation for the pair

$$\dot{\rho}_{ij} \approx -\frac{i}{\hbar}[\hat{H}_0 + \hat{Y}_i + \hat{Y}_j + K_{ij}\hat{x}_i\hat{x}_j, \rho_{ij}] - \Gamma_{ij}\left([\hat{x}_i,[\hat{x}_i,\rho_{ij}]] + [\hat{x}_j,[\hat{x}_j,\rho_{ij}]]\right)$$

is thus obtained, where $\Gamma_{ij} \equiv \frac{1}{4D} + \frac{K_{ij}^2 D}{4\hbar^2}$. Defining $K_{ij} := 2Gm_i m_j \frac{(d_{ij}^{\parallel})^2 - \frac{1}{2}(d_{ij}^{\perp})^2}{d_{ij}^5}$, $Y_i := -Gm_i m_j(\frac{1}{2d_{ij}} - \frac{d_{ij}^{\parallel}}{d_{ij}^3}x_i + \frac{(d_{ij}^{\parallel})^2 - \frac{1}{2}(d_{ij}^{\perp})^2}{d_{ij}^5}x_i^2)$ the master equation describes the induced (approximate) Newtonian interaction between $m_i$, $m_j$ (since $\hat{Y}_i + \hat{Y}_j + K_{ij}\hat{x}_i\hat{x}_j \approx V_{ij}$, eq. (C.1)) with the decoherence term including a gradient of the Newtonian force between the pair in three dimensions. Note that the $x$-axis is defined by the direction of the superposition; that is why decoherence terms included in the model also act only in this direction. The dynamics of all $N_1 + N_2$ constituents, described by $\rho_{tot}$, reads

$$\dot{\rho}_{tot} = -\frac{i}{\hbar}[\hat{H}_0 + \sum_{i<j}^{N_1+N_2} V_{ij}, \rho_{tot}] \quad - \sum_{i<j}^{N_1+N_2} \Gamma_{ij}\Big([\hat{x}_i, [\hat{x}_i, \rho_{tot}]] + [\hat{x}_j, [\hat{x}_j, \rho_{tot}]]\Big). \tag{C.2}$$

Introducing the displacement $r_1$ ($r_2$) of the CM of $s_1$ ($s_2$), and $\hat{x}'_i$ as the displacement relative to the CM, the displacement of any individual constituent can be described by $\hat{x}_i = \hat{r}_1 + \hat{x}'_i$ for $i < N_1$ (for constituents of $s_1$) and $\hat{x}_i = \hat{r}_2 + \hat{x}'_i$ for $i > N_1$ (for constituents of $s_2$). With the above $[\hat{x}_i, [\hat{x}_i, \rho_{tot}]] = [\hat{r}_1, [\hat{r}_1, \rho_{tot}]] + [\hat{x}'_i, [\hat{x}'_i, \rho_{tot}]] + [\hat{r}_1, [\hat{x}'_i, \rho_{tot}]] + [\hat{x}'_i, [\hat{r}_1, \rho_{tot}]]$, for $i \leq N_1$ and analogously (with $\hat{r}_2$ instead of $\hat{r}_1$) for $i > N_1$. From the assumed rigidity of the bodies it follows that relative degrees of freedom are uncorrelated with the CM and their displacements remain negligible; see fig. C.2 for an illustration (i.e. a rigid body whose CM is in a superposition of locations $a$ and $b$ is described by a correlated state where all its constituents are at fixed distances relative to the CM position $a$ and at the same fixed distances relative to the CM position $b$).

Tracing over the relative degrees of freedom and keeping the CM positions of $s_1$ and $s_2$ results in the following master equation (in performing the trace, for simplicity one can assume that the CM of $s_i$ coincides with the position of one of its particles)

$$\begin{aligned}\dot{\rho}_{s_1 s_2} = &-\frac{i}{\hbar}[\hat{H}_0 + V, \rho_{s_1 s_2}] - 2\sum_{i<j=1}^{N_1} \Gamma_{ij}[\hat{r}_1, [\hat{r}_1, \rho_{s_1 s_2}]] - 2\sum_{N_1<i<j}^{N_1+N_2} \Gamma_{ij}[\hat{r}_2, [\hat{r}_2, \rho_{s_1 s_2}]] \\ &- \sum_{i=1}^{N_1}\sum_{j=N_1+1}^{N_1+N_2} \Gamma_{ij}\Big([\hat{r}_1, [\hat{r}_1, \rho_{s_1 s_2}]] + [\hat{r}_2, [\hat{r}_2, \rho_{s_1 s_2}]]\Big)\end{aligned} \tag{C.3}$$

where $V = \sum_{i<j}^{N_1+N_2} V_{ij} \approx -G\frac{M_1 M_2}{|d + r_1 + r_2|}$; $M_1$ and $M_2$ are correspondingly the total masses of $s_1$ and $s_2$.

Finally, tracing over the degrees of freedom of $s_2$ one obtains the master equation for

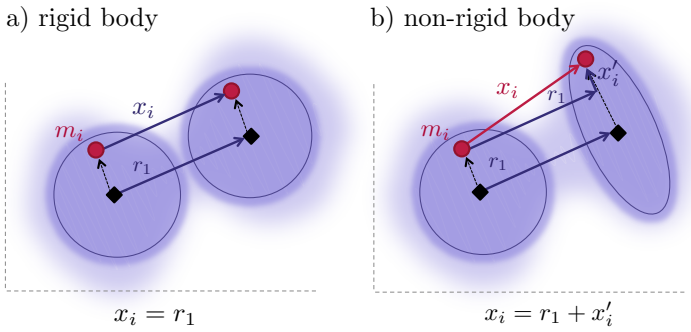


Figure C.2: Displacement $x_i$ of the $i^{th}$ constituent of a) rigid body, b) non-rigid body. For a rigid body each constituent remains at the same distance (dashed arrow) from from the centre mass (black diamond), and its displacement is the same as that of CM $x_i = r_1$. For a non-rigid body, the displacement of a constituent can differ from that of the centre of mass, $x_i = r_1 + x_i'$. This work only considers case a).

the CM of $s_1$:

$$\dot{\rho}_{s_1} = -\frac{i}{\hbar}[\hat{H}_0 + V, \rho_{s_1}] - \big(2\sum_{i<j=1}^{N_1}\Gamma_{ij} + \sum_{i=1}^{N_1}\sum_{j=N_1+1}^{N_1+N_2}\Gamma_{ij}\big)[\hat{r}_1, [\hat{r}_1, \rho_{s_1}]], \tag{C.4}$$

We are particularly interested in the case when $s_1$ is a single atom, $N_1 = 1$, and $s_2$ is the entire Earth. Minimising the decoherence rate for each pair $(1, j)$ gives $\Gamma_{1j}^{min} = \frac{K_{1j}}{2\hbar}$ and the total decoherence rate is given by $\sum_{j\in\text{earth}} \frac{K_{1j}}{2\hbar}$. Note, that every constituent of the Earth acts so as to increase the decoherence rate of $s_1$. Here we seek to relate the resulting decoherence to that given by the Earth's CM, as in the original model. (For some geometries, the multi-particle formulation of the model, and the original CCG prediction for the CMs of the bodies give different results[1].) Since $K_{1j}$ as a function of $(d_{1j}^{\parallel}, d_{1j}^{\perp})$ is convex only for $|d_{1j}^{\parallel}| < |d_{1j}^{\perp}|/\sqrt{2}$ we consider only a portion $\mathcal{C}$ of the Earth's mass, which lies within the volume where $K_{1j}$ is convex, see fig. C.3.

The overall decoherence rate is greater than that stemming from particles in $\mathcal{C}$, which itself is greater than decoherence coming from the centre of mass of $\mathcal{C}$. Since $|d_{1j}^{\parallel}| <$

[1]Let $s_2$ to be a spherical shell of radius $r$ comprising N particles of mass $m$, and $s_1$ – an elementary particle inside the shell. Sum over the constituents of the shell yields a finite decoherence rate, which can be made arbitrarily small by increasing $r \to \infty$. However, decoherence predicted by the model applied directly to the CM of $s_2$ is arbitrarily large for $s_1$ arbitrarily close to the shell's centre, independently of $r$.

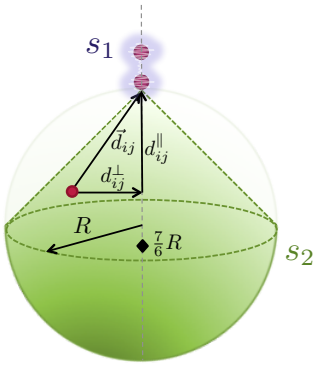


Figure C.3: Estimation of the decoherence effect on a single atom, $s_1$, due to Earth: for simplicity we consider only the portion of Earth for which the decoherence rate is always greater than the effect stemming from matter concentrated at its centre of mass . This portion of Earth's mass is defined as all constituents (atoms) for which $d^{\perp}_{1j} < d^{\parallel}_{1j}$ – inside the cone-and-half-ball, shaded green in the figure. The total mass of the region is 3/4 of the mass of Earth $M$, and its centre of mass is 7/6 of the Earth's radius $R$.

$|d^{\perp}_{1j}|/\sqrt{2} < |d^{\perp}_{1j}|$, the region $\mathcal{C}$ can be taken as a cone of height $R$ and support of area $\pi R^2$ together with a half ball of radius $R$. Assuming a constant density for body $M_2$, the mass of $\mathcal{C}$ is $\frac{3}{4}M_2$ and its CM is at a distance $\frac{7}{6}R$ from the top surface, as depicted in fig. C.3. The quantity

$$\Gamma^{min}_{M_2;R} = \frac{3}{4}\left(\frac{6}{7}\right)^3 \Gamma_{CCG}(M_1, M_2, R) = 0.47\, \Gamma_{CCG}(M_1, M_2, R)$$

where $\Gamma_{CCG}(M_1, M_2, R) = \frac{GM_1M_2}{R^3}$ is the lower bound on the decoherence rate of mass $M_1$ due to the presence of the homogeneous ball of mass $M_2$ and radius $R$. Note that in the above the $\Gamma_{CCG}(M_1, M_2, R)$ is the decoherence rate as per the original CCG model for elementary masses $M_1, M_2$ at a distance $R$.

Note that our overall result is lower bounded by the decoherence rate calculated as if the entire body were concentrated in the centre of mass. Hence the predictions of the CCG model for the experiments we analyze will not change if we choose constituents of the Earth that are different from atoms.

We close this section by noting that in general there will be decoherence also in the transverse directions. However the setup we analyze is not sensitive to any loss of coherence in transverse directions. Furthermore, any such effects will further increase decoherence rates, and thus will not affect our results.